UNIVERSITY OF COPENHAGEN
FACULTY OF SCIENCE

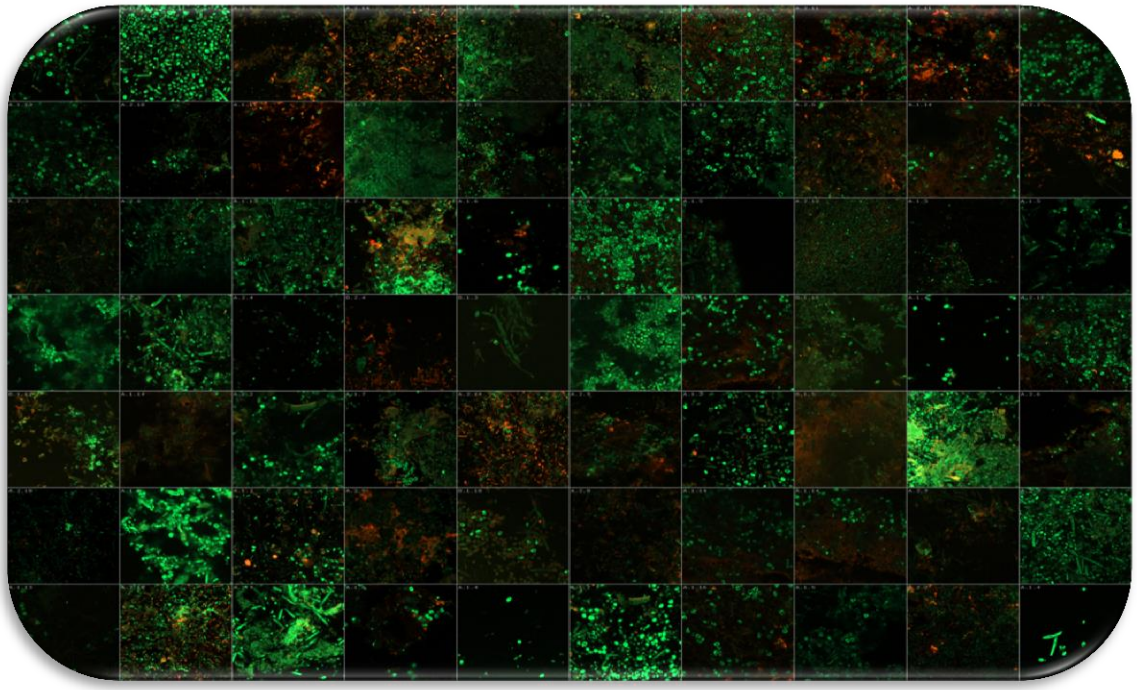

Characterization of surface fouling and biofilm formation under water reuse scenarios in dairy and meat industry

PhD thesis 2018 • Iuliana Madalina Stoica

Characterization of surface fouling and biofilm formation under water reuse scenarios in dairy and meat industry

PhD thesis

by

Iuliana Madalina Stoica

Frederiksberg, 2018

Department of Food Science

Faculty of Science
University of Copenhagen

Title
Characterization of surface fouling and biofilm formation under water reuse scenarios in dairy and meat industry.

Submission date
July 31, 2018

Supervisors
Associate Professor Frans van den Berg
Department of Food Science, Faculty of Science
University of Copenhagen

Professor Søren Balling Engelsen
Department of Food Science, Faculty of Science
University of Copenhagen

Assessment committee
Assistant Professor Åsmund Rinnan (chair)
Department of Food Science, Faculty of Science
University of Copenhagen

Professor Lisbeth Truelstrup Hansen
DTU FOOD, Research Group for Microbiology and Hygiene
Technical University of Denmark

Professor Royston Goodacre
School of Chemistry / Institute of Biotechnology
Faculty of Science and Engineering
The University of Manchester

ISBN: ……
Printed by SL grafik, Frederiksberg,Denmark (slgrafik.dk)

Table of Contents

Preface

This thesis is submitted in order to obtain the PhD degree from the PhD school of Science, University of Copenhagen. It was conducted as part of the Reuse of Water in the food and bioprocessing industry (REWARD) and RENPÅNY projects.

REWARD is a project funded by the Danish Council for Strategic Research, Programme Commission on Health Food and Welfare and REWARD partners which include University of Copenhagen (KU FOOD), Technical University of Denmark (DTU), Technical University of Munich (TUM), Arla Foods Ingredients, Novozymes A/S, DHI, LiqTech International A/S, TetraPak, and NIRAS.

RENPÅNY is a project funded by the Green Development and Demonstration Programme (GUDP) of the Ministry of Food and Pig Levy Foundation, including as industry partners: Danish Crown (DC), Tulip, Tican, 3-stjernet Stryhns, ISS and Danish Meat Research Institute (DMRI).
Acknowledgement goes to my principal supervisor, Associate Professor Frans van den Berg and co-supervisor Professor Søren Balling Engelsen, University of Copenhagen.

Most of the work was carried out in the section of Chemometrics and Analytical Technology (CAT), Department of Food Science, University of Copenhagen and for a couple of months at DMRI. Therefore, I would like most of all to express my special thanks to Frans in whom I have always found support and motivation even in the most challenging times.
I also thank to Anette Granly Koch and operators from DMRI who helped with the several trials and providing me with the results for the microbial analysis. A great thank goes as well to Dorrit Thaysen from Arla Foods Ingredients, for her positive attitude, critical discussions and her time in helping me to collect all membrane elements.
I would like to thank to all co-authors for their contribution, in particular to Eirini Vitzilaiou with whom I have done most of the microbial analysis in tandem and to Henriette Lyng Røder for helping with Confocal Laser Scanning Microscopy even if pressed by time due to her PhD thesis deadline.

Not last, I would like to thank to all my colleagues from CAT, for their special power to provide a unique and always entertaining atmosphere. Especially to Peter Bæk Skou, I want to thank him for being a great colleague, for helping me with transportation of instrument at DMRI, for all encouragements and help in getting rid of some frustrating MATLAB errors.

Iuliana Madalina Stoica
Frederiksberg, July 2018

List of publications

Paper I

Iuliana Madalina Stoica , Hamid Babamoradi, Frans van den Berg. A statistical strategy to assess cleaning level of surfaces using Fluorescence spectroscopy and Wilks' ratio. Chemometrics and Intelligent Laboratory Systems, Volume 165, 15 June 2017, Pages 11–21

Paper II

Iuliana Madalina Stoica , Eirini Vitzilaiou, Henriette Lyng Røder, Mette Burmølle, Dorrit Thaysen, Susanne Knøchel, Frans van den Berg. Biofouling on RO-membranes used for water recovery in the dairy industry, Journal of Water Process Engineering, Volume 24, 15 May 2018, Pages 1–10

Abbreviations and notation

AFI	Arla Foods Ingredients
APC	Aerobic plate count
ATP	Adenosine triphosphate
ATR	Attenuated total reflectance
BCA	Bicinchoninic acid protein assay
BEOP	Biofilm enhanced osmotic pressure
CCD	Charged –coupled device
CIP	Clean-in-place
CLSM	Confocal laser scanning microscopy
DOE	Design of experiments
DMRI	Danish Meat Research Institute
EEM	Emission-excitation map
EPS	Extracellular polymeric substances
FAD	Flavin Adenine Dinucleotide
FTIR	Fourier Transformed Infrared
GMP	Good manufacturing practices
HACCP	Hazard analysis and critical control points
ICP-OES	Inductive coupled plasma-optical emission spectroscopy
IR	Infrared
LED	Light emitting diode
MSPC	Multivariate statistical process control
NADH	Nicotinamide adenine dinucleotide
NIR	Near infrared
NF	Nano filtration
PARAFAC	Parallel factor analysis
PAT	Process analytical technology
PCA	Plate count agar/ Principle component analysis
PCR	Polymerase chain reaction
PLS	Partial least square
PMT	Photomultiplier tube
QbD	Quality by design
RLU	Relative light units
RO	Reverse osmosis
ROP	Reverse osmosis polisher
SPC	Standard plate count
TVC	Total viable counts
UF	Ultrafiltration
UV-VIS	Ultraviolet-Visible

Abstract

Food industries still depend to a large extent on potable water in conducting their routine operations. Equipment cleaning, in particular, is a water intensive process which results in considerable volumes of wastewater. Considering the high environmental impact and increasing costs for water treatment before discharge, they are exploring alternatives to minimize their water waste production. Optimization of cleaning recipes towards less use of water and chemicals or replacing the necessary volumes with process water recovered from various effluent streams by reverse osmosis (RO) filtration, are some of the main routes explored. However, the success and cost efficiency of any of these strategies depends on good process control and efficient evaluation of safety aspects, which ideally should be done based on real-time measurement techniques.

First aim of this thesis was to show how spectroscopic techniques combined with chemometric modeling techniques may be used to achieve a solution for a non-destructive - preferably real-time - monitoring system over the hygiene and microbiological level of different surfaces involved in different production processes. More specific, the scenario of monitoring hygienic status of conveyor belts under slaughterhouse processing conditions.

An algorithm based on Wilks ratio statistics applied on fluorescence recordings was developed and demonstrated in pilot-scale for its potential to monitor online hygienic status of conveyor surfaces. Strong background interferences and changes in surface physical properties due to processing conditions are identified as main challenges. The algorithm is designed to neutralize such interference and high potential for reaching a valid monitoring solution is expected when using more advanced fluorescence spectrophotometers.

The second aim was characterization of RO membrane fouling to map and potentially optimize performance and cleaning strategies. Several industrial-scale RO membranes used for recovery of process-water from whey ultrafiltration permeate have been examined for their fouling tendency. At the end of a complete cleaning-in-place (CIP) protocol, biofouling appears to be the main issue in most RO-elements. Significant yeast contamination was found on the membrane permeate surfaces of these particular elements. Microbiological analysis performed on RO permeate streams indicated that minimal loads of microorganisms pass into the permeate streams, however being inactivated by UV treatments proceeding the RO units. Therefore, the identified biofouling appears to have primarily technological and economic implications, whereas the process water streams a have suitable quality for reuse.

Resume′

Fødevareindustrien er i høj grad stadig afhængig af drikkevand for at kunne udføre rutineopgaver. Særligt rengøring af udstyr er en vandintensiv proces, som resulterer i betragtelige volumener af spildevand. Den høje miljøpåvirkning og øgede omkostninger for vandrensning før udledning gør at fødevareindustrien undersøger alternativer til at minimere spildevandsproduktionen. De primære alternativer som undersøges er optimering af rengøringsprocedurer som mindsker vand- og kemikalieforbrug samt erstatning af det nødvendige volumen med procesvand genvundet fra omvendt osmosefiltrering af forskellige spildevandsstrømme. Succesen og omkostningsniveauet af disse strategier afhænger dog af god proceskontrol og effektiv evaluering af sikkerhedsaspekter, hvilket ideelt bør baseres på måletidsteknikker i realtid.

Det første mål med denne afhandling var at vise hvordan spektroskopiske teknikker, kombineret med kemometrisk modelleringsteknikker, kan bruges til at opnå et ikke-destruktivt – helst realtids – målesystem som dækker hygiejne- og mikrobiologiniveauet af forskellige overflader involveret i forskellige produktionsprocesser.

En algoritme baseret på Wilks ratio statistik anvendt på fluorescensmålinger blev udviklet og eftervist i pilot-skala for dets potentiale til direkte at monitorere hygiejne status af transportbåndsoverflader. Stærk baggrundsinterferens, samt forskelle i overfladens fysiske egenskaber som konsekvens af proceseringsforhold, er identificeret som de væsentligste udfordringer. Algoritmen er designet til at neutralisere sådanne interferenser og metoden forventes at have stort potentiale for at blive en effektiv monitoreringsmetode når mere avancerede fluorescensspektrofotometre benyttes.

Det andet mål var at karakterisere omvendt osmose membran-fouling (tilgroning) for at kortlægge og potentielt optimerer ydelse og rengøringsstrategier. Adskillige industrielskala omvendt osmosemembraner brugt til genindvinding af procesvand fra valle ultrafiltrerings permeat er blevet undersøgt for deres evne til at blokere. Til slut i en rengøringsprotokol lader biofouling til at være hovedproblemet i de fleste omvendt osmose filtreringselementer. Betragtelig gærkontaminering blev fundet på permeat siden af membranerne af disse bestemte elementer. Mikrobiologisk analyse, udført på omvendt osmosepermeatstrømme indikerede at minimale mængder af mikroorganismer passerer ind i permeatestrømmen, men bliver inaktiveret af efterfølgende UV-behandling. Derfor lader det til, at den identificerede biofouling primært har tekniske og økonomiske implikationer, hvorimod procesvandstrømmene har en passende kvalitet for genindvinding.

Chapter 1

Introduction

Water is a valuable utility that food industries highly depend on in their daily manufacturing and cleaning operations. By comparison to other industries (e.g. chemical, pharmaceutical or oil refineries), large volumes of fresh water are involved in food processing operations which results in significant volumes of effluent with notable organic loads[1]. Owing to the negative impact this may have on environment if released as is, such effluents require treatment before discharge in order to comply with quality standards[2]. With climate change as an ongoing global challenge and the adoption in 2000 of the European Union (EU) Water Framework Directive[3], which puts priority on water protection among the main environmental issues, more strict effluent discharge regulations[4] have been adopted within the EU, and also worldwide. Therefore, in a context of water stress and changes in legislation that open up to the use of alternative water qualities in food applications[5], industries have started to shift their vision towards more sustainable use of water resources. Depending on the particularities of their processes, different food and beverage industries adopt different strategies to cope with the need for water conservation; some examples are summarized in Table 1.1. Sustainable water practices may begin with process optimization by rationalizing industrial water use practices, fixing spillage and prevent leaks, or store and include product residues in future production batches. Also, if the nature of the process allows, substituting a wet process with a dry one or selling some of the effluent streams as by-products are generally strategies with a higher impact on water savings.

Comparing the water consumption among different food sectors, dairy and meat processing industries have the largest dependence on fresh water in their production processes, Figure 1.1. Obviously, this is partly an inherited fact due to the susceptibility of dairy and meat products to be more easily spoiled by microorganisms, hence requiring more hygienic conditions and use of water, compared to other food products. When looking at the water usage among the different food industries in Denmark in the past years, a reduction can be noticed in the water consumption in particular within dairy and meat, in spite of the current trend of increased production demands[6]. This suggests an ongoing change of vision where process optimization and rethinking cleaning strategies are increasingly implemented in their daily practices, especially when identifying that less environmental impact, competitiveness on the market and savings come as main benefits.

In dairy, the opportunity to recover water from cheese whey has been driven over the years by the advances in membrane technology[7] combined with the increased interest to harvest the nutritional components of whey (e.g. protein, lactose and fat). The typical composition of cheese whey is 0.8% proteins, 0.05% fat, 5% lactose, 0.7% minerals and 94% water[8]. When employing ultrafiltration

(UF), the protein part can be concentrated at the retentate side of the UF membrane, allowing only lactose, minerals and water to permeate through. By further treatment, the purified whey protein products are of high nutritional and functional value and can be sold on the market as alternative sources of proteins[9]. Similarly, lactose and minerals can be recovered by feeding the UF permeate to a Reverse Osmosis (RO) system and the liquid that permeates is generally water with good properties, suitable for e.g. clean-in-place (CIP) operations[10]. This is obviously a valuable route for dairies to reduce their fresh water intake, convert their main by-product into a financial gain and minimize the effluent that goes typically to (biological) water treatment.

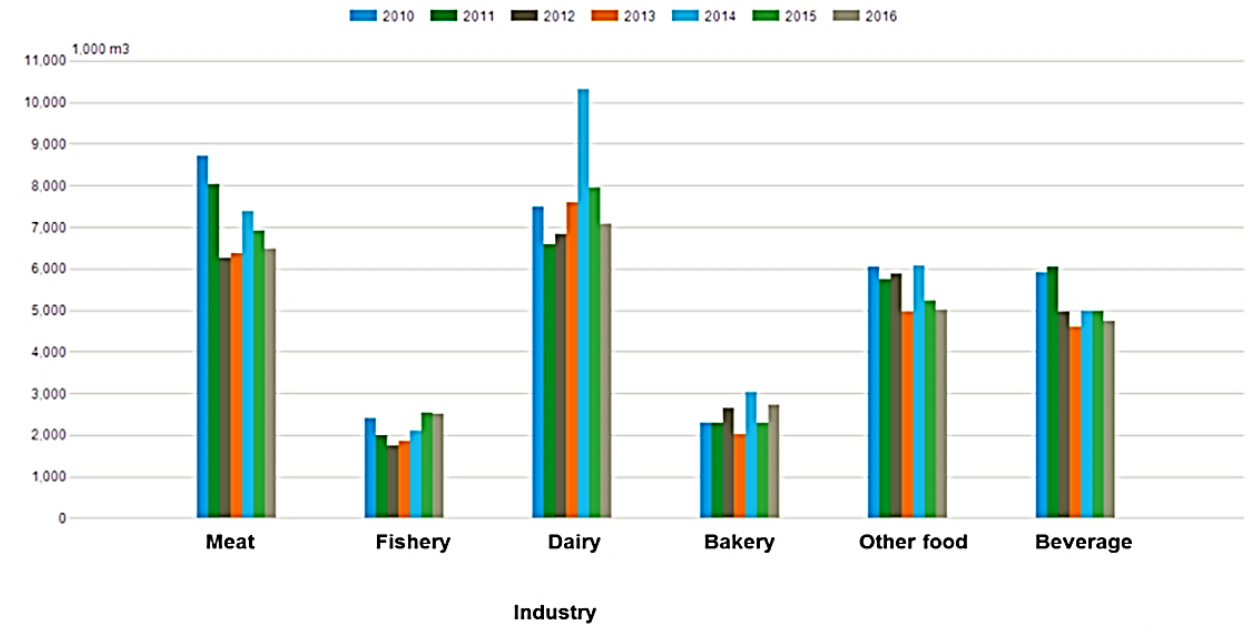

Figure 1.1 Water consumption by the food industry, according to Statistics Denmark; accessed 02 July 2018

In parallel, in the meat manufacturing, cleaning of slaughterhouse facilities generates the largest amount of wastewater. At this level, conveyor belts used both during processing (such as cutting) and transportation account for one of the largest *equipment* that if not cleaned properly can become a vector for microbial contamination[11]. Cleaning of such systems occurs at fixed schedules based on recipes designed according to risk-based analysis and at the recommendations of chemical and equipment suppliers. But all cleaning is at the cost of shutting down production, use of energy and manpower and extensive volumes of water and chemicals. Consequently, if possible to minimize the frequency of cleaning operations and/or the amount of necessary fresh water without compromising the safety and quality parameters of meat products, less wastewater would be generated[12].

Table 1.1. An overview of different strategies for water recovery and reuse in various food and beverage industries; adapted from Ölmez et al. 2013 [1].

Processing industry	Description	Reference
Poultry processing	Reuse of desensitization tank effluents for pre-washing of plastic transportation cages after preliminary treatment	
	Reuse of cooling tank, cooling tunnel and storage chamber effluents in washing the live poultry receiving and unloading yards	Amorim et al. (2007)[7]
	Reuse of effluent from final rinising of cleaning operation for pre-washing the by-product room	
	Rational water use practices: replacement of main chiller with air chilling, adoption of high-pressure washing can be coupled with reduction of truck shower time	
	Reuse from pre-chiller after UF, from gizzard machines to viscera flume without pre-treatment, from freezing	Matsumura & Mierzwa (2008)[8]
Meat processing	Reuse of chiller shower water for warm cleaning after preliminary treatment, nanofiltration and UV disinfection	Mavrov & Bélières (2000)[9]
	Reuse of cooling water from sausage products after treatment with nanofiltration	
Dairy processing	Reuse of UHT flash cooler condensate after preliminary treatment, nanofiltration and UV disinfection	Suárez et al. (2015)[10]
	Recovery of detergents and process water by nanofiltration treatment	Suárez & Riera (2015)[11]
	Treatment of dairy industry wastewater by reverse osmosis for water reuse	Vourch et al. (2005)[12]
	Reuse in CIP operations of process water recovered from cheese way after ultrafiltration combined with reverse osmosis and UV disinfection	Aydiner et al. (2014)[13] Meneses & Flores (2016)[14]
Shrimp processing	Recycling water in peeling operation after treatment with reverse osmosis	Casani et al. (2005)[15]
Fruit processing industry	Reuse of spent process water from mixing and equalizing tank for boiler make-up,cooling, pasteurisation or bottle pre-washing after preliminary treatment, nanofiltration and UV disinfection	Blöcher et al. (2002)[16]
	Ozonation and O3–UV are alternatives to other sanitizers used in the fresh-cut washing processes, allowing less frequent changing of spent water	Selma et al. (2008)[17]
Beverage industry	Reuse of chiller showers or bottle washing water after treatment with nanofiltration, low-pressure reverse osmosis membrane and UV disinfection.	Mavrov & Bélières (2000)[9]
	Use of vapor condensate as boiler make-up water	

The common point of any strategy for sustainable use of water resources within food processing plants is that process monitoring and control play a crucial role. When cleaning less or using recovered water for cleaning purposes, one should pay attention that no chemical, physical and more likely microbial hazards emerge. When looking at the reported cases of altered quality and safety properties of food products, the issue is mostly associated with microbial hazards, suggesting that microorganisms represent probably the main danger for food industry. Microorganisms are well known to acquire persistence in the processing environment and resistance to antibiotics, disinfectants and cleaning chemicals when embedding themselves in a self-produce extracellular polymeric substances (EPS), hence developing in what is normally known as biofilm[23]. When associated with food processing equipment, the term biofouling is alternatively used. The regular cleaning and sanitizing operations are aimed to restore the hygiene status of surfaces and prevent the development of biofilms. However, organic material and microorganisms may still accumulate on food-contact surfaces. Through cross-contamination such deposits may lead to food spoilage or foodborne illnesses in case pathogens are involved, or in the least critical scenario affect negatively equipment performance.

When assessing surface cleanliness, traditional culture procedures are the standard method to determine the total number of viable microorganisms or indicator microorganisms. Despite their wide acceptance, these tests are very slow and results are obtained first after 48-72h[24]. Although extensive trials to develop fast, robust, non-destructive and accurate tool for bacterial enumeration, few methods have proven their applicability in full scale production conditions[25]. Therefore, the steps conducted in this thesis were with the mindset to bring the detection of microbial hazards closer to the food process own dynamic and achieve a more comprehensive overview.

Detection of microorganisms on surfaces becomes even more important when intended to change the nature of the cleaning operations by substituting the involved volumes of fresh water with recovered water. In this case the importance of appropriate monitoring of equipment hygiene and water fitness for use is enhanced since the likelihood of using contaminated water for cleaning is considerably higher and can exacerbate the biofilm development. Therefore, with an overall aim to bring a contribution in the area of surface fouling and biofilm formation under the current and rather new movement towards water reuse practices, this thesis has been focused on:

- Characterizing the incidence and implications of microbial hazards under the conditions of the two cases: RO water recovery and conveyer systems in the meat industry.
- Develop spectroscopic methods combined with multi-way data analysis into monitoring systems or strategies applicable in these industrial set-ups that can bring an advantage in identifying, preventing and reacting more promptly to emerging microbial contaminants in comparison with current employed methods.

1.1 Outline

The thesis is developed around two investigations conducted during the project. In order to create a better understanding of the research, the published papers are integrated in the thesis and the additional text is intended to offer an introduction on the established techniques used in the investigations, followed by a discussion of main results and perspectives.

Chapter 2 outlines the practical and legal frame of food hygiene, describes the implications of hazards in the food industry and discusses the main challenges in achieving proper monitoring of surface hygiene. The chapter includes a description of Process Analytical Technology (PAT) as a support for new concepts in cleaning validation and risk assessment.

Chapter 3 opens with an introduction on fluorescence spectroscopy principles and an overview of state-of-the art in monitoring surface fouling. Then the multivariate data analysis techniques employed in Paper I are explained in more detail. In this paper a statistical algorithm was developed that can demonstrate the use of fluorescence spectroscopy as a potential PAT tool to support fouling monitoring on conveyor belt surface. The chapter continues with a follow-up investigation on Paper I and describes the outcome of additional trials with a hand-held fluorescence device.

Chapter 4 moves the focus to the application of RO membranes for recovery of process-water in the dairy industry. It offers an overview of the existing types of membrane fouling as main causes of failure, combined with an introduction over the chosen techniques to evaluate the type of fouling present on industrial RO membranes as detailed in Paper II. In this paper biofouling is discussed as the main issue on the investigated RO membranes, and the chapter is supplemented with results obtained from other techniques that address scaling and protein fouling as well.

Chapter 5 consists of a general discussion on the main outcomes of the project and gives perspectives for future research in relation to the implementation of PAT in validating surface cleaning efficiency.

Chapter 2

Surface monitoring with a focus on fouling and microorganisms detection

2.1. Legal frame of food hygiene

Food borne illnesses have been consistently among the top ten causes of death in the world. According to the World Health Organization (WHO), in spite of continuous efforts to mitigate the issue, still almost 1 in 10 people in the world fall ill after eating contaminated food and 420,000 die every year[26]. In light of these facts which - scored more dramatic figures in the past - Codex Alimentarius Commission (CAC) was established in 1963 by the Food and Agriculture Organization of United Nations (FAO) and WHO, with the purpose to harmonize safe food practices on a global level by developing food standards and guidelines, collectively called Codex Alimentarius[27].

The risk of contamination with microbiological, chemical, physical or allergenic hazards[28], is inherent at all stages across the food chain and may have a tremendous impact on public health. With the publication of the Commission's White Paper on Food Safety[29] in 2000, emphasize on food safety increased. Over the years it became a legal requirement for any food manufacturer or business operator to implement effective controls of their operations and ensure the production of safe foods suitable for consumption. If not handled and/or manufactured properly, food products may carry contaminants introduced during growth and harvesting of raw materials, storage, transport, processing into final products or re-contamination may occur during subsequent storage and transportation until the final consumer is reached. Therefore, hygiene in the food industry is of paramount importance and as defined by Codex Alimentarius, represents "*all measures necessary to ensure the safety and suitability of food at all stages across the food chain*". In Europe, the hygiene of food stuff is regulated by the Regulation (EC) No. 852/2004[30], Regulation (EC) No 853/2004[31] for the specific hygiene rules for food of animal origin and Regulation (EC) No 183/2005[32] on the requirements for feed hygiene, which are all incorporated further in the national legislation of each country. The General Food Law (Regulation (EC) 178/2002)[33] serves as the basis of all hygiene regulations[34].

The *microbiological contamination* is the major safety concern for food industries since most food outbreaks are directly linked to the presence of pathogenic microorganisms and in fewer cases due to chemical or physical contaminants[35]. This may be partly due to the fact that by comparison, the latter ones can be better avoided and controlled through a well implemented risk management system and surveillance programs. Microorganisms, on the other hand, are unavoidable in food

production environments. They may be introduced by air, contact with surfaces, water or humans[36]. Microbial hazards can be high risk pathogenic bacteria[37] responsible for causing diseases or low risk spoilage bacteria[38] that have instead a negative effect (most often economic) on product quality and shelf-life. Both categories thus present a major concern and great effort is made within the food industry to avoid their spread and development. To reach this goal, Good Manufacturing Practices (GMP) and Hazard Analysis Critical Control Point (HACCP) based procedures are a requirement and used to control the incidence of any food related hazards[27]. This requires more effort and alignment of hygiene practices across the entire food chain, since factors like temperature, humidity, pH, availability of nutrients, and presence or absence of oxygen may easily influence bacterial growth and thus recontamination[36].

GMP offer guidelines that deal with all aspects of production, from design of premises and equipment, to control of the production process, plant maintenance and cleaning, personal hygiene, storage and transportation, product information and staff training. GMPs are rather subjective recommendations of a qualitative nature, but important prerequisite programs for the HACCP system[39]. The HACCP concept is a risk management methodology aimed to identify safety risks based on scientific knowledge and defines quantitative measures to control, validate and prevent safety issues that may occur across the production stages[40].

With the adoption of EU Water Framework Directive[41], the reuse of treated wastewater has been prioritized within the food industry and it is seen as a tool to achieve the objectives set in the mentioned directive. The entire movement is primarily targeted to loosen the current dependence on natural resources, such as water, and achieve minimal discharges. For safe integration, implementation of any water reuse practice should be carefully designed and included in the HACCP program as recommended by the Codex Alimentarius.

2.2. Type of surface materials used in food industry during manufacturing

Secure products are a direct result of safe production practices - hence hygienic food processing environments are a mandatory factor to achieve food products suitable for consumption. Generally, any type of surface may pose the risk of becoming a source of contamination at some point if not maintained and cleaned properly. Cross-contamination may occur in various ways along the manufacturing process, either through direct contact of food with contaminated equipment surface or indirectly when exposed to potential contaminants from the processing environment, such as dirt falling from the ceiling, splashes from floor cleaning, dust, fuel equipment leakages, etc. Therefore, a hygienic design of the environment and more extensively of the processing equipment has an important role in ensuring a safe food production free from physical, chemical and microbiological contaminants. To meet the hygienic design criteria, materials of construction, equipment geometry and cleaning protocols are the key elements to be addressed[42].

Materials of construction are probably the first element to consider when designing food processing equipment for a specific application. The European Framework Regulation (EC) No.1935/2004[43] regulates and outlines the safety requirements necessary to be fulfilled by any type of materials of

construction intended for use in the food industry. It is important to stress that the food contact materials must be first of all mechanically stable as no or minimal damage should occur during normal processing operations, resistant to a high range of harsh chemicals that are generally included for cleaning purposes is needed, but also to high temperatures if steam sterilization or hot water are intended to be applied. Also, since most food products are characterized by high water content, food contact materials must be corrosion-resistant and chemically inactive avoiding leaching out into the product of any toxic compounds. Besides these aspects, surface topography plays an important role as well when considering that microbial contaminants can easily find favorable growth conditions in crevices that are hard to be spotted and consequently cleaned. Thus, all surfaces that come in direct contact with food must be smooth, non-porous and easy to clean. Evidently, it is not always easy to fulfill all these different characteristics in applications, which determines that new material development and improvement are continuously sought. Today, in the food industry, stainless steel, plastics and rubber-based elastomers are the most common types of materials used for the construction of different food processing equipment[44].

Stainless steel is a popular metal that enters in the construction of a vast number of food processing and storage applications due to its high corrosion resistance compared to other metals such aluminum, copper or carbon steel. Also, it is the metal of choice for food industry in particular due to its great mechanical strength, great endurance to heat and chemicals, ease to clean even when handling strong coloring agents but also due to its property to be easily shaped in the necessary format during fabrication[45].

Through a process called passivation, a thin layer containing a mix of iron, chromium and optionally molybdenum oxides is typically formed on metal's surface in order to increase its resistance to corrosion. In the manufacturing of stainless steel, the last step of final surface finish has a high importance in rendering the metal's required smoothness. Depending on its composition, crystalline textures (e.g., ferrite, austenite, pearlite, martensite, ledenburite, spheroidite, and cementite) and the selected combination of alloys, stainless steel comes in various grades; each of them with specific properties that cover endurance to a vast range of food processing conditions[45].

The largest quantities used are the austenitic stainless steels which are a system of Fe-Cr-Ni alloys. Most commonly are AISI 304 (18%Cr-10%Ni) and AISI 316 (17%Cr-12%Ni-2.5%Mo) stainless steel due to their suitable hardness and corrosion resistance in most food applications[46].

If low chloride levels are expected (up to 50 ppm) under neutral pH (between 6.5 and 8) and at low temperatures (up to 25°C), the AISI 304 stainless steel types can be the metal of choice. From a long term perspective of use at slightly higher chloride levels and moderate temperatures the molybdenum-containing AISI 316 together with its lower carbon version AISI 316(L) types are superior to AISI 304 and become preferred. Thus, pipework, vessels, valves, pump castings and rotors are frequently made of AISI 316/316(L)[47]. However, under high levels of chlorine combined with high temperatures (more than 60°C), even AISI 316 stainless steels may show stress-corrosion cracking. In such cases, super austenitic stainless steels with higher chromium, nickel, molybdenum, copper and nitrogen contents or duplex steel and nickel alloys are required for their higher strength and greater resistance to stress corrosion cracking[48].

Plastics are high molecular weight polymers that besides their high use in food packaging are also an important equipment construction material due to their high plasticity and corrosion resistance. They may be used to avoid metal-to-metal contact, for conveying food products, used as covers and guides, for storage containers or molds. The main concerns when selecting the type of plastic is their ability to withstand the production and cleaning conditions such as temperatures, pressures and chemical concentrations without cracking, breaking or releasing toxic compounds. Also, when dedicated for food contact, the plastic materials should be easy to clean, with smooth surfaces, free from cracks, not absorbent to food constituents or microorganisms and with good wear/abrasion resistance[47].
Polypropylene, polyvinyl chloride, acetal copolymer, polycarbonate and high-density polyethylene are among the few types of plastics considered safe and suitable for hygiene applications. Compared to stainless steel that is manufactured according to standard specifications, plastic grades may depend on supplier's own specifications. Thus, the selection of appropriate plastic for specific food contact applications must always be done based on tests that demonstrate their regulatory compliance and compatibility with manufacturing conditions[44].

Once approved, maintenance of plastic based equipment is important. Conditions that may induce failures of plastics should be minimized or better avoided if possible, since it may impact the safety and quality aspects of food products. At low temperatures combined with high mechanical stress some plastics may become brittle with sharp components detaching, which can ultimately result in food contamination with physical hazards. Also, plastic surface damage acquired through abrasion due to high shear forces between solids, slurries or pastes transferred along plastic's surface will promote the accumulation of soils, sustain biofilm formation and challenge the cleaning procedures. Moisture but also some cleaning detergents and sanitizing agents may be absorbed by plastics causing swelling, material shedding and generally poor surface hygiene. Similarly, plastics should be protected from UV and ozone as such exposure will degrade material properties and sometimes cause embrittlement. Electrostatic charges acquired through friction or rubbing operations are also sought to be avoided. Such charges attract and favor the attachment of dust and bacteria to surface. To mitigate the issue, food grade anti-static agents are added to polymer's formulation[44].

Rubbers are the type of material whose high elasticity recommends them primarily in the composition of seals, gaskets, caps and hoses. Depending on their formulation, different rubbers come with different elasticity, resistance to chemicals and strength. They contain a mix of polymers, fillers, plasticizers, activators, antioxidants, accelerants, and cross-linking (or vulcanizing) agents. There may be natural and synthetic rubber, thermoplastic elastomers, and silicone rubber. In all cases, when selecting for food-contact purposes the most important aspect of all types of rubbers is their property to be chemical inert and not leach any toxic compounds into food.[49]

2.3. Biofilm formation

Biofilm formation is a practice that microorganisms undertake in order to achieve protection and withstand unfavorable physical and chemical conditions. Briefly, biofilms are microbial communities that bridge themselves in self-produced extracellular polymeric substances (so-called EPS) while (firmly) attaching to a surface. The practice of switching from a planktonic state (free floating) to the biofilm state is preferred by all microorganisms since is a self-defense mechanism to harsh conditions normally encountered during food processing and cleaning operations. A general accepted theory is that biofilms follow five (more or less) distinct stages along their formation: 1 the initial attachment of planktonic bacteria to the surface, 2 replication and production of extracellular polymeric substances (EPS), 3 formation of micro-colonies, 4 maturation (development of biofilm architecture) and 5 detachment, see Figure 2.1[50].

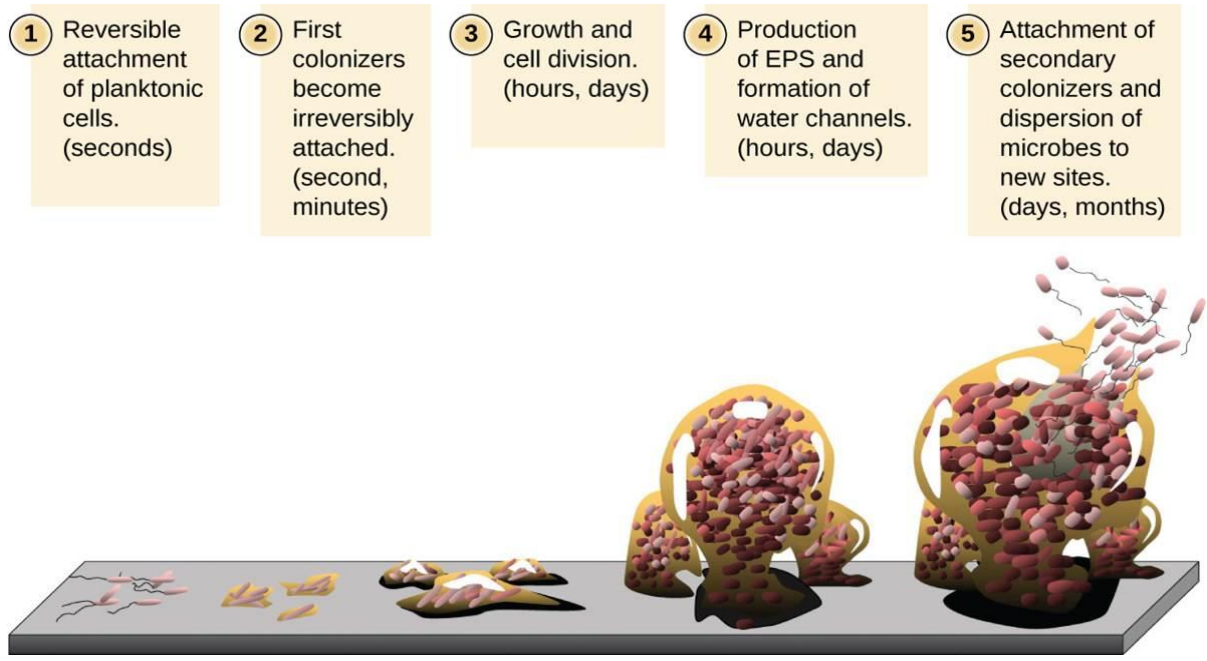

Figure 2.1 Stages of biofilm formation; adapted from Monroe (2007)[51]

The instalment of biofilms is closely linked with the production of EPS, which has a role in attachment and also in building the biofilm matrix that acts as a barrier between embedded cells and environmental stresses. EPS are high molecular weight compounds that include primarily polysaccharides, proteins, nucleic acids, humic substances, and ionisable functional groups like carboxylic, phosphoric amino and hydroxyl groups; it can account for 50% to 90% of the total bio-film material[52]. There is evidence that the production of EPS type and their amount differs among bacterial strains even within the same species[53]. More important, when associated with other cells, microorganisms appear to create synergies, expressing changes in their phenotype that

down-regulate or up-regulate different functions influencing the biofilm forming strengths, functions and final architecture. Overall, environmental biofilms are complex and commonly found to contain mixed microbial populations distributed in layers.

The attachment and development into mature biofilm structures undertakes complex mechanisms that are regulated by a set of factors related to surrounding particularities, substratum, cell surface and other aspects as summarized in Figure 2.2. The initial phase (attachment) is dependent on the physicochemical interactions between cells and surfaces, whereas its subsequent phases (development) corresponds to molecular mechanisms that lead to metabolic cooperativity between cells through quorum sensing and their acquisition of new genetic traits by gene expression. Through Brownian movement, van der Waals attraction, gravitational forces, surface electrostatic charges and their intrinsic motility, microorganisms arrive inevitably on surfaces. Their adhesion is then influenced most importantly by the availability of nutrients and the type of absorbed organic molecules on surface. Other factors such as surface roughness or smoothness, hydrophobicity, pH and temperature come as supportive factors for biofilm formation. Porous surfaces are generally more difficult to clean and thus can offer more opportunities for cells to remain hidden and develop into microhabitats[54]. Even though not a clear trend, hydrophobicity may also have an influence in surface attachment. For instance, Salmonella and Listeria have been shown by Sinde & Carballo (2000)[55] to attach better on hydrophobic surfaces than hydrophilic ones. The composition of the organic material and environmental conditions determine the type of cells attaching to surfaces and their biofilm architecture. More dense and compact biofilms are formed under high shear forces compared to low shear flows that promote thick multi-layered biofilm structures with different architectures[56].

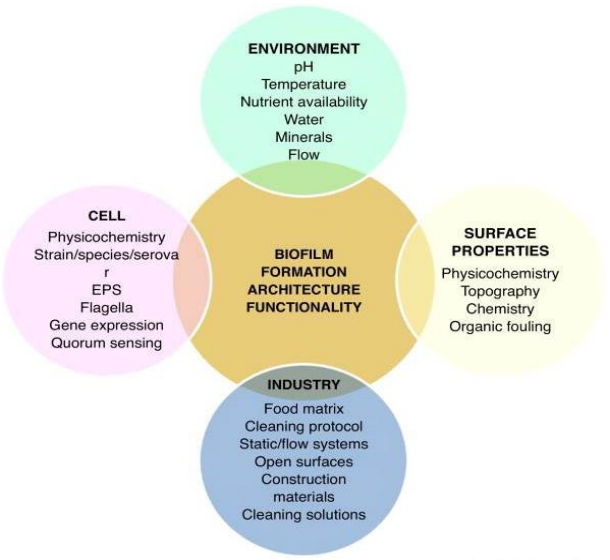

Figure 2.2. Factors impacting on biofilm formation, its architecture and functionality; source : Whitehead et al.(2015)[57]

One should note that on engineering surfaces with food contact, the scheduled cleaning operations are aimed to remove and avoid the development of microorganisms into biofilms. Regularly cleaned surfaces may still accumulate organic material and bacteria, but in the case of open type of surfaces (easy access) the likelihood of reaching advanced biofilm morphologies is minimized due to the constant disturbance by cleaning (with possibility for mechanical cleaning) and sanitizing procedures and the possibility to directly check their efficiency. In such cases, the term *biofouling* is alternatively used and refers to the organic material associated with microbial cells retained on the particular surface; it is what would typically correspond to the first biofilm stage in Figure 2.1 - the reversible attachment. However, in closed and difficult to access systems such as pipes, membranes, tubes, corners, interior of processing equipment, *true* biofilms are more likely to be found.
The accumulation of bacteria on a food-contact surface under the biofilm umbrella is undesirable since by cross-contamination, it might lead to lower shelf life of products and pathogenic strains will render food products unsafe for consumption and might cause diseases. Salmonella spp, Listeria monocytogenese, E. coli O157:H7, Campylobacter spp., Bacillus cereus and Staphylococcus aureus are some of the primary bacterial pathogens associated with food borne illnesses and have been shown to adhere to food-contact surfaces and acquire persistence in food environments[58].
Besides the impact on safety and quality aspects of the food products, biofilm formation can be associated also with technical issues. Losses of heat-transfer efficiency may be encountered in heat-exchangers under the development of biofilms on their surface or even blockage of tubes may happen when biofilms reach proportions that can restrict the normal flow[59]. Corrosion and material deterioration can be promoted by biofouling, depending if the bulk biofilm contains sulfate-reducing, iron-oxidizing or hydrogen producing bacteria, whose secreted metabolites are capable to attack the colonized substratum[60]. In pressure driven processes, biofouling of membranes increases the hydraulic resistance and lowers the unit performance. In reverse osmosis membranes biofouling may accumulate high salt concentration near the membrane, creating the *Biofilm Enhanced Osmotic Pressure* (BEOP), which results in turn to enhanced salt passage[61].

One of the main concerns related to biofilm formation is that when part of a biofilm structure, microorganisms acquire certain levels of resistance to disinfection agents and implicitly persistence in the processing environment, compared to when present in a planktonic state. The resistance of microorganisms to biocides under the biofilm umbrella is attributed to several mechanisms where EPS and changes in bacterial phenotypes play important roles. First, depending on their complexity and amount, the EPS may act as a physical barrier and hinder the penetration of antimicrobial agents through the bulk matrix. Also, biocides may partly react with matrix components such as proteins, nucleic acids or carbohydrates, which determines that overall only sub-lethal doses of antimicrobial agents reach bacterial cells present in the deeper level of biofilm. Complementary, as an adaptive response to repeated exposure of non-critical concentration of disinfectants, bacteria may change their phenotype and develop tolerance to present conditions[62].

Whether it is tolerance or *true* resistance to biocides, biofilm formation must be avoided especially because pathogenic bacteria like E. coli O157:H7 that has poor biofilm production power when alone[63], tends to interact instead with other microorganisms in order to benefit of the protective advantage of biofilms. Depending on the type of surface-associated community, E. coli O157:H7 may exhibit synergistic or antagonistic behavior. Numerous bacterial isolates from food processing environments have been shown to boost E.coli adhesion and proliferation on food contact surfaces. Liu et.al (2014)[64] observed for instance that especially strong biofilm producing strains such as Burkholderia caryophylli and Ralstonia insidiosa favored the persistence of E.coli in production plants, exhibiting 180% and 63% increase in biofilm biomass, and significant thickening of the biofilm, when co-cultured with E. coli O157:H7. However, other strains like Pseudomonas grimontii may inhibit the proliferation of Escherichia coli[65].

Salmonella, a pathogen related to numerous foodborne infections can persist on food-processing equipment by its ability to form biofilms on all contact materials (plastic, rubber, glass and stainless steel) involved in the food industry. It produces cellulose as the main matrix component and the biofilm-forming ability differs among strains in relation to environmental conditions such as pH, temperature and salt content[58]. Lianou & Koutsoumanis (2012)[66] showed by evaluating a total of 60 different Salmonella enterica strains that the highest amount of biofilm was achieved at pH 5.5 (35 strains; 58.3%), at 0.5% NaCl (29 strains; 48.3%) and at 25°C (32 strains; 53.3%).
Bacillus cereus is a spore forming, motile bacteria associate with milk spoilage but also responsible for foodborne illnesses[58]. They possess the ability to survive pasteurization and form biofilms in pipelines and stainless steel. The resistance of spores to hot alkaline solutions (pH>13) and hot acidic solutions (pH<1) makes their removal more challenging and requires thorough hygiene practices[67].
Staphylococcus aureus, commonly found also in human flora, is responsible for intoxications of humans when producing enterotoxins in meat associated products. It has high biofilm formation power on both stainless steel and polypropylene surfaces[68]. Consequently, the ability of most pathogens to survive and be involved in biofilm formation requires processing conditions that limit their development. Additionally, proper monitoring and cleaning operations are highly important to ensure safe final products.

2.4. Challenges when monitoring surface hygiene

While there are regulations such as Regulation (EC) No 2073/2005[69] that specify the acceptable microbial limits for different food products in relation to the aerobic colony count or specific pathogenic microorganisms, surface hygiene does not have any *specific limits of acceptability* defined by authorities. Baseline acceptable limits are instead set internally within food companies and these should be meaningful in relation to hazard analysis and critical control points for each product and process.

As an overall aim, the cleaning and disinfection procedures are targeted to achieve at minimum significant bacterial reduction and eliminate pathogenic bacteria from production environments. However, due to various factors, among which one can list ineffective soil removal, instalment of biofilms, faults in reaching the suitable temperature or chemicals concentration etc., the bacterial removal may not be absolute and low number of bacteria can still remain on equipment surfaces or machines. Thus, sampling and testing are necessary to monitor the remaining levels of microorganisms, identify any potential instalment of biofilms and validate the efficiency of cleaning programs. Monitoring surface hygiene level is however not trivial. Especially when considering that *estimations* of the microbial population are to be done *on a microscopic level in relation to surfaces* that in some cases may *reach square meters* for e.g. conveyor belts, industrial membranes, fermentation and storage thanks. Also, easy access is not always possible for some processing systems such as pipelines, tanks, containers or for those that may require dismantling as in the example of meat grinders, filters, etc. In such situations, indirect methods are sought for conducting representative sampling and microbial analysis. One strategy most commonly used is the rinse method[70] which involves the rinse of the specific unit with sterilized water added upstream and collected downstream at different points (in space and/or time), followed by the estimation of colony forming units in the collected rinse water. In this way bacteriological samples can be taken from large surfaces that otherwise would be inaccessible for direct sampling. For this procedure to work large rinsing volumes may be required and it thus result in increased disposal costs while biofilms attached firmly to the surface of for instance pipes may not be detected.

Surfaces are generally challenging to monitor also due to the fact that their topology may change over time as a consequence to process operations, such wear-and-tear on cutting tables in slaughterhouses. Therefore both the cleaning and microbial assessment method needs to adapt and take into consideration the presence of potential cracks, scratches and grooves. One should note that such damages do not necessarily need to be visible to the human eye as even micro-crevices that if not detected and cleaned properly are enough to harbor microorganisms and provide suitable environments for growth. The world of microbiology on surfaces has still lots of unknowns since there is no easy accessible technology or method that can assess directly and non-destructively their presence in their microhabitat. The errors in estimating microbial levels and detection of bacteria on surfaces are inherently higher when compared to liquid samples where plating is applied directly. In the case of surfaces results are always dependent of the intermediate extraction step performed by e.g. swabbing. All these aspects render production surfaces to be difficult to monitor and it is nearly impossible to have a true estimate of actual microbial levels colonizing a surface. Rapid microbiological testing is one area that lacks in accurate quantitative methods. There is not yet a method to assess the microbial level of surfaces without having involved a recovery step via the swab method. Thus, a direct non-destructive method would be far superior to the reference method.

2.5. Current methods to validate cleaning on surfaces in industrial setups

2.5.1. Direct - culture based techniques

Conventional plating is the reference method of use for either quantitative purposes when intended to enumerate microorganisms in a given sample, but also for qualitative analysis when isolation and identification of targeted microorganisms is sought. Aerobic Plate Count (APC), referred in literature also as Standard Plate Count (SPC), mesophilic count or Total Viable Count (TVC) is the measure of Hazard Analysis Critical Control Point Effectiveness[71]. The method is based on allowing the growth of microorganisms retrieved from sample of interest, on the non-selective enrichment media, followed by enumeration of the individual colonies visible on the plate, which will provide an estimate of sample population, expressed as Colony Forming Units (CFU). Typically Plate Count Agar (PCA) serves as the non-selective media of use in quantitative determinations of the *total level* of a sample's viable bacteria, since media composition will allow the growth of a wide range of microorganisms. If on the other hand the interest is to detect and test for specific bacterial strain like pathogenic bacteria or e.g. yeasts, selective enrichment media is required. The principle remains the same, except for the media being used which is designed to support and emphasize the growth of the microorganism of interest. These selective media typically contain in their formulation antimicrobials, dyes, or alcohol meant to inhibit the growth of other strains[72]. Most pathogenic bacteria like E.coli, Listeria, Salmonella etc., have well defined standards and are routinely used for their identification and enumeration in environmental and food samples, as indicated in Regulation (EC) No 2073/2005[69].

Although considered the standard method, the culture based technique is not absolute. Besides being time-consuming and requiring trained personnel, it is unfit for real-time monitoring since results are obtained at minimum after one day of incubation. Conventional plating has a series of limitations that should be considered when interpreting the results. First, it should be noted that each bacterial strain is characterized by certain cultivable conditions, among which most important are the type of media, incubation temperature, concentration of oxygen and incubation period. As a consequence, only a few percent of viable bacteria in the sample is cultivable on a given medium and results are generally biased by the method used[73]. The chosen plating technique - spread plate, pour plate or drop plate technique - have as well a great influence and results are not directly comparable even for the same type of sample. In an attempt to create consistency, spread plate and pour plate were standardized in ISO 4833-1:2013[74]. Another crucial factor in reaching *true* estimations of the microbial level is played by the representativeness of sampling and retrieval of microorganisms from surfaces[70]. Direct sampling done via contact plates or swab techniques are the primary methods used to account for all types of surfaces and have been standardized in ISO 18593:2018[75].

While the *contact plate method* comes as a ready to use plating solution with minimal sample preparation and work load, it is recommended strictly for smooth, flat surfaces provided that they have been previously cleaned and sanitized. It consists in a pre-made culture media plate that is pressed against the area of interest for 5 to 10 seconds followed by incubation and colony counting.

The possibility to conduct multiple sampling in short time periods and ease of use are the main advantages of this sampling method. This makes it suitable to validate if surface sanitation has been achieved. 3M™ Petrifilm™ Plates (3M) and dip slides (BIOSAN Laboratories, Inc.) are some of the commercial available solutions that incorporate the contact plate method principle[73].

The swab contact method is done either via stick swabs, see Figure 2.3,when surfaces are less than $100cm^2$ or via sterile cloths or sponges when more than $100cm^2$ is targeted for testing. The pre-moistened swabs can be useful in sampling from porous, irregular surfaces or corners. After wiping thoroughly the area of interest, the stick swab bud is collected in a sterile recipient containing a buffered rinse solution with neutralizers[70]. After extraction of microbial cells in the rinse solution, the resultant liquid can be subsequently plated and used for quantitative or qualitative analysis.
The reproducibility and repeatability of sampling via stick swabs is rather poor since it's mostly subjective to the operator skills, pressure applied and extent of the swabbing pattern which are hard to standardize. Also, in case of organic residues or severely fouled areas, the stick swabs are limited by the sample load. In this case the sponge and sterile cloth are the alternative swabbing techniques that have a higher power of recovery and sampling is slightly more reproducible. This way they may be used not only for cleaning validation but also for testing during production cycles, when the organic load is typically higher. Gloves must be used and sanitized with e.g. 70% alcohol prior holding the sterile sponge or cloths. The swab needs to be moistened in a sterile rinse solution, commonly saline peptone in water 0.9%(v/v), rub over the surface and placed in a sterile plastic bag filled with diluent in which microorganisms are to be released via stomaching.

In spite of the well acknowledged limitations, the conventional methods are still considered the golden standard for bacterial detection and enumeration, due to their inclusion in the legal frameworks. It is indeed true that no perfect methods exists so far, but to some extent this may also be attributed to the fact that any new technology or measurement technique would have to be validate against this reference plating.

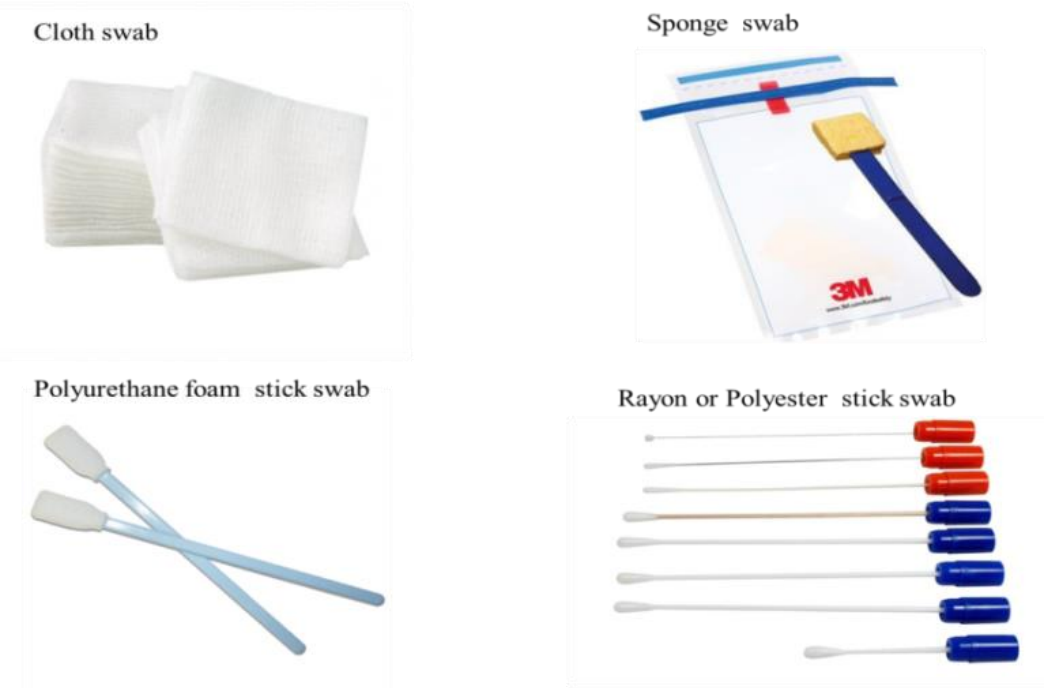

Figure 2.3 Examples of common types of swabs used in food industry for cleaning validation purposes.

2.5.2. Indirect - marker based techniques

ATP based assay-adenosine triphosphate (ATP) is the common molecule found in all living organism. It is indispensable for intracellular energy transfer and cell metabolism. This is attributed to the high energy stored in its phosphate bonds serving as a main source of energy in cell functions with energy release when cutting one of the phosphate bonds. Reversed, when in the presence of luciferase with luciferin as a substrate, ATP may be converted into light and offers a direct measure of the amount of ATP consumed, hence present, in a sample. The ATP bioluminescence method uses a luminometer to measure the low amounts of light produced. Results are acquired fast and are expressed in relative light units[76]. Various commercial solutions like CleanTrace (3M), Hy-Lite (Merck), Lightning (BioControl) and EnSURE (Hygiena) are available and their various sensitivities are the main competing advantage. Different cell types are characterized by different amounts of ATP. Typically one bacterial cell contains 1/1000 of the level present in an eukaryotic animal, plant, yeast or mould cell (approx. 10^{-12} g)[77]. Additionally, ATP levels are also dependent of cell structure, stage of growth or growth temperature.

In the food industry, where it is generally difficult to distinguish between microbial ATP and other sources of non-microbial ATP, the method has been established mainly as a rapid way to assess the *total surface hygiene*, considering that organic matter improperly removed during cleaning may hinder the efficiency of disinfection and contribute instead to faster instalment of microorganisms on surfaces. Similar to plating techniques, the sample collection is again a critical phase due to sampling which is conducted via a stick swab method. Also, one should note that diverse ATP tests,

see Figure 2.4, are not compatible with luminometers from other manufacturers. Hence, for valid results it is important to use the device and reagents from the same manufacturer.

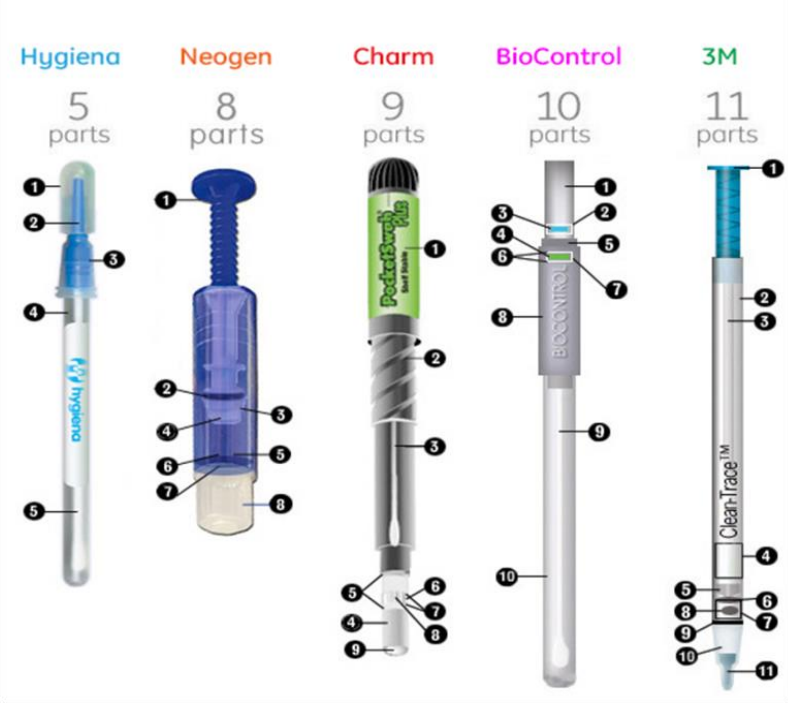

Figure 2.4 Commercial examples of various ATP tests; source: hygiene.com.

2.6. Process analytical technology (PAT)- for cleaning validation and risk assessment

Using the definition given by the FDA in their Guidance for Industry, PAT is "a system for designing, analyzing, and controlling manufacturing through timely measurements (i.e., during processing) of critical quality and performance attributes of raw and in-process materials and processes with the goal of ensuring final product quality"[78]. Ever since the PAT initiative was started by the FDA in 2002, a recommendation primarily for the Pharmaceutical industry, the food industry has also been increasingly embracing the PAT principles. The trend is driven by the complex and dynamic processes that may turn out to be more cost and operational effective if tuned appropriately to the unavoidably variable and complex composition of raw materials or other unforeseen interferences.

The ultimate goal of PAT, especially from a food safety perspective, is very much in line with the scope of HACCP programs. When comparing their particularities, one can notice the compatibility of the two frameworks. In the HACCP systems quality and safety of final products is ensured through monitoring defined process parameters (e.g. temperature, pressure, turbidity, conductivity, pH, etc.) in critical control points (CCPs) and take corrective actions whenever established control limits are exceeded. Complementary, in PAT systems the critical process parameters identified as

linked to a product's quality and safety, are monitored in strategic points, but not necessarily considered CCPs. Additionally, in the PAT case, corrective actions and modulation of the process are implemented continuously (so-called continuous optimization) using measurements that link the evolution of all process parameters with their predicted effect on final product properties. Therefore, the HACCP's risk mitigation strategy is based on creating local hazard gates along the process, and act as a result to their individual responses; non-conformities being registered whenever unexpected input variability is encountered (i.e. seasonal variation of raw material properties). By comparison, the PAT strategy aims to homogenize the variability at such hazard gates through appropriate measurements combined with a holistic analysis that can give better insights over true process dynamics and tune the process parameters in such way that the non-conformities are minimized or reduced to zero even in the context of unforeseen interferences[78].

A typical sequence of steps in designing and optimization of a manufacturing process based on PAT principles includes: 1 a start-up phase in which (critical) material and process attributes related to product quality are identified and measured, 2 the design phase of a process measurement system that accounts for monitoring all critical attributes in real time or near real time (e.g., on-, in-, or at-line), and finally 3 the control phase where process adjustments are designed and implemented to support the control of all critical process and product features. In order to achieve this, a set of PAT tools are required and they may generally be classified into:

- Multivariate tools for design, data acquisition and analysis (Design of Experiments/ DOE, chemometrics)
- Process analyzers (instrumentation, Process Analytical Chemistry)
- Process monitoring and control tools (Multivariate Statistical Process Control / MSPC, Quality-by-Design / QbD)
- Continuous improvement and knowledge management tools (statistical optimization)[78]

Without doubt, process analyzers and multivariate tools represent the engine and the core of PAT. In food processing, the main challenge is on the one hand finding the optimal way to cope with the dynamic of processes towards particular output quality and on the other hand, the continuous change in chemical and physical composition of raw materials and end-products as a result of environmental factors (e.g. humidity, temperature, pH, level of microorganisms, etc.). Thus, following one critical parameter at a time (i.e. flowrate, temperature, pH, dissolved oxygen, conductivity, etc.) as measured by traditional univariate instruments often has limited power in predicting the quality performance of outputs at various manufacturing steps. However, employing multivariate tools that consider in the analysis the cumulative effect of all univariate parameters, patterns specific to particular changes may be identified and help in taking appropriate corrective measures. Obviously, any instrument that can measure the one process parameter linked directly to output's attributes would be superior. But such parameters do not exist in most of the cases and statistical inferences need to be made based on appropriate mathematical modeling of relevant measured variables[79].

The advances in fiber optics, spectrometer technology and computers lead to more sophisticate instruments (primarily chromatography and spectroscopy based techniques) that are capable to measure variables that relate directly to the chemistry, physiology and biological properties of organic and inorganic matter. A large body of research has been focused on finding the application of such instruments when combined with the appropriate data modeling in reaching measurement systems that can capture more of the process signatures and explain better the kinetics involved in food production. This is illustrated in Figure 2.5 from Munir et al. (2015)[80], which depicts that a great deal of PAT related publications focused primarily on the development of commercial solutions for instruments and/or mathematical tools suitable for various issues. However, finalizing the PAT loop and having such solutions integrated in an active and efficient process control at industrial scale is minor. Especially in food industry, where the unavoidable raw material variation, complex physical and chemical matrix combined with high susceptibility for spoilage under various combinations of environmental factors make process monitoring challenging[81].

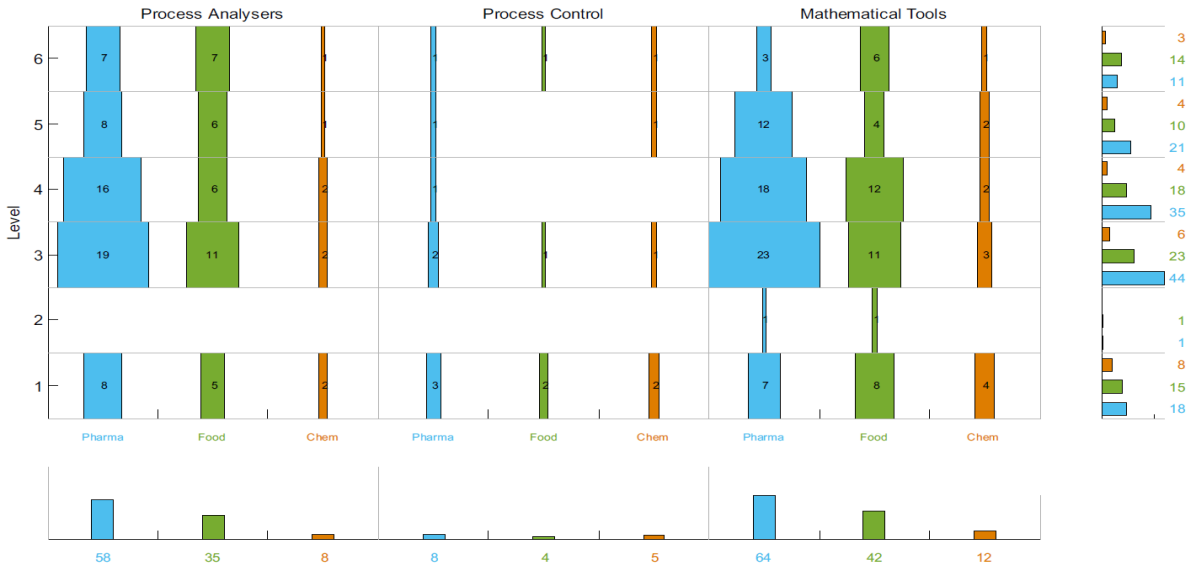

Level	Description	Comment
1	Fundamentals	Article is concerned primarily with the fundamentals
2	Regulatory	Concerned with issues pertaining to rules and regulations such as FDA
3	Commercialization	Concerned with issues when commercializing the strategy or measurement technology
4	Widely adopted	Concerned with the favorite tools for the practitioners and academia from different process industries
5	Review articles	Concerned with critical and constructive analysis of the PAT, literature extending explanation of PAT
6	Mature field	Concerned with successful, well adopted and mature fields of PAT

Figure 2.5 Overview of the extent of PAT research concerning different tools across different industries; source Munir et al. (2015)[80]

Nonetheless, even not used according to their original recommendation for a feed-forward in real time type of situations, PAT tools, in particular the spectroscopic type of analyzers and multivariate data analysis may still come useful in improving the overall performance of food manufacturing processes by:

- Speeding up the validation steps in HACCP systems, through their faster and more comprehensive way of data acquisition and analysis, hence higher promptness in corrective actions.
- Supporting process innovation and sustainability by taking decisions on when to stop or initiate a process as a function of whenever specific quality or process set points are achieved[82].

To illustrate the point, under the HACCP concept cleaning of equipment (for instance filtration membranes), is a recipe–based process with a fixed end-time determined based on previous research and risk-analysis derived data. Briefly, alkaline-acid chemicals (optional enzymatic formulations and sanitizing agents) recirculate in steps within the unit for defined periods of time (or fixed volumes in combination with recirculation time) with clean water flushes in between. During cleaning, parameters like chemical concentration, pH, conductivity and flowrates are measured in order to ensure that conditions according to the established recipe are met. In a subsequent validation step, at the end of cleaning, the hygiene attributes (i.e. aerobic plate count, ATP test) would be measured and if not comprised within control limits, additional cleaning is applied as a corrective action. However, for this particular case, accessing the membrane surface and conduct such tests is impossible unless performing destructive membrane autopsy, hence compromising the system. For that reason the validation step mainly consists in checking if water flux over transmembrane pressure is restored within acceptable limits and performing microbiological test on e.g. the clean water flux as an indirect marker for the equipment cleanliness.

By comparison, in a PAT based process, end-of-cleaning would be the achievement of established parameters related to hygiene. An example is given by Lyndgaard et.al (2014)[83] that describes the use of UV-VIS in reaching a decision when appropriate CIP of whey filtration units has been achieved. In the process of whey filtration, protein fouling caused by absorption and accumulation of whey proteins on membrane surface is one of the main causes for decreased unit performance. Thus, the CIP operations are intended to remove this protein layer, whose extraction rate from surface into the cleaning solution can be monitored by following tryptophan (a UV chromophore present in whey protein) levels in CIP liquids via UV-VIS instrument with the appropriate multivariate tools, in this case exploratory tools such as Principal Component Analysis (PCA). This leads to a monitoring system that captures the protein release trend from membranes, which is more intensive during enzymatic treatment, see Figure 2.6.

One can also notice that flushing steps within enzymatic and peroxide cleaning can be shorten since the system reaches water purity level much earlier than their set end-time. Obviously, such end-points defined within the (fixed) CIP recipe are intended to account for a reasonable compromise that will cover most cleaning dynamics, but using a PAT approach the CIP operations could be adjusted accordingly (optimized continuously) and save the amount of water involved in

the unnecessary extra flush period. The validation step will still be required, but the real-time modulation of the process will generate fewer incidences of non-conformities.

Figure 2.6 also addresses another issue, namely that the (biological) residual fouling present on the membranes is not directly observable, but must be related to the observed cleaning performance/clean water flux and the residual organic load[84] observed during cleaning, both over a longer period of production time including period CIP's. To have a full QbD solution, this residual fouling must be known (or maybe understood) and characterized for the production system under investigation. This (statistical) characterization[85] of the membrane system could be called the Design Space, and is an important part of a full PAT implementation.

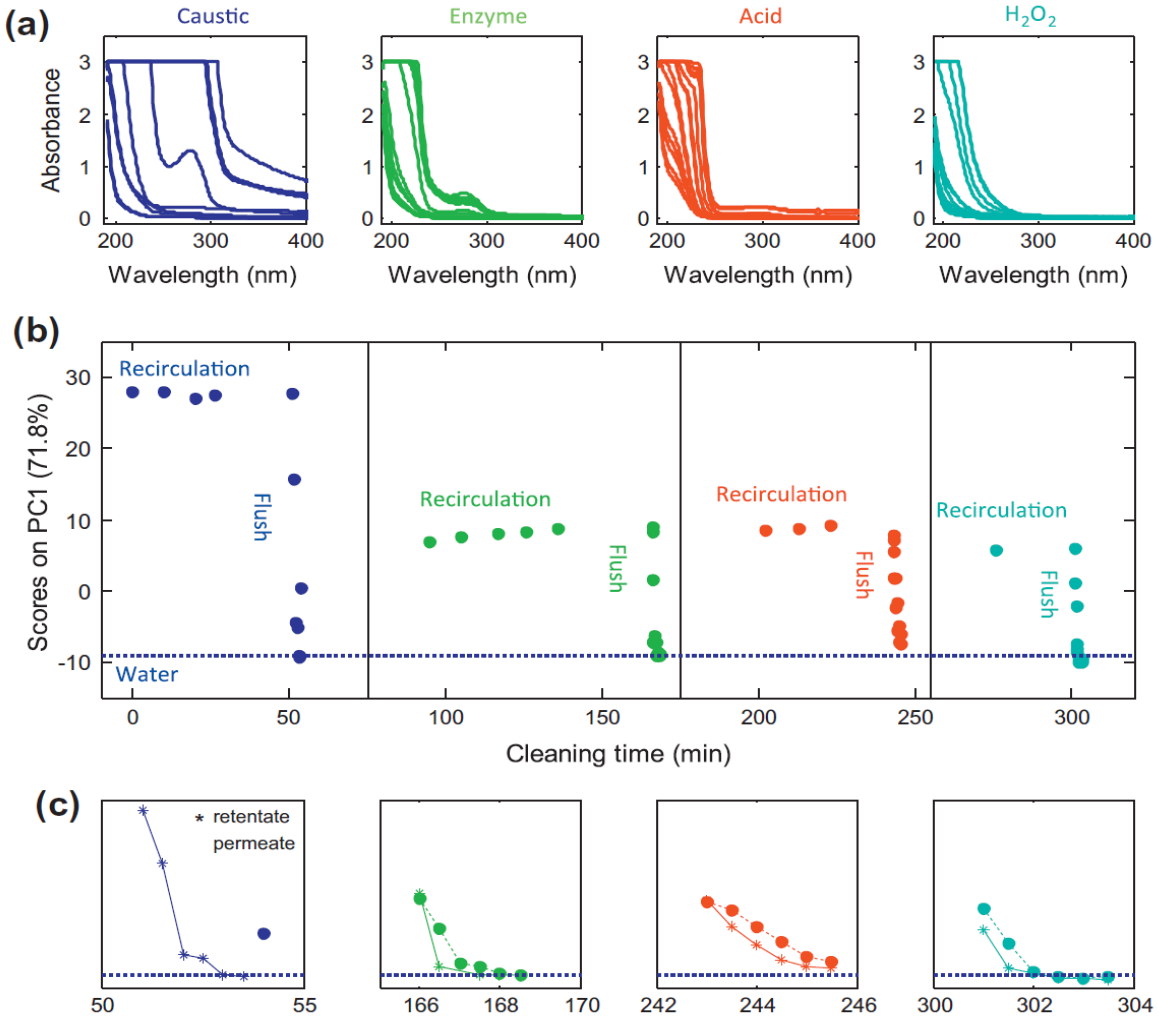

Figure 2.6 Example of a PAT approach for water reduction in CIP process of whey filtration units; source Lyndgaard et al.(2014)[83]

Chapter 3

Fluorescence spectroscopy as tool to support fouling monitoring on conveyor belt surfaces

3.1. Fluorescence spectroscopy principle

Before introducing the investigation presented in Paper I, a brief overview of basic principles of fluorescence spectroscopy is presented, as the technique has been at the basis of data collection. Only main aspects of relevance for the investigations presented here are discussed; for detailed knowledge in the field of fluorescence spectroscopy the reader is referred to Lakowicz (1999)[86].
When interacting with matter, light or radiation from different regions of the electromagnetic field can be absorbed, transmitted or scattered. Under the absorbance phenomena, if the wavelength (energy level) of light matches the required energy for a molecule to reach one of its electronic excitation states, the corresponding photons are absorbed with the remaining part being transmitted and/or scattered. In the case of most molecules, the relaxation from excited state to ground state takes place rapidly as a non-radiative decay. For a limited number of molecules however, such relaxation happens as a radiative-decay, hence with emission of light. This commonly happens through a phenomenon known as fluorescence[87].

Phosphorescence and chemiluminescence are two other luminescence phenomena where emission of light occurs as well. In chemiluminescence the electrons of a molecule are excited upon a chemical reaction, while fluorescence and phosphorescence are similar in the sense that both require the absorption of photons in the UV-VIS range to achieve an excited state[86]. The Jablonski diagram in Figure 3.1, helps in explaining the occurring transition processes and to distinguish between the two phenomenon. Considering the case of molecules that can undergo either fluorescence or phosphorescence, at room temperature such molecules are almost exclusively present in their ground electronic singlet state (S_0) the lowest of the vibrational energy levels, symbolized as 0, 1 and 2. Upon absorption of light and depending on the energy level (wavelength) of the electromagnetic radiation, the molecules can reach one of the excited singlet states, hence transit either from S_0 => S_1 or S_0 => S_2 or even higher; in all cases transitioning to any of the corresponding excited vibrational states. Next, the return to a vibrational level associated with the ground state happens only with release of light (photons) via one of two pathways:

- Most common through *the fluorescence path* that can only occur from S_1 to S_0; the emission rates are fast with a fluorescence lifetime around 10 nanoseconds.

- In special situations when the transition to the ground state is forbidden, the phosphorescence path can alternatively happen from T1 to S0 and requires first a so-called intersystem crossing process to reach the triplet state; in this case the emission rates are slow with phosphorescence lifetimes in the order of milliseconds to seconds[86,88].

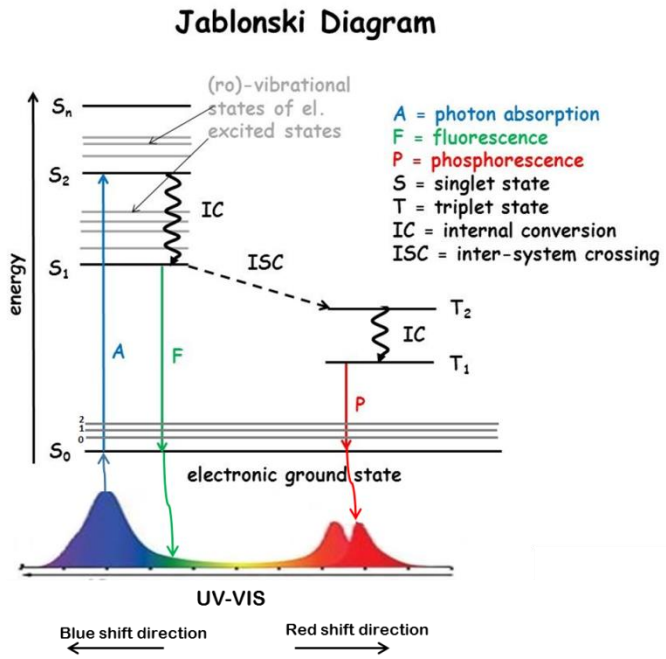

Figure 3.1 The Jablonski diagram; adapted from https://slideplayer.com/slide/9006507/

Important to note is that if present in one of the higher vibrational levels associate with an excited state, the molecule loses its excess of vibrational energy through collision with other molecules. Also, more energy is lost via internal conversion in order to reach the lowest excited state S_1 or T_1. Given such energy losses, if there are no other interferences, the emitted light is always red shifted (towards longer wavelengths = less energy) in relation to the excitation light. The fact that fluorescence only describes the S_1 to S_0 path, which is specific to each molecule, makes fluorescence a selective method and offers the possibility to identify the nature of present molecules in relation to their specific combination of excitation/emission spectrum[88].

Molecules that have the property to fluoresce are called fluorophores and typically contain an aromatic ring or conjugated double bounds. There are synthesized[89] fluorophores designed to bind to specific molecules such as the fluorescence dyes used in Paper II[85] (SYTO™ 9, SYPRO® Ruby Protein Gel Stain and Concanavalin A) or natural occurring fluorophores (intrinsic fluorophores) whose emission is called autofluoresence. This chapter deals primarily with intrinsic fluorophores, since microorganisms are known to contain fluorescence active compounds[90], and their detection may help in reaching a solution to quantify the level of microorganisms on surfaces without

labeling or using other destructive methods. Primary target molecules are the aromatic amino acid tryptophan, the coenzymes NAD(P)H and FAD, porphyrins and ATP[91].

Box 1: Instrumentation and measurement principles

A fluorescence spectrophotometer consists in several components:

- Light source – typically a high-pressure xenon (Xe) arc lamp that has the property to provide continuous light output from 250 to 700 nm, a pulsed xenon lamp or in simplified instruments a single or (small) array of light emitting diodes (LED) may be used to emit light at a specific wavelength.
- Monochromators - are used to disperse the polychromatic light into its individual wavelengths by means of prisms or more often by diffraction gratings. It allows to selected single wavelengths at a time to reach the sample or to scan a wavelength-separated spectrum of the emitted light. An important aspect of monochromators is their property to reject stray light, which essentially is any unwanted light that passes the monochromator and is not due to fluorescence, hence scatter
- Slits - the slit widths can vary and has a role in dictating the light intensity that passes through a monochromator, hence signal-to-noise ratios, but at the same time the selectivity/resolution in the emission and excitation spectrum. A tradeoff between these two aspects – signal-to-noise and resolution – needs to be established.
- Detectors - usually a photomultiplier tube (PMT), where one wavelength at a time is detected, or a charge-coupled devices (CCD), that allows the detection of all wavelengths simultaneously resulting in less recording times and makes the emission filters or mono-chromators to be unnecessary[98].

Depending on the geometry of measurements, two methods can be distinguished,

- *Right angle geometry* - collection is done at a right angle relative to the incident beam; this is suitable for transparent samples (most often liquid samples). In this geometry the stray light is minimal.
- *Front-face arrangement* - collection of light takes place at e.g. a 30° angle relative to the incident beam; suitable for solid samples. If stray light is too high the collection angle can be increased, all the way to a 180° geometry. In such cases, the instrument may be coupled to a fiber optic making it possible to bring the light to and from the sample[88]. Both configurations can be seen in Figure 3.3.

The instrument must obviously fit the type of samples intended to be analyzed. In this thesis, front-face fluorescence is addressed.

Box 1: Instrumentation and measurement principles

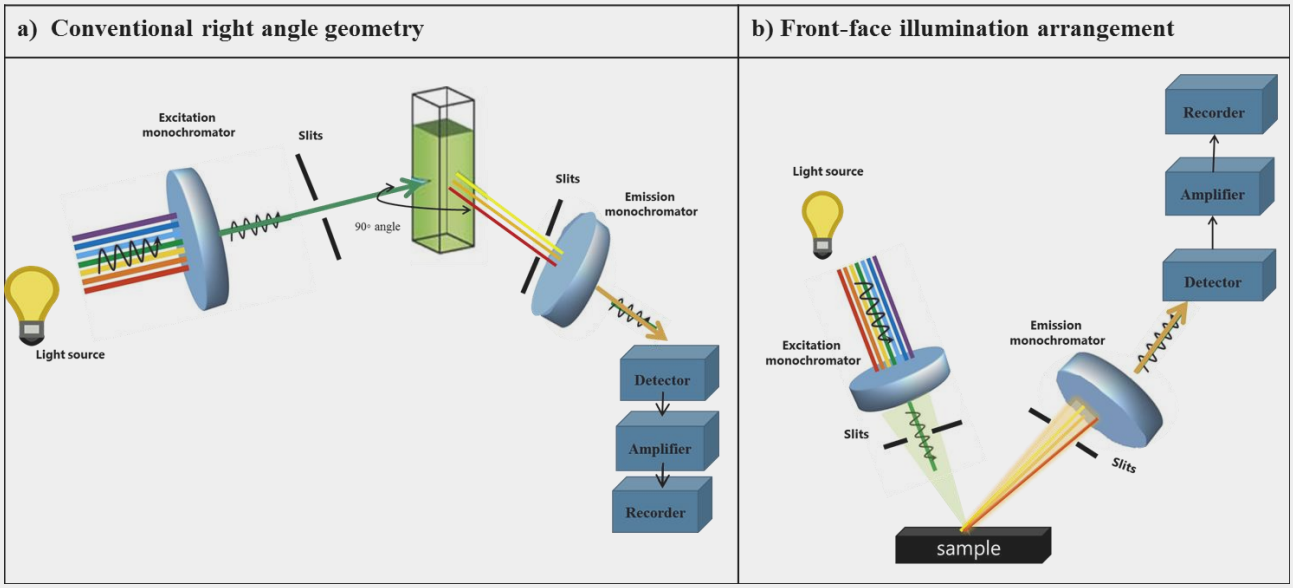

Figure 3.3. Geometric arrangements for steady state spectrophotometer a) conventional right-angle geometry b) front-face illumination arrangement.

3.2.Factors affecting the fluorescence emission

In fluorescence spectroscopy, the measuring systems are based on photon counting, which facilitate low detection ranges and high sensitivity (in the order of ppb-levels) when compared to other spectroscopic methods[86]. The emission spectrum is broad following a Gaussian profile and its intensity at a specific excitation wavelength is linear and direct proportional to the concentration of detected species, following the Lambert-Beers law. However, there are situations when the fluorescence intensity is affected by – often uncontrollable - environmental conditions. As a consequence, the linear relationship with the fluorophore concentration might no longer be valid. These phenomena are collectively called quenching and may happen when:

- *Dynamic quenching* - where due to temperature effects the collision of molecules is enhanced which in turn results in deactivation of the excited-state fluorophores, hence the higher the temperature, less fluorescence intensity is expected.
- *Static quenching* – may happen under the presence of quencher molecules that react with the present fluorophores forming non-fluorescent complexes.
- *Inner filter effect* - may happen due to a concentration effect or mixture with other fluorophores, where the emitted light may be partially absorbed by the fluorophore itself or may match the excitation of another molecule, leading to losses in the detected fluorescence intensity[92].

Besides reductions in intensity, the emission spectrum may also be red shifted (towards higher wavelength) or blue shifted (towards lower wavelength) as a function of pH[93] and solvent polarity[94], causing difficulties in identifying correctly the fluorescing molecules.

3.3. Emission-Excitation maps (EEM)

A common way of presenting the fluorescence spectra is as an emission spectrum that is measured at a specific excitation wavelength, see Figure 3.2a. Such emission spectra are useful in simple systems where the nature of the fluorophores is known, plus no overlapping peaks and minimum or no interferences are expected. However, in complex samples it is preferred to record the emission spectra at different excitation wavelengths, which results in a fluorescence landscape known as excitation-emission matrixes (EEM), see Figure 3.2c. The EEMs have the benefit of capturing more information, which gives an advantage in resolving overlapping peaks, achieve better identification of fluorescing species and estimate their concentrations. Since not all the light arriving at the detector is fluorescence (i.e. light emitted from S_1 to S_0), both the emission spectra and the EEMs need to be cleared of the scattering information before interpretation or analysis[95,96]. The two types of scattering present in EEM are:

- *Rayleigh scatter* – is the elastic type of scatter caused by the solute or fluorophores themselves where light is absorbed and emitted at the same wavelength as the incident light. The Rayleigh signal can be recognized based on its sharp peaks and presence at multiples of the excitation wavelength, hence in an EEM only 1st order Rayleigh (emission wavelength = excitation wavelength) and 2nd order Rayleigh (emission = 2 x excitation) can be observed.
- *Raman scatter* – is the inelastic type of scatter caused by the solute which absorbs light and emits at a lower energy level compared to incident light. The energy loss depends on the nature of solute; the Raman scatter line can be recognized by its constant distance from the 1st order Rayleigh scatter line throughout the EEM[86,97]. Both types of scattering can be noticed in Figure 3.2b.

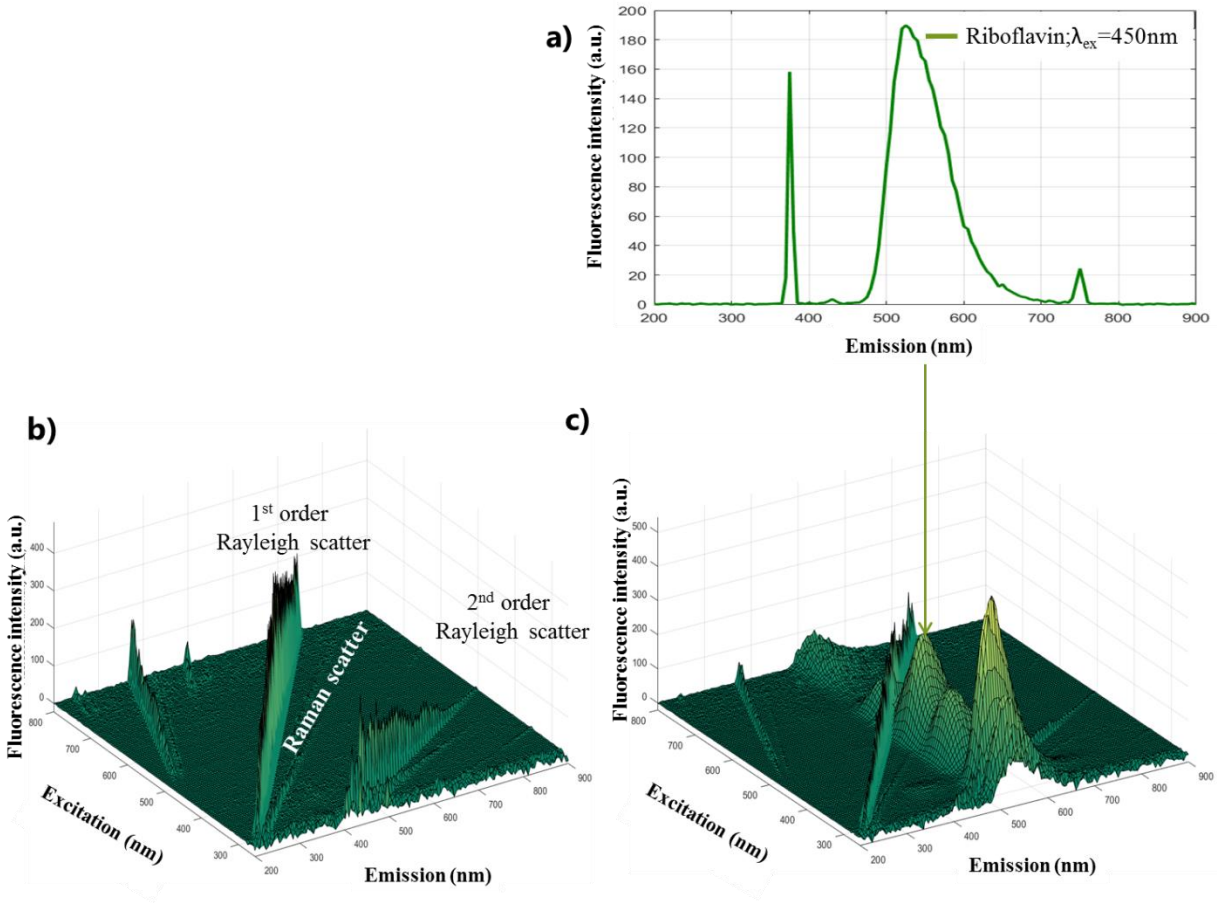

Figure 3.2. Typical fluorescence measurements; a) Emission spectrum of riboflavin solution at single excitation wavelength (450nm), b) Emission-Excitation Map (EEM) of riboflavin solution, c) Rayleigh and Raman scatter in EEM of deionized water.

Box 2: PARAFAC

When recording EEMs at discrete time points during a process or over a set of samples, the stacked 2D fluorescence landscapes result in a three-way (or 3D) array **X** (IxJxK), as shown in Figure 3.4. A suitable way to resolve and extract valuable information from such data cubes is by decomposing the three-way array into its components by means of PARAllel FACtor analysis. The PARAFAC model decomposes the data into a systematic part composed of three loading matrices **A**, **B** and **C** with elements $a_{i,f}$, $b_{j,f}$ and $c_{k,f}$, which are found by minimizing the sum of squares of the residuals or unsystematic part $e_{i,j,k}$:

$$x_{i,j,k} = \sum_{f=1}^{F} a_{i,f} \cdot b_{j,f} \cdot c_{k,f} + e_{i,j,k}$$

where $x_{i,j,k}$ is the intensity of sample number i at emission wavelength j and excitation wavelength k; F represents the number of components extracted (the chemical rank).

Box 2: PARAFAC

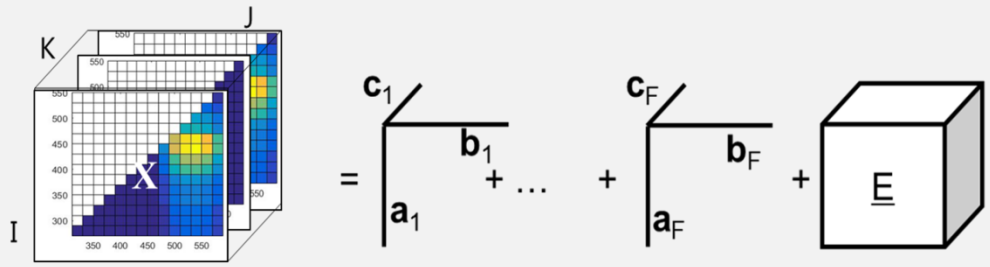

Figure 3.4. Illustration of PARAFAC decomposition

Due to its three-way decomposition nature, PARAFAC is a curve resolution method, meaning that if the right number of components (the correct chemical rank) is selected the PARAFAC solution is unique and the calculated loadings represent the true underlying excitation and emission spectra. Keeping the same dimensionality as the original data in the decomposition method cancels the rotational freedom that the two-way analysis methods (for example PCA) have and leads to the uniqueness feature[99]. This is obviously an advantage when intended to resolve complex mixtures with unknown and emerging fluorescing species, hence without knowing in advance their spectra. Such case is illustrate in Paper I[100] where the underlying fluorescing species of conveyor belt surface are identified together with riboflavin, which in this case is used to demonstrate the situation of an emerging contaminant. The uniqueness feature of PARAFAC attracts also the fact that calibration can be done on limited number of measurements, compared to the exhaustive datasets necessary in the case of two-way analysis methods.

In order to reach a valid PARAFAC solution, data must have a trilinear behavior, the noise should be random and not too severe and the appropriate number of components must be determined. By its nature, fluorescence is a trilinear system[86]; the intensity of absorbed and emitted light (emission as a function of excitation) is directly proportional with the concentration of absorbing species (under the conditions indicated in 3.*2. Factors affecting the fluorescence emission*). Exception from the trilinear behavior is the scattering effects. Therefore, before the PARAFAC analysis, all EEMs are cleared from any influence of scatter by inserting zeros/missing values in regions correspondent to Rayleigh and Raman scatter but also where the emission is below the excitation wavelengths since no information is expected. The most critical issue is deciding on the right number of components. Prior knowledge of expected complexity is always useful, but even under lack of such knowledge, decisions can be made by assessing the residual matrix (check if systematic patterns are still left in the data) and applying the core consistency diagnostic[101].

3.4. State-of-the art and challenges

Considering the potential impact of microorganisms on food spoilage and consumer safety, the development of rapid monitoring systems able to provide information during production and during storage stages is highly desired, but also a fundamental challenge. Such solutions not only will have a positive impact in protecting consumers from pathogenic agents, but they will also help food producers to react promptly, increase their products' shelf-life and reduce number of recalls by ensuring proper food quality. Several fast monitoring techniques have been developed over the years for microorganism detection. Most often these are based on electrical impedance[102,103], ATP based bioluminescence[104,105] , flow cytometry[106], electronic noses[107], PCR based methods[108,109] or vibrational spectroscopy[110–114].

Obviously, sensing the presence of microorganisms in a remote, non-destructive, rapid way would be superior to methods that require certain levels of sample preparation (i.e. typical sample collection via a swab method and extraction of microorganisms into solution followed by a detection technique, accompanied by labeling with fluorescing dyes or nano-particles). Therefore, when addressing the remote, non-destructive way of quantification of microorganisms, spectroscopic based methods are the ones investigated the most, in particular NIR[115,116], IR[117–120] , Raman[121,122] and fluorescence spectroscopy[123,124].

The IR-absorption bands can provide a fingerprint over proteins, lipids, polysaccharides and other functional groups present in microorganisms. With respect to sensing of microorganisms that mostly develop at the surface of food products or of food-contact equipment, the Fourier-transformed infrared attenuated-total-reflectance (FTIR-ATR) is a promising version of IR spectroscopy that focuses its collection of information from the vicinity of a sample's surface as a function of the penetration depth of the evanescent wave (typically only a few μm). Raman spectroscopy which is based on the inelastic scattering of photons, offers complementary information to the IR technique. High resolution spectral signatures can be acquired in relation to the present proteins, nucleic acids, carbohydrates and lipids[125], which have been proven useful in distinguishing between bacterial strains[126]. Compared to IR, water absorption does not represent a drawback in Raman spectroscopy, but the signals are generally weak, with high fluorescence background especially when analyzing biological samples. Surface enhanced Raman spectroscopy (SERS)[127] is one variant of the Raman technique to increase the signal and overcome the fluorescence background. However, this is achieved with the addition of nanoparticles, which requires special, delicate conditions (pH, particle size considerations in relation to bacteria, etc.) and the variation of the local field enhancement usually makes it challenging to achieve quantitative results[128].

Compared to FTIR-ATR and Raman spectroscopy, fluorescence techniques are much more sensitive (reported 100-1000 times more sensitive than other spectroscopic methods[86]). Even though it is based on limited chemical information (only a few active fluorophores compared to the high resolution spectral signatures recorded in Raman and IR spectroscopy), the intrinsic fluorescence is

specific and can be linked to the microbial activity, biomass and cellular components[125]. Also, the instrumentation can be quite simple and robust, and the possibility to acquire measurements fast, remotely and under ambient light are some of the features that make fluorescence spectroscopy suitable for reaching monitoring systems that can function under industrial conditions.
However, the intrinsic fluorophores that the method relies on are not present only in microorganisms but also in the food product. Therefore, discriminating with good accuracy the microbial information from the food matrix is the primary challenge. Extensive studies have been conducted over the years; some of them summarized in Table 3.1 and demonstrate that when combined with the appropriate multivariate techniques the aerobic plate count (APC) levels on different food products can be predicted based on the fluorescence data. Looking through the studies in Table 3.1 it is evident that most studies focus on prediction of APC in particular on meat products and only few address the hygiene status of food-contact equipment/surfaces. One reason for this trend may be due to the high perishable nature of meat, especially beef, which determines a priority for developing methods that can rapidly assess the spoilage level of such products in order to prevent any potential incidents of foodborne illnesses associated with spoiled food consumption.

Under the main mechanisms of meat spoilage that may occur as lipid oxidation, enzyme reactions and microbial growth, the chemical composition of meat products will change. Meat spoilage is typically a result of microbial development, which results in development of off-odors, off-flavor and slime formation[129]. Hence, having a spectral fingerprint of the specific meat products in relation to their freshness status and periodic monitoring during its spoilage process, such structural changes can be captured in the wealth of information acquired by either IR, Raman or fluorescence techniques; sensitivity making the difference between methods. With the appropriate multivariate tools (most often PLS) the link between observed changes with the reference aerobic plate count can be established. The estimation of APC levels can therefore be achieved indirectly as a response to the changes of meat composition that microorganisms may induce. While the working principle can be proved under lab conditions, the main challenge in reaching robust commercial solutions is that the models are not transferable; extensive calibrations must be done in relation to each type of meat (beef, chicken, pork, fish) and different muscle types (plain muscle fibers with or without presence of fat and connective tissues) in order to define the appropriate baselines generally valid for real-life situations.

When extending the same measuring principle to equipment food-contact surfaces for their APC evaluation, the issue is even more challenging. Detection of microorganisms would have to be based preferably on the direct detection of a microbial fingerprint, since the equipment surface will not change its chemical properties as a function of bacterial growth, unless extreme. The two situations when surfaces might require hygiene assessment are *after cleaning operations* and – preferably - *continuously during production.*
Determining the hygiene status of surfaces after cleaning mostly summarizes to answer the question: Is there anything left on the surface? This is typically answered via ATP assays. Having a

good picture of what the clean surface should look like, then detecting with high accuracy any product residuals and microorganisms depends on the capabilities of selected technique. However, even in this situation several sources of error and challenges may appear, in particular due to the fact that surfaces are not always homogenous (i.e. the sample collection for ATP swab methods will be negatively affected by wear-and- tear). Additionally, surfaces may have their own signal with certain level of interference (background interference) in relation to the chosen measurement technique. These aspects make quantification of residual fouling/biofouling on equipment surfaces a difficult task. Most studies conducted on surface hygiene with a goal of rapid remote sensing are only qualitative indicating the presence/absence and distribution of contaminants.
The other case, setting up a real-time measuring system while production is running, has obvious benefits (real-time reaction to hazards, fine tuning cleaning operations in relation to actual hygiene necessities etc.). But isolating a bacterial fingerprint from a high and variable interference caused by the food matrix is another issue that comes on top of the challenges related to surface physical properties and potential strong background information.

From Table 3.1, it is apparent that most studies do not take benefit of the full dimensionality of fluorescence landscapes. In the majority of cases, recordings are done at a single excitation wavelength characteristic for a specific fluorophore (results in a two-way data array), or when the full fluorescence landscape is recorded the three-way fluorescence data is unfolded and reduced to a two-way array that fits the two-way modeling methods such as PCA[130] and PLS[131] (first order calibration). The weakness of using a first-order calibration (based on two-way array data) is that any interference with the analyte signal would have to be identified and modeled in the calibration, which comes at the cost of large sets of calibration samples in order to have a good estimate of their effect. This may be suitable for the case of evaluating the freshness level of meat products, assuming that under controlled storage conditions the only interference that may occur is due to bacterial spoilage. Consequently, having their effect included and modeled in the calibration data, the estimation of true spoilage level can be determined in new samples. However, such first-order calibrations lack in their power to give the true estimate of analyte signal when new/unknown interferences occur (which have not been included in the calibration model) as it may result for instance due to different backgrounds from variable sources (such as surface wear-and-tear induced by processing operations or variable background interference from e.g. short-term or permanent color changes caused by the food matrix). Second-order or trilinear calibration (PARAFAC based models) can on the other hand compensate for both new and modeled interferences. In such cases the calibration can be based on a limited number of samples since by keeping the original dimension of data (three-way structure), a true signal would be identified using the simultaneous response in relation to two vectors this time (i.e. excitation and emission in the case of fluorescence; Box 2), which can be decomposed also in the presence of interference, reducing ambiguities. Such trilinear calibrations have higher power to resolve overlapping peaks and filtering out any new interference not included in the calibration set.

Based on the different considerations mentioned above, one of the aims of this thesis was to explore the full properties of emission-excitation matrices by employing trilinear calibration and test the fitness of such approach for its power to estimate the microbial level on conveyor belt surfaces. Conveyor belts are *equipment* found throughout slaughterhouses and represented the test surface for this investigation. While the construction material of such conveyor belts (in this case polyacetal, POM) has its own auto-fluorescence signature and strongly interfering with most fluorophores of interest it was noticed that its signal would also vary as a function of different levels of wear-and-tear. Therefore, as a first step in Paper I a statistical approach to minimize the strong interference of conveyor background information is presented and used to demonstrate its ability to detect emerging contaminants under on-line monitoring conditions.

Table 3.1 Literature overview of application of fluorescence spectroscopy for detection of microorganisms.

Type of surface	Purpose/results	Type of fluorophores	Multivariate tools	Reference
Bacterial suspensions	Discrimination between 25 different strains of bacteria based on their pure dilute suspensions	Ex. 250 nm (aromatic amino acids+nucleic acids) Ex.270 nm (tryptophan residues) Ex.316 nm (NADH)	PCA Hierarchical clustering	Leblanc& Dufour (2002)[89]
Minced beef	Portable fluorescence spectrometer was tested to quantify minced beef spoilage stored aerobically and under vacuum at 5 and 15 °C.	Different excitation LEDs (280, 320, and 380 nm).	PLS-R models	Aït-Kaddour et al. (2011)[131]
Chicken breast fillet	Determining of microbial load on chicken breast fillets stored aerobically at 5 °C for 8 days, and 15 °C for 5 days.	Synchronous fluorescence spectra were collected in the 250–550 nm excitation wavelength range using offsets of 20, 40, 60, 80, 100, 120, 140, 160 and 180 nm between excitation and emission monochromators.	PARAFAC N-PLS	A. Sahar et al. (2011) [132]
Pipe systems	Monitoring biofilm growth and microbial activity on pipe surface in a pilot plant set-up by OPTIQUAD sensor system	Tryptophan Ex.290nm/ Em.340nm (presence of bacteria) NADH Ex.340/Em. 460 nm (for microbial activity)	Fluorescence intensity regressed against APC.	M. Strathmann et al.(2013) [133]
Water	Continuous real-time detection of microbial contamination in water (based on lab trials)	10 LEDs-4 amber, 4 red and 2 UV (reduced pyridine nucleotides (RPNs), flavins and cytochromes to distinguish live cells; cytochromes for dead cells; calcium dipicolinic acid (DPA) for spores. UV (Ex 365 nm/Em 440 nm) ; amber (Ex 590 nm/Em 675 nm) ; red (Ex 635 nm/Em 770 nm)	the detection limit for viable bacteria ~50 cells/L. Fluorescence intensity regressed against APC.	A.P. Kilungo et al.(2013) [134]
High-density polyethylene (HDPE) cutting boards and stainless steel (SS)	Assess surface cleaning efficiency by detection of produce residues. The system can be used to detect wear on HDPE surfaces as well as the presence of produce residues	Ex. 405 nm by four 10-watt,, LEDs Em. 475nm, 520nm, 570nm, and 675 nm.	Fluorescence imaging	A.M. Lefcourt et al.(2013) [135]
Wheat flour and beef surface	Detection of mycotoxin in wheat flour and prediction of APC on beef surface stored for 2 days at 15°C	tryptophan (Ex) 290 nm/ (Em) 330& 660 nm), NAD(P)H (Ex 320 nm / Em 460 nm), Porphyrins (Ex 430 nm / Em 600 nm), and Flavins (Ex 460 nm / Em 520 nm).	PLSR on unfolded data	J.Sugiyama et al. (2013) [90]
Fish fillets	Determine the freshness of fish fillets when stored at 4°C for 12 days in presence of light and vacuum packaging	tryptophan (Ex) 290 nm/ (Em) 305-450 nm), NADH (Ex 340 nm / Em 360-660 nm),	PCA and PLS-DA	A. Hassoun & R. Karoui (2015) [136]
Deli slicer	Detection of residues from cheese and meat slicers after cleaning and sanitation	Hyperspectral imaging based on fluorescence recorded at 475, 520, and 675 nm excitation		E.A. Beck et al.(2015) [137]
Pork and lamb meat	Pork and lamb meat stored at 5 °C for up to 20 days	NADH Ex.340/ Em. 460nm; protoporphyrin (PPIX)& zinc protoporphyrin (ZnPP) Ex.420nm/ Em.592nm & 636nm & 705nm	Fluorescence intensity regressed against APC.Better correlations for protoporphyrin (PPIX)& zinc protoporphyrin	J. Durek et al. (2016) [138]
Pork loin surface	Aerobic plate count(APC) prediction when meat samples stored for 3 days below 15°C	Tryptophan (Ex.295nm/Em.335 nm) ; NADPH (Ex.335 nm/Em.450 nm); ATP	PLSR on unfolded data; second derivative	N. Oto et al.(2013) [139]; H. Shirai et al. (2014) [140]; H. Shirai et al. (2016) [141]
Beef surface	Aerobic plate count prediction on beef slices stored for 3 days at 15°C	Tryptophan, NAD(P)H, Vitamin A, porphyrins, and flavins	PLSR on unfolded data; normalization	M. Yoshimura et al.(2014) [142]; D. Mita Mala et al. (2016) [123];
High-density polyethylene (HDPE) and food grade stainless steel (SS)	Hand-held fluorescence imaging device was assessed for detection of three types of food residues that have been associated with foodborne illness outbreaks, i.e. spinach leaf, milk, and bovine red meat, on two commonly used processing surfaces	Four 405 nm 10 W LEDs with interchangeable optical filters (470, 515, 640 and 680 nm with 10 nm bandwidths and CCD camera with high quantum efficiency in the spectral range 400-700 nm	Fluorescence imaging	C.D. Everard et al. (2016) [143]

Paper I

A statistical strategy to assess cleaning level of surfaces using fluorescence spectroscopy and Wilks' ratio

Iuliana Madalina Stoica , Hamid Babamoradi, Frans van den Berg

Chemometrics and Intelligent Laboratory Systems 165 (2017) 11–21

Chemometrics and Intelligent Laboratory Systems 165 (2017) 11–21

Contents lists available at ScienceDirect

Chemometrics and Intelligent Laboratory Systems

journal homepage: www.elsevier.com/locate/chemometrics

A statistical strategy to assess cleaning level of surfaces using fluorescence spectroscopy and Wilks' ratio

Iuliana Madalina Stoica[a,*], Hamid Babamoradi[b], Frans van den Berg[a]

[a] Chemometrics and Analytical Technology section, Department of Food Science, Faculty of Science, University of Copenhagen, Rolighedsvej 26, DK-1958 Frederiksberg C, Denmark

[b] Surface Engineering, Department of Micro- and Nanotechnology, Technical University of Denmark, Produktionstorvet, 2800, Kgs. Lyngby, Denmark

ARTICLE INFO

Keywords:
Biofouling
Fluorescence
Wilks' ratio statistics
Conveyor belts
Process monitoring
PARAFAC

ABSTRACT

There is a high demand for techniques able to monitor on-line, in real-time, the bio-contamination level of contact surfaces in the food industry. Such techniques could help to react promptly whenever failures in the cleaning or sanitation operations occur, keep the safety parameters in control at any time during production, and ultimately tailor the operations towards more sustainable and efficient practices. However, monitoring surface areas such as conveyor belts comes with a distinct set of challenges from the construction materials used in food processing equipment such as compositional-heterogeneity, background signals and continuous changes due to wear and tear. In this work we demonstrate the potential of front-face fluorescence spectroscopy in combination with Wilks' ratio statistics for monitoring large surface areas fouled under industrial working conditions. The technique was tested in both off-line and on-line mode, for a polymer-based conveyor surface, which presents an intrinsic natural variation across its running length and which was contaminated artificially for a proof of principle. Results show that any potential contamination will shift the variance and covariance structure of the in-control fluorescence landscapes modeled with PARAFAC, and detected this shift as a deviation from the reference clean state in a Wilks' ratio based monitoring charts.

1. Introduction

Biofilm formation is a practice that microorganisms adopt in order to withstand harsh environmental conditions, conditions which would be fatal if undertaking a bachelor type of life [1]. Consequently, by modulating their own phenotype in response to the physiological stress, induced on e.g. the equipment surfaces under food production conditions, and creating synergies [2], bacteria and yeasts succeed to survive and develop in microbial communities by encapsulating themselves in a self-produced extracellular polymeric matrix (EPS) [3]. The available knowledge on biofilm points out that the EPS matrix has two purposes [4]. First, it serves as an adherent to the various types of surfaces and second, the EPS matrix acts as a protection shield against surfactants and disinfectants [5]. This self-defense mechanism adds a challenge for cleaning and sanitation operations in the food industry. Therefore, cleaning procedures within food production facilities must be designed towards an optimal fouling removal to minimize the risk of building-up in hot-spot contamination points which could be detrimental for food security.

Conveyor belts, for instance, represent an important food contact surface in meat related industries. They may easily become a vehicle for bacterial contamination and impact directly the quality of meat and ready-to-eat products due to the direct contact [6]. Previous research has shown that both spoilage bacteria such as Listeria monocytogenes [7] and Pseudomonas spp. and more dangerously, pathogenic bacteria such as E.coli O157:H7 [8] and Salmonella serovars [9] may survive the common hygiene operations of conveyors under the biofilm *umbrella*. Through the prerequisites of HACCP plans, the conveyor belts must be designed and made of materials that favor less bacterial attachment. In spite of this precaution, studies have shown that biofilm is still prone to develop on the different types of widely used materials for conveyor belts [10]. The phenomenon is mainly assigned to the remarkable property of bacteria to change their physiology in relation to the environmental conditions, to the unique production of EPS and strengthen by inefficiencies or failures in cleaning [11]. This suggests that biofilms will always be present to some degree in different levels of maturity across the entire food production chain. Therefore, tools or monitoring devices aimed at detecting whenever cleaning and disinfection procedures failed represent one important element in a holistic approach to avoid irreversible instalment of biofilms.

To the best of author's knowledge, not many industrial applications are available to assess on-line or *real-time* the cleaning status of large

* Corresponding author.

http://dx.doi.org/10.1016/j.chemolab.2017.03.014
Received 13 January 2017; Received in revised form 1 March 2017; Accepted 31 March 2017
Available online 05 April 2017

surfaces such as conveyor belts. The conventional ATP (adenosine triphosphate) swab-test might fail in giving an appropriate picture of the true contamination level since most likely the exo-polymeric matrix shielding the bacteria will hinder the reaction between the firefly enzyme luciferase and the ATP of living microorganisms. Additionally, swab-testing is by definition a manual operation that can only be performed on an intermittent basis. Never the less, ATP swab-tests are the main analysis used to evaluate cleaning level of surfaces. Despite its easy to use, the ATP swabbing method is not cost effective or suitable to inspect large areas like conveyor belts [12]. At present, the normal plating methods are the most reliable, but they require one to several days before a result is obtained, which is too long in most food processing applications. Additionally, the plating method suffers from the same shortcoming as ATP rapid testing, namely selective swab sampling of a relatively small area.

Fluorescence spectroscopy is a technique which can map relatively large surfaces in a short time and has the potential of detecting on-line and remotely bio-contamination or organic residues, based on the auto-fluorescence signatures of molecules such as proteins, vitamins and co-enzymes of microorganisms and food products. For a detailed explanation of fluorescence principle, the reader may refer to Lakowicz [13]. Scanning simultaneously through both excitation and emission, information about multiple fluorophores and their interaction with the surrounding environment can be captured in one single measurement. In complex systems, such as detection of biofilms on food related surfaces, the signal of different fluorophores may strongly overlap and/or the chemical information may be at low intensities compared with the strong signal originating from the background. Pu et al. [14] addressed the problem of distinguishing multiple overlapping signals by a *peak picking* method, using emission profiles recorded at one single relevant excitation wavelength. They recover the contributions of each fluorophore by means of multivariate curve resolution. The same principle of scanning only through emission wavelengths at selected excitation wavelengths was applied by Aït-Kaddour et al. [15] for a portable spectrofluorometric device to predict the bacterial load of minced beef by the partial least square regression algorithm (PLS-R). Shirai et al. [16] showed that by applying a two dimensional second-order Savitzky-Golay to a fluorescence excitation-emission map (EEM), overlapping peaks could be distinguished. The resolved EEM maps could then be used to predict by PLS-R the ATP content on a meat surface, as implemented also by Oto et al. [17]. Not many studies address the hygiene level of surfaces with spectroscopic background interference. Both Wiederoder et al. [18] and Everard et al. [19] showed how a hyperspectral fluorescence imaging system can be used to tune the cleaning practices on HDPE (high density polyethylene) conveyor belts. When the surface was subjected to a violet LED, potential organic residue was easily observed based on the fluorescence response at discrete wavelengths. Following the same principle of hyperspectral fluorescence imaging, but this time combined with an algorithm using the ratio between two-bands, Jun et al. [20] were able to distinguish the Escherichia coli O157:H7 and Salmonella biofilm on a similar type of HDPE conveyor belts.

Many of the mentioned studies in on-line, real-time bio-contamination detection are of an academic nature. One of the factors that might limit the success of the discussed applications in an industrial surrounding is the difficulty to distinguish between the low-intensity chemical or biological signal and a high background response. The auto-fluorescence characteristics of the polymer construction materials used could lead to false alarms due to the heterogeneous signal over the conveyor belt area and overlap with the auto-fluorescence originating from fouling. Segmented conveyor types can show considerable variation in age plus *wear and tear*, and e.g. cleaning-in-place (CIP) procedures involving mechanical and chemical stress can change the spectroscopic response considerably on both the short (in between shifts) and long (over a lifespan) terms. Generally, monitoring the surface of equipment is a challenging task. The initial topology of the surface may change during the production processes - i.e. processing meat on conveyors for an extended running time - which deprives most classical monitoring methods of their success in assessing on-line, real-time surface safety. Consequently, there is a need for strategies which can adapt periodically to the physical changes of the surface to be monitored. We present here an approach based on advanced chemometric methods which can potentially tackle this problem and lead to the design of on-line monitoring instruments for bacterial development under working conditions. More precise, we describe the theoretical bases of a statistical decision algorithm based on Wilks' ratio statistic for multivariate measurements from fluorescence landscapes extracted by PARAFAC modelling to assess the contamination level on a conveyor belt surface. For illustration, the principle of the statistical decisional algorithm will be explained on an artificial data set containing only one chemical compound (riboflavin) used to *spike* a conveyor material in order to simulate the scenario of surface fouling. Riboflavin (aka. vitamin B2) was chosen as a model fluorophore, primarily based on its spectral overlap with the conveyor's belt auto-fluorescence, ease of handling in a food-grade environment and its acceptable quantum yield. Taking into account that bio-contamination will be generally characterized by weak and overlapping spectral signatures with the background information, we considered riboflavin a representative model compound to illustrate the capability of our proposed statistical algorithm to target the occurrence of weak information in relation to a strong and inhomogeneous background. The end goal of our research will be to define an optimized fluorescence recording technique suitable for on-line mode. As a first step, the focus of this work is to demonstrate the fitness of the statistical model in combination with fluorescence spectroscopy while its implementation for a real bio-fouling scenario will be investigated in future work.

2. Methods and materials

2.1. Fluorescence spectroscopy

Fluorescence emission-excitation maps (EEMs) were non-invasively recorded using a non-contact fiber probe mounted approximately 5 mm above the conveyor surface, resulting in a circular measurement spot roughly 10 mm in radius. The instrument used was a BioView (Delta Light & Optics, Hørsholm, Denmark) process spectrometer, which uses a pulsed xenon lamp in combination with filters as excitation source (270 to 550 nm, 20 nm intervals), while emission wavelengths are selected by a second filter wheel (310 to 590 nm, 20 nm intervals). One recording will result in one EEM map of 15 excitation and 15 emission wavelengths, which corresponds to $15 \cdot (15+1)/2 = 120$ permitted excitation-emission pairs [13], taking 2.5 min per measurement (gain 1200, 10 scans averaged). The most attractive feature of the BioView sensor is its process-ready design suitable for industrial applications. However, the sensor comes with a standard optical set-up characterized by low resolution (20 nm), which results in recordings with low information contents. Some examples of EEMs are shown in Fig. 1.

2.2. Off-line EEM recording

A two-fold dilution series of riboflavin in water at ten levels was prepared, ranging from $50 \cdot 10^{-3}$ mM down to $0.19 \cdot 10^{-3}$ mM. Plastic rings were glued across the length of a used (and visibly damaged) polyacetal conveyor belt element, in order to create wells for the purpose of depositing a thin film layer of the riboflavin dilutions. First, in each of the created wells (8 in total), a volume of 2 ml tap water was added and EEMs were recorded, with four replicate measurements done within each well. This resulted in a total of 8 wells times 4 replicates giving 32 *blank* EEMs over the entire conveyor element. The cleaned element - having water deposited - is intended to mimic a production line start right after cleaning. Next, in order to include representative variation of the background, for every riboflavin dilution, volumes of

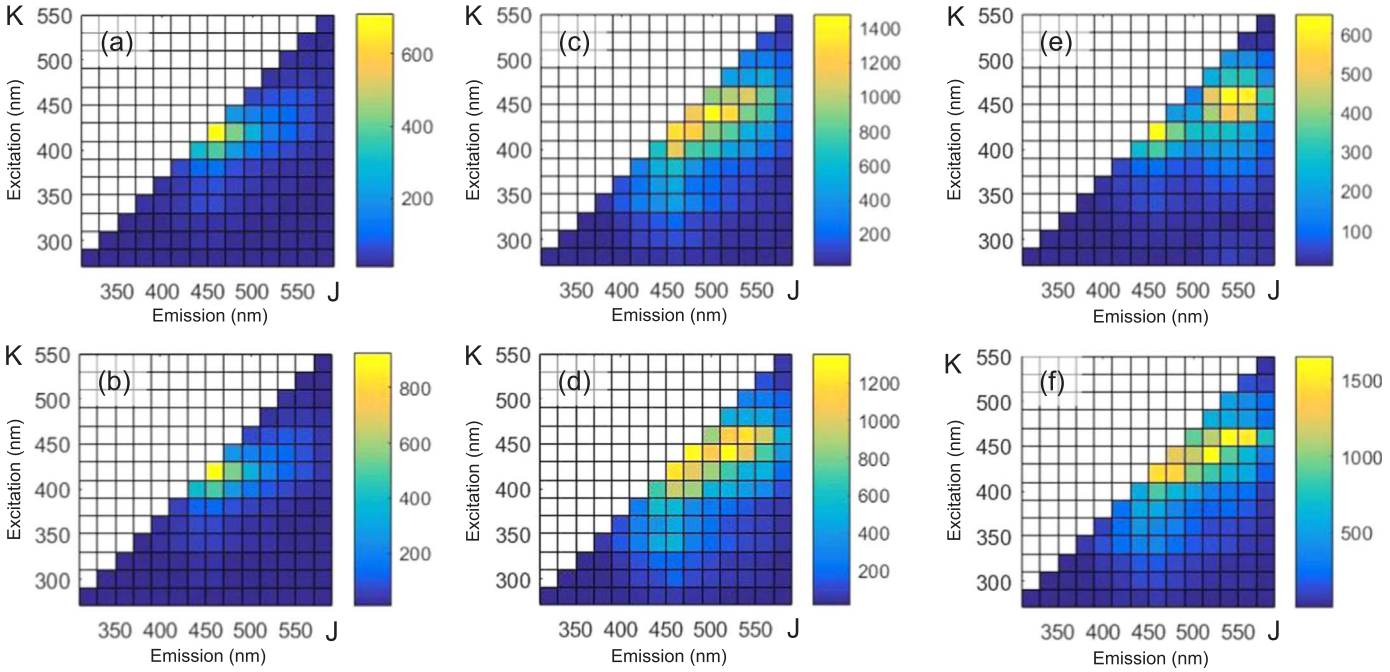

Fig. 1. (a), (b) Off-line recorded EEMs of wet conveyor surface at two random positions; (c), (d) on-line recorded EEMs of cleaned conveyor surface at two random positions; (e) off-line recorded EEM of conveyor spiked with $6.2{\cdot}10^{-3}$ mM riboflavin; (f) on-line recorded EEM of conveyor spiked with $50{\cdot}10^{-3}$ mM riboflavin. Note different intensities in photon counts.

2 ml solution were deposited in four random wells and EEMs recorded for each of them (10 dilutions times 4 random wells equals 40 riboflavin EEMs). Washing with soap and intensive rinsing with tap water was done before a new dilution level was measured.

2.3. Multiway data analysis

Parallel factor decomposition (PARAFAC) is a multidimensional decomposition method suitable to extract the unique underlying fluorescence structure contained in three-way fluorescence EEMs organized in a data cube $\underline{\mathbf{X}}$ [21]. PARAFAC decomposes data into F trilinear distinct factors, which estimate the systematic part of the measurements by spectral and concentration loadings (Eq. (1); Fig. 2a).

$$x_{i,j,k} = \sum_{f=1}^{F} a_{i,f} \bullet b_{j,f} \bullet c_{k,f} + e_{i,j,k} \quad (1)$$

Interpretation of the PARAFAC factors as EEMs is assisted by the uniqueness property of tensor algebra [21]. A strong identification of the chemistry is provided via the outer-product of the excitation and emission, namely the spectral loadings vectors $\mathbf{b}_f$ and $\mathbf{c}_f$ (Fig. 2a), while the first loading vector in the sample direction $\mathbf{a}_f$ – usually called sample scores – provides a direct quantification of the relative amount chemical f was present for each particular sample i. During model building the number of factors F must be determined; the sample score $a_{i,f}$ (and residual matrix or landscape $\mathbf{E}_i$) for each new measurements can be estimated by a projection on the F spectral loading vectors [21]. All data analysis was performed using Matlab version R2015b using the PLS Toolbox (Version 8.1.1) and in-house routines.

2.4. Strategy for process monitoring of surface fouling

Given a multivariate system whose variation depends on several varying and co-varying parameters, Wilks' ratio statistics is one method to detect if a set of new samples have potentially moved the process from its *normal variation*. Our basic monitoring strategy is: given a training data set collected on a clean/recently cleaned surface, the model space determined by the scores $\mathbf{a}_f$ from Eq. (1) and Wilks' ratio statistics, can we distinguish future clean or normal surface measurements from fouled surface measurements? This strategy is characterized by two steps: in the first step (called Phase I) we calibrate the models using normal, *blank* or *null* data – including the considerable variability that will be present over a larger conveyor surface, see Fig. 1a-d – and thus not towards any specific contaminant. Here we must guarantee that the normal variation over the conveyor surface is statistically represented in the Phase I calibration set. In the second step (called Phase II) we project new samples on the normal variability space only. Here, any deviation from normal surface measurements should be detected and flagged as potential surface fouling. This *not-normal*-detection concept has the advantage that it might function with a calibration set of limited size used during Phase I. This calibration set can e.g. be collected each time right after a conveyor system has been cleaned, under the assumption that after CIP the system will be in the desired (clean) state. This is a very attractive feature when the measurement system is prone to change as is e.g. the case for conveyors due to wear and tear, the harsh chemicals and physical treatment during CIP, or repositioning the spectrometer after a CIP cycle where the exact same location cannot always be guaranteed. The change we want to monitor/detect in Phase II must break the covariance structure of the calibration set. As multivariate monitoring tactic we use Wilks' ratio statistic using the framework detailed in Appendix A.

2.5. On-line EEM recording

In a pilot plant facility (Danish Meat Research Institute, Taastrup, Denmark), on-line, real-time detection of an ongoing fouling, on a conveyor belt, under normal operating conditions was simulated by wetting progressively different areas of an initially clean system. Over the entire simulation run the fluorescence probe was mounted in a horizontal front-face orientation at one end/bend of the conveyor (at 5mm distance) and set to measure continuously while the conveyor passed the probe. At the beginning of the experiment, 23 blank EEMs were recorded on the surface of conveyor belt, just as it was found after cleaning-in-place overnight. In the second experimental phase three distinct molar concentrations of riboflavin solutions ($25{\cdot}10^{-3}$, $37.5{\cdot}10^{-3}$ and $50{\cdot}10^{-3}$ mM) were then used to gradually contaminate the conveyor belt while recording the area. The contamination in itself

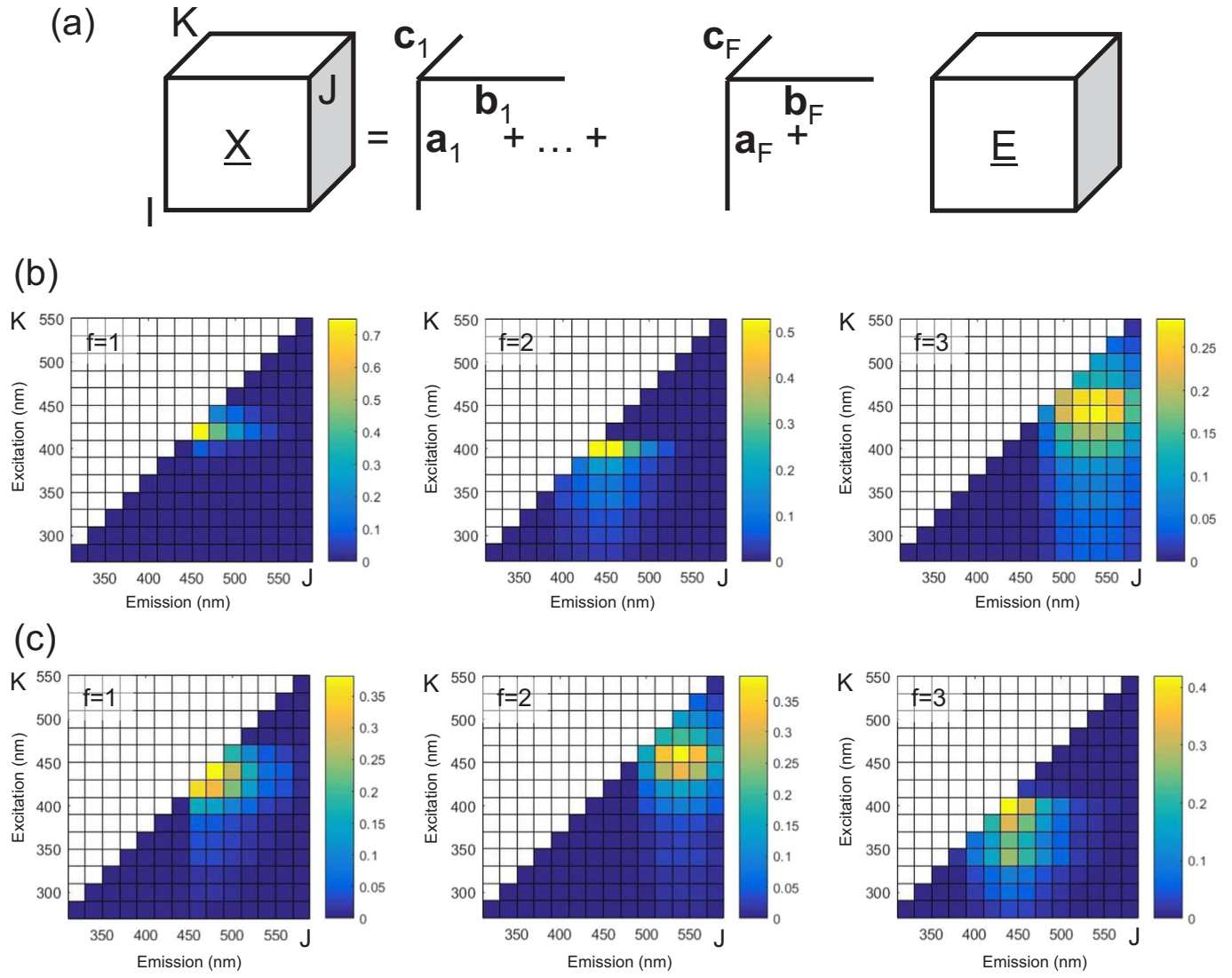

Fig. 2. (a) Graphical representation of the PARAFAC algorithm used to decompose EEM landscapes; (b) outer-products of spectral loading vectors $\mathbf{b}_f$ and $\mathbf{c}_f$ in off-line mode after PARAFAC modelling (n = 32); (c) outer-products of spectral loadings in on-line mode after PARAFAC modelling (n = 23).

was performed by soaking a tissue in the respective solution and subsequently using it to wet the conveyor belt in a specific area – more precisely a band of approximately 10 cm wide over the entire length of the conveyor - where the recording was performed. The exact procedure was as it follows: the contamination was initiated with placing on a randomly selected monitored area of the conveyor belt a thin layer of the lowest concentration of riboflavin ($25{\cdot}10^{-3}$ mM) and allowing 5 EEMs to be recorded. Then, without any interruption of the process, a new area of the conveyor belt was contaminated with the same $25{\cdot}10^{-3}$ mM riboflavin solution, and 5 other new EEMs were recorded. This way each stock solution was applied three times in distinct areas of the conveyor belt and every 15 EEMs the concentration of it was increased. Contaminating in this fashion way was considered to be more proper rather than spraying the solution. This way a homogenous layer could be achieved, resembling to the film-like fouling seen on meat processing equipment.

It should be noted here that the exact total concentration of riboflavin present on the conveyor belt surface is unknown given how the fouling simulation was carried out. However, it is evident that the information contained in steps of 5 EEM landscapes should reflect a general increase over time. The conveyor belt was again composed of visibly damaged polyacetal elements, arranged in a loop with a total length of 4.3 m, rotating at a fixed speed of 8.6 m min^{-1}, which corresponds to approximately five loops completed during one EMM recording. Therefore, one EEM recording in on-line mode will not correspond to information solely contained in one conveyer element, but it will rather show an averaging across the entire length of the conveyor belt.

At the end of applying the different riboflavin fouling steps, a cleaning procedure was initiated using standard industrial wipes with soap (Novadan, Kolding, Denmark). The purpose of this cleaning step was to check if it is possible to restore the original status of the conveyor belt. This was performed in a comparable way as the contamination, meaning that the conveyor belt was cleaned gradually in four steps and 5 EEMs recorded in between each stage. The full fouling-and-cleaning simulation ended with a total of 70 EEM recordings representing the different contamination levels followed by cleaning.

3. Results and discussion

3.1. Off-line

We simulated contaminations with riboflavin on a clean conveyor surface to investigate the feasibility of using a Wilks' ratio statistic based control chart to detect unusual measurements. Inputs to the

multivariate control chart are the concentration score values retrieved from PARAFAC after modelling the fluorescence landscapes. Initially, the method was tested off-line with inputs containing EEMs collected on conveyor surfaces under static conditions. The methodology of Wilks' ratio statistics is summarized in Appendix A and its implementation in this work is explicitly described in Appendix B. Throughout this article, it is assumed that contamination is a special event emerging within the incoming data during process monitoring stages, the so-called Phase II, which was not initially present in the reference or calibration set in Phase I. During the calibration the process was considered to be in an *in-control state*. Therefore, in reaching a diagnosis of fouled surface, the form of Wilks' ratio statistics implemented in our proposed method, as described by Mason et al. [22], is designed both to detect general changes in the variance-covariance matrix, but also to compensate for a relatively small test sample size m in relation to the multivariate process dimension p. The latter is an appealing feature for the method's industrial fitness, where due to recording data under working conditions, coupled with the need to account for reasonable scanned surface areas, the process can produce a new test evaluation within a short time interval.

Given the high number of variables scanned within each EEM landscape and the interest to monitor the within variability, PARAFAC was used for spectral curve resolution to reduce the dimensionality of the original measurements and to estimate new vectors of latent process quality characteristics. During model building, neighboring values below the excitation wavelength have been set to missing, in order to avoid misleading results induced by the absence of emission below the excitation wavelength. Zero values in this area do not conform to the trilinear property of the rest of the landscape and may thus estimate wrongly the underlying latent variables. As can be seen from Fig. 1a–b, even the same conveyor material can vary considerably as a function of spatial location, ageing/wear, etc. This results in intensity differences for different measurement locations on the same surface, and also in distinct intensities for the chemical entities in the surface material. This dissimilarity is even stronger for an equivalent conveyor material with a different history in use and cleaning, observable in Fig. 1c–d. It should be noted that the difference is both a function of true surface composition, but also of the instrument-surface interface (distance from the surface, angle between the surface and measurement probe, stationary versus moving conveyor belt, etc.). The latter highlights an additional challenge when monitoring surfaces compared to e.g. a liquid stream sample for which interfacing is generally easier. It can also be observed from Fig. 1e–f that there is a considerable overlap between riboflavin and natural conveyor background signals that challenge the statistical control, in particular when the interest is to detect low levels of contaminants on the surface. Additionally, recalibration for each process start was possible owing to the second-order advantage carried by PARAFAC (the capability of handling an unknown background), which enabled to reach representative models based on relatively small number of samples/recordings n. Three factors gave the optimal model complexity for the off-line data set; Table 1 summarizes details on model building.

During Phase I, after PARAFAC modelling, the concentration scores of the calibration set must be tested for outliers; if outliers are not removed the test statistics in Phase II would be unfit for process monitoring. For this purpose the Hotelling's T^2 statistics is used as shown in Fig. 3a (details can be found in Appendices A and B); no outliers were identified. It should be remembered here that the conveyor element was visibly damaged, locally to different extents, and the sampling strategy during data collection was to incorporate these differences. Table 1 summarizes the details and Fig. 2b shows the reconstructed loading-landscapes of the auto-fluorescence active chemicals found in the polyacetal conveyor material. It shows fairly strong correlations between the concentration scores of factors 1 and 2, and factors 2 and 3. Polyacetal is one of the polymers shown to have their own auto-fluorescence signals [23], and is moreover known to be unstable under UV light which is commonly counteracted with light stabilizers [24]. Thus, we speculate that two of the fluorophores identified originate from the type of stabilizers used in this particular conveyor belt, and the changes in ratio are likely caused by the degree of surface damage.

In Phase II (monitoring) the model space defined by the concentration scores $a_{i,f,}$ from Phase I (calibration) can be used to test weather new sample sets of $m = 4$ measurements carry solely chemical information which can be explained as a function of the clean conveyor material, and thus fall within the control limits of the $a_{i,f}$ scatter matrix (see Appendix A for details). This is symbolized in Fig. 4, where the sample scores corresponding to a conveyor surface spiked with two known riboflavin concentrations are expanding – or better, exceeding – the Phase I reference space. The proportion of expansion follows the concentration gradient, which implies that the greater the contamination of the surface, the more the reference space volume will increase. The expansion is also more dominant in the third direction, which is associated with the loading landscape $f = 3$ in Fig. 2b.

The Wilks' ratio statistics W control chart for the off-line Phase II data set is shown in Fig. 5a (for computational details see Appendices A and B). Data was recorded in a random order but is plotted here from the lowest to the highest riboflavin concentration in order to illustrate a contamination gradient on the conveyor. This gradient should be reflected in data points that score *W values* closer to zero. Every point on the Wilks' control map represents the statistical inference done for a set of $m = 4$ recordings. As anticipated, each stock solution is flagged as alarm, but with the lowest dilution level moving towards what would be considered a clean conveyor. It is interesting to investigate the pattern of individual variable contributions to the alarms in multivariate monitoring tasks [25], presented in Fig. 5b (for computational

Table 1
PARAFAC model building details on Phase I data.

	PARAFAC model details			Model details			Constrains
Off-line	Recordings n = 32 Factors F = 3			Core-consistency: 96% Explained variance: 99.7%			Non-negativity in all three modes
On-line	Recording n = 23 Factors F = 3			Core-consistency: 88% Explained variance: 99.2%			Non-negativity in all three modes
	Correlation matrix for Phase I data sets						
	Off-line			**On-line**			
	f_1	f_2	f3	f_1	f2	f3	
f_1	1.0000	0.8097	0.1710	1.0000	−0.4385	−0.0790	
f_2	0.8097	1.0000	0.6529	−0.4385	1.0000	0.1560	
f_3	0.1710	0.6529	1.0000	−0.0790	0.1560	1.0000	

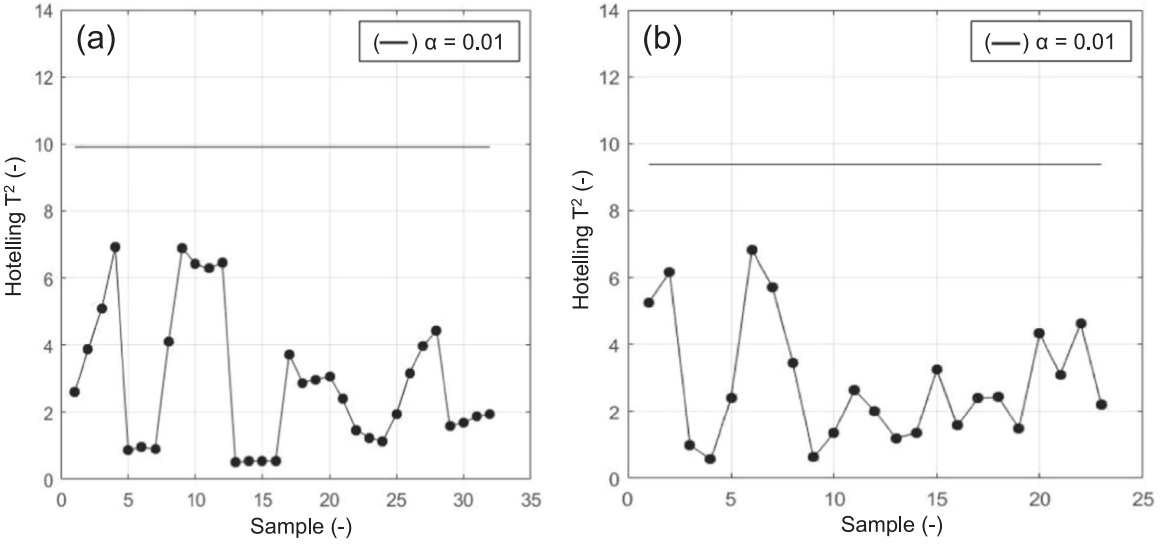

Fig. 3. (a) Hotelling's T^2 controls for off-line Phase I data set; (b) Hotelling's T^2 controls for on-line Phase I data set.

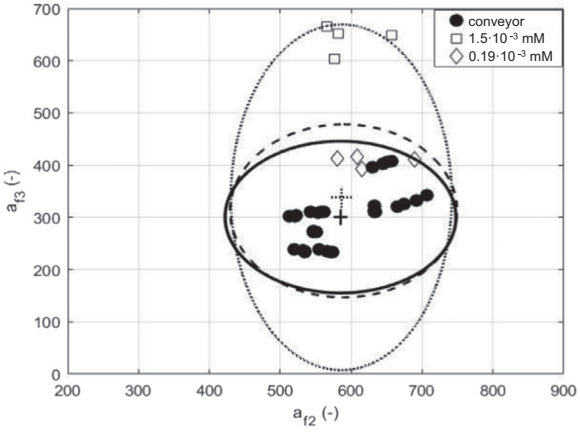

Fig. 4. Graphical representation of Wilks' ratio principle, shown for dimensions f = 2 and f = 3 only. Note that the true variance space used during computation of the Wilks' ratio statistic is three-dimensional (F = p = 3) for the conveyor system.

details see Appendices A and B). Again, as was expected, for high contaminations levels all individual contributions flag an abnormal or *out-of-control* situation. Moving to lower contamination levels the contributions for variables 1 and 2 move towards normal signals, and for the lowest levels also contribution 3 reaches the no suspicion zone, without restoring completely the original space of the conveyor belt. Hence, though the individual variable contributions are not flagged at the lowest contamination level, the variance-covariance signal in the Wilks' statistics indicates an alarm.

To interpret the detection mechanism we construct a new PARAFAC model combining clean conveyor measurements and one contamination level, extracting $F = 4$ components. The fourth component, which can be identified as riboflavin [26] is shown in Fig. 6. When comparing this landscape with the one shown in Fig. 2b it becomes clear why the third variable in our Wilks statistic is the one most influenced by the riboflavin contamination. In summary: at a visual inspection of raw measurements and loading landscapes (Figs. 1, 2b and 6), riboflavin information mostly overlaps with factor $f = 3$ PARAFAC component for the off-line measurements. This suggests that incoming data with

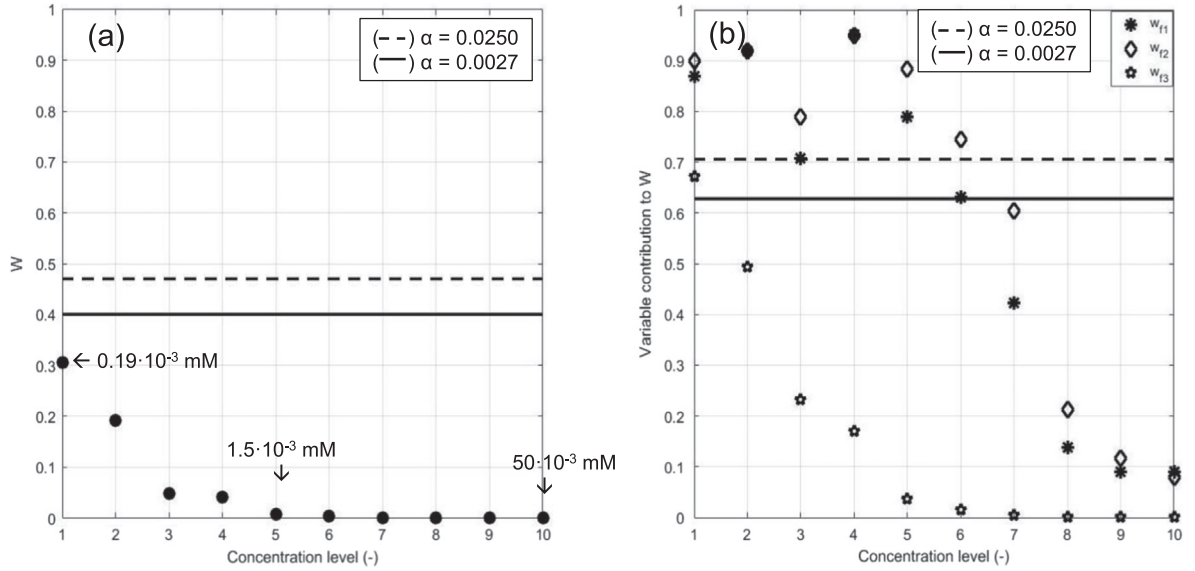

Fig. 5. Wilks' ratio control charts for off-line data (m = 4) with warning limits set at α = 0.025 and alarm limits at α = 0.0027 (a) full model and (b) off-line variable contributions.

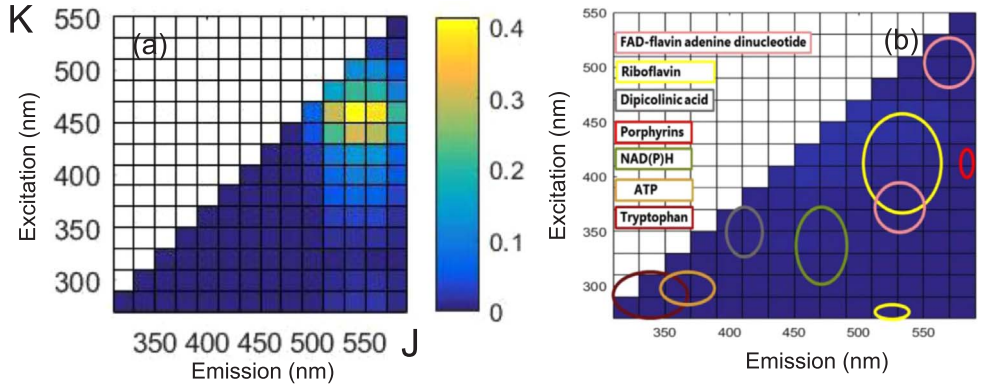

Fig. 6. (a) Outer-products of spectral loading vectors $\mathbf{b}_f$ and $\mathbf{c}_f$ for dimension f = 4 in off-line mode after PARAFAC modelling (n = 36) using F = 3 + 1 factors, including clean calibration data (n = 32) and contamination level $6.2{\cdot}10^{-3}$ mM measurement (n = 4). (b) Tentative assignment of different fluorophores superimposed on a BioView EMM landscape based on Quality & Technology, Food Fluorescence Library, 2005.

riboflavin will disrupt the ratio in which the three conveyor-related factors normally vary. The Wilks' ratio statistic is targeting these shifts in the covariance structure induced by future newly collected process data and translates the multivariate process signal into a univariate parameter *W*. This parameter *W* takes a value equal to 1 if the process did not undergo any statistically significant change, or approaches 0 the more changes occur in the new sample.

3.2. On-line

Having established the method, our monitoring strategy can be applied to the on-line task. A Phase I calibration set of $n = 23$ fluorescence landscapes was recorded on a newly cleaned conveyor belt in motion. The PARAFAC model building indicated $F = 3$ factors to be optimal (see Fig. 2c, and Table 1). Phase I outlier detection using Hotelling's T^2 showed no suspicious recordings (see Fig. 3b). The conveyors used in both the off-line and on-line cases have the same chemical composition and their fluorescence signatures are thus expected to be similar. Owing to the averaging happening across the large surface area in on-line mode – a moving surface, 10 recordings averaged per excitation-emission combination, sequentially for the 120 excitation-emission combinations, plus the different wear-levels – the PARAFAC components in on-line mode seem to have slightly more broad shapes. In the on-line data the three factors also have comparable intensities, whereas in the off-line mode component one was more dominant compared to the second, followed by the third component. Observe also that in the on-line mode the correlations between the different concentration scores are broken due to the moving conveyor and averaging across the entire surface (Table 1). It was decided that $m = 5$ measurements, corresponding to ~12 min of processing time or five decisions per hour, was a good compromise between sufficient accuracy/sensitivity and *real-time* surface fouling detection. Fig. 7a shows the Wilks ratio statistics control chart, marking the different stages in the simulated fouling (70 consecutive EEMs leading to 14 decision time points on $m = 5$ recordings each), while Fig. 7b shows the corresponding individual variable contributions. Fig. 7a shows that the thin film with the first two concentrations (stage A and B) is not flagged, while the variable contribution patterns do change for the two stages (Fig. 7b). A more concentrated film is being detected and is flagged in stage C; we emphasize again that the true concentration at the surface is not known but the expected pattern of fouling is clearly observed. During the cleaning (stage D) the Wilks' ratio (Fig. 7a) still indicates an out-of-control situation, but the variable contributions (Fig. 7b) show a different pattern. This is most likely related to the detergents being deposited on the conveyer surface. During rinsing (stage E) the system moves back to a clean phase and in principle a new Phase I calibration could be recorded (assuming there is sufficient confidence in the cleanliness of the system).

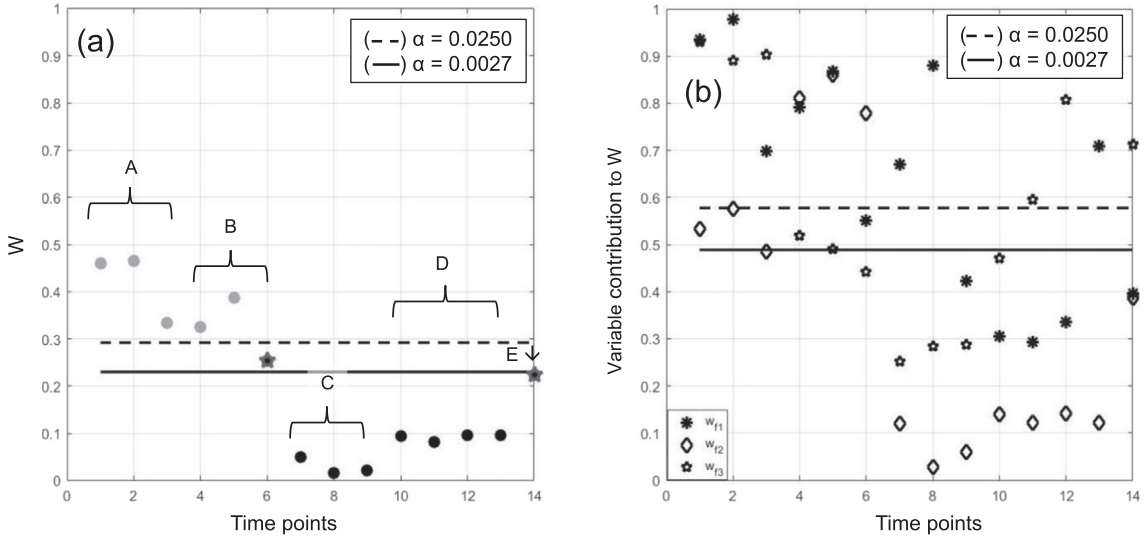

Fig. 7. Wilks' ratio control charts for on-line data (m = 5) with warning limits set at α = 0.025 and alarm limits at α = 0.0027 (a) full model containing contamination levels at $25{\cdot}10^{-3}$ mM (group A), $37.5{\cdot}10^{-3}$ mM (B) and $50{\cdot}10^{-3}$ mM (C), and a cleaning step with industrial wipes (D) followed by a rinsing with water (E); (b) on-line variable contributions.

4. Conclusion

The overall conclusion is that the Wilks' ratio monitoring charts succeeded to flag the presence of unusual measurements in relation to a calibration phase. Given that the aim of our investigation is to develop an on-line, real-time detection method for a biofouling type of contaminations on surfaces, the decisional algorithm was tailored for fluorescence measurements. Fluorescence has been extensively suggested in literature as an attractive method to detect biofouling, due to its high sensitivity, fast response time and potential to scan non-invasively. Characteristic signals such as NAD(P)H and FAD, nucleic acids and aromatic amino acids like tryptophan, tyrosine and phenylalanine are the common type of information comprised within the recorded biofouling related EEMs. They can thus be used to indicate the presence of live bacterial cells and/or a protein fouling layer. We observed that background signal from polymer conveyor belts, a low signal-to-noise ratio and other signal interferences are hindering a simple univariate data analysis, and add a challenge in extracting the different fouling signatures. Process monitoring and diagnose based on analyzing the entire fluorescence landscapes is generally a more valid solution, rather than using solely the emission spectrums at specific wavelengths. The latter scenario has been used in several studies [14,15]; the results however may lack in capturing the real picture since potentially valuable information about interferences may not be identified due to the selective way of recording raw data.

Most standard methods would require us to know beforehand the identity of the contaminant and have it included in the calibration set. Consequently, this would also result in the need for a large number of calibration samples. Thus, for the case illustrate in this work, where the background itself has a strong and varying signal, combined with an unknown identity of the contaminant, setting up a standard method is a challenging task. Note that our proposed strategy turns this issue into an advantage by setting the statistics to answer the general question: *is the new measurement similar with the in-control clean conveyor?* Further, if an unusual behavior is detected, a decision is taken by inspecting in more details the source causing the event via individual variable contributions. The first key step in our strategy is the unique decomposition of fluorescence data by PARAFAC. As a result, good performances can be achieved with calibrations based on a small number of samples. Additionally, we can handle and identify the presence of emerging interferences in the monitoring Phase II without having them included in the calibration data based on the uniqueness property. Note that even under on-line recording mode, PARAFAC is able to handle the noisy type of data and extract the true underlying information contained in the EEMs (Fig. 2b–c). The second key step in performing monitoring is the Wilks' ratio statistics which is targeting shifts in the variance and covariance parameters that translate ultimately in deviations by the process. We are making use of the model space of the clean conveyor, the way it looks at the start of the process, and consider that the initiation of a fouling layer will result in one or more fluorescence signals that will interfere with conveyor's auto-fluorescence. As a consequence, the covariance of the three components will be changed and signaled in the Wilks' ratio based chart. For illustration purposes we used riboflavin as a fouling simulant which has a fluorescence signal that strongly overlaps with one of the three conveyor components.

In an alternative scenario not pursued here, an emerging new and unidentified chemical component may not necessarily interfere with the normal display of conveyor's auto-fluorescence, which would render it *invisible* for the monitoring chart described in this work. Therefore a parallel question could be considered: *does the conveyor look different from its initial stage?* During PARAFAC modeling the normal variation spanned by the clean conveyor is explained through the spectral loadings and concentration scores. The residual matrix $\mathbf{E}_i$ from Eq. (1) will thus include the unexplained or new information. Given that the PARAFAC model is fitted on data originating from Phase I characterized by an acceptable level of cleanliness, upon projection of new observations into this model an additional signal from the new and unidentified component will not fall in the clean conveyor *p*-dimensional space. Therefore, answering the second question narrows down to a check for similarity between the defined residual-error structure of Phase I – e.g. using the sum of squared residuals in combination with a weighted chi-square test – and the new residuals during Phase II. We do not explore this alternative because this would come down to straight forward residual-based outlier detection, which could easily be implemented parallel to our suggested strategy. Moreover, given the broad nature of fluorescence spectrums and the intrinsic information of this particular conveyor covering the general areas where bio-based signals are expected, it was considered that the suggested strategy in this work is sufficient. This hypothesis has to be confirmed by additional investigations in future work.

Acknowledgements

IMS gratefully acknowledge the financial support provided by the Reuse of Water in the food and bioprocessing industries (REWARD) and both Pig Levy Foundation and the Green Development and Demonstration Programme (GUDP) of the Ministry of Food, supporting RENPÅNY programs.

Appendix A

Wilks' ratio, Hotelling's T^2 and Wilks' ratio contributions

Assume we have a training set (also called calibration or Phase I) of n independent sample column vectors $\mathbf{x}$ (of size p x 1) containing p variables, collected while our process was in-control. We can then assume that all these in-control samples are taken from the same p-dimensional normal distribution $N_p(\boldsymbol{\mu},\boldsymbol{\Sigma})$. Our best, unbiased estimates for the unknown parameters in this distribution using our training set are the mean Eq. (A.1a) and the variance-covariance matrix Eq. (A.1b).

$$\bar{x} = \frac{1}{n}\sum_{i=1}^{n} x_i \tag{A.1a}$$

$$S = \frac{1}{n-1}\sum_{i=1}^{n} (x_i - \bar{x})^T (x_i - \bar{x}) \tag{A.1b}$$

The two parameters sets $\bar{x}$ (p x 1) and $\mathbf{S}$ (p x p) together specify what is normal variation in the training set. If a new test set (also called monitoring or Phase II) of m observations becomes available we can make a new estimated of the mean and variance-covariance structure using the augmented data set via Eq. (A.2).

$$S_A = \frac{1}{n+m-1}\sum_{i=1}^{n+m} (x_i - \bar{x}_A)^T (x_i - \bar{x}_A) \tag{A.2}$$

Under the assumption that nothing has changed going from the training to the test stage, hence that our system and error structure have not changed, both $\mathbf{S}$ and $\mathbf{S}_A$ are data-derived estimates of the same unknown parameter set $\mathbf{\Sigma}$. To evaluate if our assumption was correct we can use Wilks' ratio statistics W, defined in Eq. (A.3) [22].

$$W=\left(\frac{n-1}{n+m-1}\right)^{p}\frac{|S|}{|S_A|} \tag{A.3}$$

The scalar W is a weighted ratio of the determinants of the variance-covariance matrix of the training set $\mathbf{S}$ and the augmented training-plus-test set $\mathbf{S}_A$, and it can be proven to be a value between 0 and 1 [22]. The determinants in turn can be interpreted as the volumes represented by the two $\mathbf{S}$-matrices. A value close to 1 for W thus indicates that the new test observations have not increased the volume significantly, while a small value suggested a change in the system. This is because the calibration set is included in both $\mathbf{S}$ and $\mathbf{S}_A$ and the variance will thus be equal or bigger in the denominator of Eq. (A.3).

In order to monitor a process in Phase II and make a statistical inference about the last m measurements a lower-significance limit at probability α (w_α) is needed (Eq. (A.4)).

$$P(W < w_\alpha) = \alpha \tag{A.4}$$

The statistical distribution of W cannot be determined analytically, but several approximations can be used. The most common one, and the one used by us, was suggested by Rao [27], defined in Eq. (A.5).

$$K\left(\frac{1-W^{1/b_2}}{W^{1/b_2}}\right) \approx F(1-\alpha,\, m\bullet p,\, b_4) \tag{A.5a}$$

$$K=\frac{b_4}{p\bullet m} \tag{A.5b}$$

$$b_1=\frac{2\bullet n+m-p-3}{2};\; b_2=\sqrt{\frac{p^2\bullet m^2-4}{p^2+m^2-5}};\; b_3=\frac{p\bullet m-2}{2};\; b_4=b_1\bullet b_2-b_3 \tag{A.5c}$$

It uses the well-known Fisher–Snedecor $F(1\text{-}\alpha, m\cdot p, b_4)$-distribution with $m\cdot p$ and b_4 degrees of freedom, evaluated at the 1-α probability. In the nominator of the F-ratio we have thus the number of test measurements m times the number of variables per measurement p as independents, while the denominator independents is a function of p, m and the number of training sample n, derived via the b-coefficients; if b_4 is not an integer it is customarily truncated to its integer part. The approximation in Eq. (A.5) is valid if $b_1 \cdot b_2 > b_3$. Finally, by Eq. (A.6), we can derive our α quantile for the statistical test in Eq. (A.4).

$$w_\alpha \cong \left(\frac{K}{K+F(1-\alpha,\, p\bullet m,\, b_4)}\right)^{b_2} \tag{A.6}$$

Hotelling's T^2 statistic

For the special case of $m = 1$ the statistical test presented before can be made exact (hence, without approximation) via Hotelling's T^2 statistic [26]. This inference testing should e.g. be applied to the n individual observations in the training set during Phase I to make sure that no outliers are used in determining the in-control error structure via Eq. (A.1). To evaluate one measurement $\mathbf{x}_i$ the T_i^2 value is estimated from Eq. (A.7).

$$T_i^2 = (x_i - \bar{x}_1)^T \mathbf{S}^{-1} (x_i - \bar{x}_1) \tag{A.7}$$

This statistic can in turn be assessed against a probability distribution to test likelihood using Eq. (A.8).

$$\frac{n+1}{n^2}T_\alpha^2 \cong Beta(1-\alpha,\, p/2,(n-p)/2) \tag{A.8a}$$

$$T_\alpha^2 \cong Beta(1-\alpha,\, p/2,(n-p)/2)\frac{n^2}{n+1} \tag{A.8b}$$

It employs the *Beta*-distribution with p/2 and $(n\text{-}p)/2$ degrees of freedom, which can be shown to be exact under the assumption of a p-dimensional normal distribution $N_p(\boldsymbol{\mu},\mathbf{\Sigma})$ [28].

Variable contributions in W

During statistical evaluation it might be relevant to understand which of the p variables causes a new sample in Phase II to flag a change [23,27] the so-called contribution in an alarm. To set up the test we first write out the variance-covariance matrix $\mathbf{S}$ from Eq. (A.1b) in Eq. (A.9); $\mathbf{S}_A$ from Eq. (A.2) can be written out in an analog manner.

$$S=\begin{bmatrix} s_1^2 & s_{1,2} & \cdots & s_{1,p} \\ s_{2,1} & s_2^2 & \cdots & s_{2,p} \\ \vdots & & \ddots & \vdots \\ s_{p,1} & s_{p,2} & \cdots & s_p^2 \end{bmatrix} \tag{A.9}$$

We then use the fact that W in Eq. (A.3) can be decomposed into a series of $p\cdot 2^{p-1}$ terms, which is shown for the first variable $p = 1$ in Eq. (A.10).

$$W = W_1 \bullet \ldots \bullet W_{1(2)} \bullet \ldots \bullet W_{1(2,\ \ldots,\ p-1)} \tag{A.10}$$

The decomposition in Eq. (A.10) splits the test statistic W into one unconditional factors W_p and a series of conditional factors $W_{p(\ldots)}$; for further details see [29]. Our interest lies in the unconditional parts only which we want to employ to evaluate individual variable contributions to the statistic W. This can be achieved using Eq. (A.11) (which is a special case of – and builds on the same assumptions as – Eq. (A.5) with dimensionality p set to 1).

$$W_p = \frac{(n-1)\bullet s_p^2}{(n+m-1)s_{A,p}^2} \tag{A.11a}$$

$$P(W_p < w_{p,\alpha}) = \alpha \tag{A.11b}$$

$$w_{p,\alpha} \cong \frac{n-1}{n-1+m\bullet F(1-\alpha,\ m,\ n-1)} \tag{A.11c}$$

Appendix B

Wilks' ratio statistics - a practical example for the off-line case

We illustrate Wilks's ratio statistics used here to detect unwanted chemical information, in this case riboflavin, on the surface of our conveyor belt. The Phase I set consist $n = 32$ recordings, which are from the clean conveyor measurements. The number of varying values in the calibration or training set is equal to the number of factors derived from PARAFAC decomposition, Eq. (1). Therefore, $F = p = 3$ variables are generated (see Fig. 2), leading to three score vectors $\mathbf{a}_1$, $\mathbf{a}_2$ and $\mathbf{a}_3$ of size n x 1. Using the PARAFAC outcome as our data set we can generate a vector for each measurement $i = 1\ldots n$ as $\mathbf{x}_i = [a_{i,1}\ a_{i,2}\ a_{i,3}]^T$, which via Eq. (A.1) gives us the Phase I mean and variance-covariance of the system:

$$\bar{x} = \begin{bmatrix} 1002 \\ 585 \\ 303 \end{bmatrix};\ S = \begin{bmatrix} 11341 & 5035 & 954 \\ 5035 & 3409 & 1997 \\ 954 & 1997 & 2744 \end{bmatrix};\ |S| = 7.39\bullet 10^9$$

To test the n individual recordings in Phase I as potential outliers we apply a Hotteling's T^2 statistic via Eq. (A.7) and compare this to an acceptance limit derived from Eq. (A.8) determined at, $Beta(1\text{-}0.01,1.5,14.5) = 0.320$, $T^2_{\alpha=0.01} = 9.91$ (see Fig. 3a) which in this case indicates none of the measurements is flagged as outlier.

In Phase II, we evaluate new samples based of $m = 4$ recordings (the number of measurements during one decision making). The augmented data set used for making a new estimate of the variance-covariance structure, based on Eq. (A.2), will always consist of a $n + m = 36$ size sample. Hence, the Phase I is augmented each time with only the m observations of the new sample, giving update $\mathbf{S}_A$ by Eq. (A.2), from which W is to be determined by Eq. (A.3), to be compared to the control limited found from Eq. (A.6).

$$\bar{x}_A = \begin{bmatrix} 1011 \\ 589 \\ 315 \end{bmatrix};\ S_A = \begin{bmatrix} 11548 & 5171 & 1685 \\ 5171 & 3358 & 2190 \\ 1685 & 2190 & 3621 \end{bmatrix};\ |S_A| = 1.25\bullet 10^{11}$$

For riboflavin sample $0.19\cdot 10^{-3}$ mM, this gives $W = 0.305$ (see Fig. 5a), where $b_1 = 31$, $b_2 = 2.64$, $b_3 = 5$, $df_1 = 12$, $b_4 = df_2 = 77$, $K = 6.42$, $F(1\text{-}0.0027,12,77) = 2.85$, which results in $w_{\alpha=0.0027} = 0.378$ (see Fig. 5a). This makes the sample fall (just) outside the alarm limit and thus flags the measurement as significantly deviating from the calibration Phase I.

References

[1] M.E. Davey, G.A. O'Toole, Microbial biofilms: from ecology to molecular genetics, Microbiol. Mol. Biol. Rev. 64 (2000) 847–867.

[2] D.W. Ren, J.S. Madsen, S.J. Sorensen, M. Burmolle, High prevalence of biofilm synergy among bacterial soil isolates in cocultures indicates bacterial interspecific cooperation, Isme J. 9 (2015) 81–89.

[3] H.C. Flemming, J. Wingender, The biofilm matrix, Nat. Rev. Microbiol. 8 (2010) 623–633.

[4] C. Mayer, R. Moritz, C. Kirschner, W. Borchard, R. Maibaum, J. Wingender, H.C. Flemming, The role of intermolecular interactions: studies on model systems for bacterial biofilms, Int. J. Biol. Macromol. 26 (1999) 3–16.

[5] J.S. Peng, W.C. Tsai, C.C. Chou, Inactivation and removal of Bacillus cereus by sanitizer and detergent, Int. J. Food Microbiol. 77 (2002) 11–18.

[6] G. Midelet, B. Carpentier, Transfer of microorganisms, including Listeria monocytogenes, from various materials to beef, Appl. Environ. Microbiol. 68 (2002) 4015–4024.

[7] M.R. Beresford, P.W. Andrew, G. Shama, Listeria monocytogenes adheres to many materials found in food-processing environments, J. Appl. Microbiol. 90 (2001) 1000–1005.

[8] K. Silagyi, S.H. Kim, Y.M. Lo, C.I. Wei, Production of biofilm and quorum sensing by Escherichia coli O157:H7 and its transfer from contact surfaces to meat, poultry, ready-to-eat deli, and produce products, Food Microbiol. 26 (2009) 514–519.

[9] G.A. Veluz, S. Pitchiah, C.Z. Alvarado, Attachment of *Salmonella serovars* and Listeria monocytogenes to stainless steel and plastic conveyor belts, Poult. Sci. 91 (2012) 2004–2010.

[10] Y. Chaturongkasumrit, H. Takahashi, S. Keeratipibul, T. Kuda, B. Kimura, The effect of polyesterurethane belt surface roughness on *Listeria monocytogenes* biofilm formation and its cleaning efficiency, Food Control 22 (2011) 1893–1899.

[11] J. Palmer, S. Flint, J. Brooks, Bacterial cell attachment, the beginning of a biofilm, J. Ind. Microbiol. Biotechnol. 34 (2007) 577–588.

[12] L. Farris, M.Y. Habteselassie, L. Perry, Y. Chen, R. Turco, B. Reuhs, B. Applegate, Luminescence techniques for the detection of bacterial pathogens, in: M. Zourob, S. Elwary, A. Turner (Eds.), Principles of Bacterial Detection: Biosensors, Recognition Receptors and Microsystems, Springer New York, New York, NY, 2008, pp. 213–230.

[13] J.R. Lakowicz, Principles of Fluorescence Spectroscopy, third ed, Springer, Maryland, 2006.

[14] Y. Pu, W.B. Wang, R.R. Alfano, Optical detection of meat spoilage using fluorescence spectroscopy with selective excitation wavelength, Appl. Spectrosc. 67 (2013) 210–213.

[15] A. Aït-Kaddour, T. Boubellouta, I. Chevallier, Development of a portable spectrofluorimeter for measuring the microbial spoilage of minced beef, Meat Sci. 88 (2011) 675–681.

[16] H. Shirai, S. Oshita, Y. Makino, Detection of fluorescence signals from ATP in the second derivative excitation-emission matrix of a pork meat surface for cleanliness evaluation, J. Food Eng. 168 (2016) 173–179.

[17] N. Oto, S. Oshita, Y. Makino, Y. Kawagoe, J. Sugiyama, M. Yoshimura, Non-destructive evaluation of ATP content and plate count on pork meat surface by fluorescence spectroscopy, Meat Sci. 93 (2013) 579–585.

[18] M.S. Wiederoder, N. Liu, A.M. Lefcourt, M.S. Kim, Y.M. Lo, Use of a portable hyperspectral imaging system for monitoring the efficacy of sanitation procedures in produce processing plants, J. Food Eng. 117 (2013) 217–226.

[19] C.D. Everard, M.S. Kim, H. Lee, Assessment of a handheld fluorescence imaging device as an aid for detection of food residues on processing surfaces, Food Control 59 (2016) 243–249.

[20] W. Jun, M.S. Kim, B.K. Cho, P.D. Millner, K.L. Chao, D.E. Chan, Microbial biofilm

detection on food contact surfaces by macro-scale fluorescence imaging, J. Food Eng. 99 (2010) 314–322.
[21] R. Bro, PARAFAC. Tutorial and applications, Chemom. Intell. Lab. Syst. 38 (1997) 149–171.
[22] R.L. Mason, Y.M. Chou, J.C. Young, Monitoring variation in a multivariate process when the dimension is large relative to the sample size, Commun. Stat. Theory Methods 38 (2009) 939–951.
[23] H. Langhals, D. Zgela, T. Schlücker, High performance recycling of polymers by means of their fluorescence lifetimes, Green. Sustain. Chem. 4 (2014) 144–150.
[24] M. Chanda, S.K. Roy, Plastic Technology Handbook, fourth ed, CRC Press, Florida, 2007.
[25] H. Babamoradi, F. van den Berg, Å. Rinnan, Confidence limits for contribution plots in multivariate statistical process control using bootstrap estimates, Anal. Chim. Acta 908 (2016) 75–84.
[26] Quality & Technology, Food Fluorescence Library, ⟨http://www.models.life.ku.dk/foodfluor⟩, (accessed 12.01.17), 2005.
[27] C.R. Rao, An asymptotic expansion of the distribution of Wilks' criterion, Bull. Int. Stat. Inst. 33 (1951) 177–180.
[28] R.L. Mason, Y.M. Chou, J.C. Young, Identifying variables contributing to outliers in Phase I, Commun. Stat. Theory Methods 37 (2008) 1103–1118.
[29] R.L. Mason, Y.M. Chou, J.C. Young, Decomposition of scatter ratios used in monitoring multivariate process variability, Commun. Stat. Theory Methods 39 (2010) 2128–2145.

3.5. Monitoring bacterial growth on surfaces under fouling conditions by meat products

In Paper I the principle of a Wilks' ratio statistic based model was demonstrated using riboflavin as an artificial emerging contaminant. In a second investigation presented here, the aim was to test Wilks model's performance also under a real bio-fouling scenario.

3.5.1. Methods and Materials

In the pilot plant facility at the Danish Meat Research Institute /Technical Institute, Taastrup, Denmark, the scenario of bacterial growth/contamination under processing conditions was simulated by allowing the surface of the conveyor belt (4.2m length) to come in contact with a meat product while set in motion, as shown in Figure 3.5. The recording of EEMs was done under the same conditions as explained in Paper I with the fluorescence probe mounted at one end/bend of the conveyor (at a 5mm distance). The entire experiment was conducted at a room temperature of 11°C for five days with the conveyor belt moving at a speed 18 (arbitrary units) which corresponds to the normal operating speed.

Prior to their placement in contact with conveyor belt surface, the three large pieces of meat (Figure 3.5) were inoculated with a Pseudomonas fragi (CC4669) culture by spreading a volume of 10ml of 4 $\log_{10}$ CFU·ml^{-1} bacterial solution over each piece. The purpose of inoculating the meat was to simulate the bacterial load that meat products would typically have in a slaughterhouse/on a slaughtering line. The bacterial strain was cold adapted, by propagating it in brain heart infusion broth at 10°C in order to reduce its lag-phase. EEMs were recorded every 10 min throughout the entire experiment via the BioView (DeltaLight & Optics, Hørsholm, Denmark) instrument taking 2.5min per recording (1200 gain, 10 scans averaged).

Water drops were supplemented in the empty space between meat pieces via a peristaltic pump set at 0.1ml·min^{-1}, in order to keep a constant humidity level and avoid drying of the meat (as was observed in previous experiments). In parallel to the EEMs recording, the aerobic plate count was determined based on the pour-plate method on PCA agar inoculated at 30°C. Thus, for the entire time of the experiment - every morning at approx. 9:00 and afternoon at approx. 16:00 - both the meat and conveyor surface were sampled for aerobic plate count determinations. Three swab samples were collected aseptically from an area of 75cm^2 via swab cloths from the conveyor surface underneath each piece of meat (one swab sample per piece of meat), while a 10cm^2 meat sample was aseptically collected from each piece (the side facing the conveyor). In the morning of day three, an intermediate cleaning was done by wiping the surface of the conveyor belt with standard industrial wipes with ethanol (Novadan, Kolding, Denmark). At the end of this intermediate cleaning, new inoculated pieces of meat were placed back on the conveyor belt and the experiment continued until day five. The purpose of the intermediate cleaning was simply to combine two experiments where the objective was to assess the power of this type of manual-intermitted cleaning in reducing the surface microbial load and assess if present CIP protocols could potentially be changed (CIP delayed).

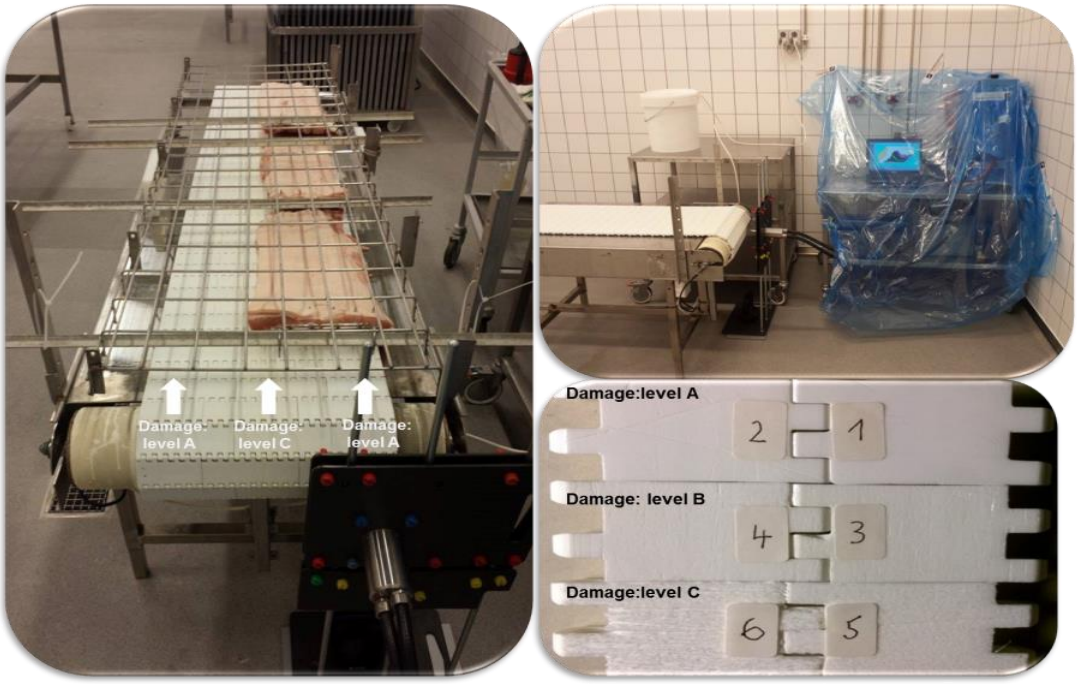

Figure 3.5. Illustration of Trial 3 setup

3.5.2. Results and discussion

Three trials were done overall. Due to several technical issues encountered in the first two runs (drying of meat in Trial 1 and ensuring the appropriate supplement of water to avoid meat drying and support microbial growth), only data from Trial 3 conducted on surface with level C of damage (Figure 3.5) is presented here.

Figure 3.6b presents the PARAFAC components of the Trial 3 calibration Phase I. In this case, calibration is done based on data collected in the first 3h of the run (59 recorded EEMs) assuming that no significant increased microbial activity occurs in this time period and the recorded EEMs are sufficient enough to capture what is considered *in-control variation*. Comparing these with the PARAFAC components of the clean conveyor surface (Figure 3.6a), it is noticed that in the calibration Phase I data, an additional component (Factor 4) is identified. This factor corresponds to the tryptophan information originating from the meat matrix. When projecting the monitoring Phase II into the calibration PARAFAC model, the concentration profiles of all components can be observed as in Figure 3.6c. Factor 1, 2 and 3 exhibit a rather stable profile apart from the last part of the experiment where their intensities (pseudo-concentrations) increase. The large variations noticed in concentration profiles of Factor 4 indicate that the meat matrix on conveyor surface varied considerably throughout the experiment. This is evident also from the intermediate cleaning step where the meat information (Factor 4) decreases and is followed by an immediate increase when the new, freshly inoculated meat pieces are brought in contact with the conveyor surface.

The Wilks' ratio control chart for the monitoring Phase II under meat biofouling is presented in Figure 3.7. Every data point in the chart corresponds to a test performed based on two consecutive measurements, hence m=2. The chart shows the onset of alarms at two different time points: first, before the intermediate cleaning point which appears to be caused by a build-up of meat matrix (unusual compared to calibration; see contribution of w_{f4}) and second in the last part of the experiment which is determined by an unusual profile of Factor 1 and 3 (see contribution of w_{f1} and w_{f3}). In a tentative to assign the information contained in Factor 1 and 3, from Paper II- Figure 6b, it can be seen that Riboflavin or FAD signals of microorganisms may be overlapping with Factor 1, while the NAD(P)H signals coincide with Factor 3. The actual growth profiles (see CFU·cm^{-2} profiles in Figure 3.9) indicates indeed more microbial load in the last part of the trial and to some extent follow the concentration profiles of F1 and F3. Figure 3.8 presents the Wilk's chart when removing the influence of Factor 4 (tryptophan) and calculated the statistics in relation to the other components Factor 1, 2 and 3. As expected, the onset of alarms is only observed in the last part of the trial corresponded to high aerobic plate count values of 6-7 log CFU·cm^{-2}, which appears to be captured in the behavior of Factor 1 and 3 (see contribution of w_{f1} and w_{f3}).

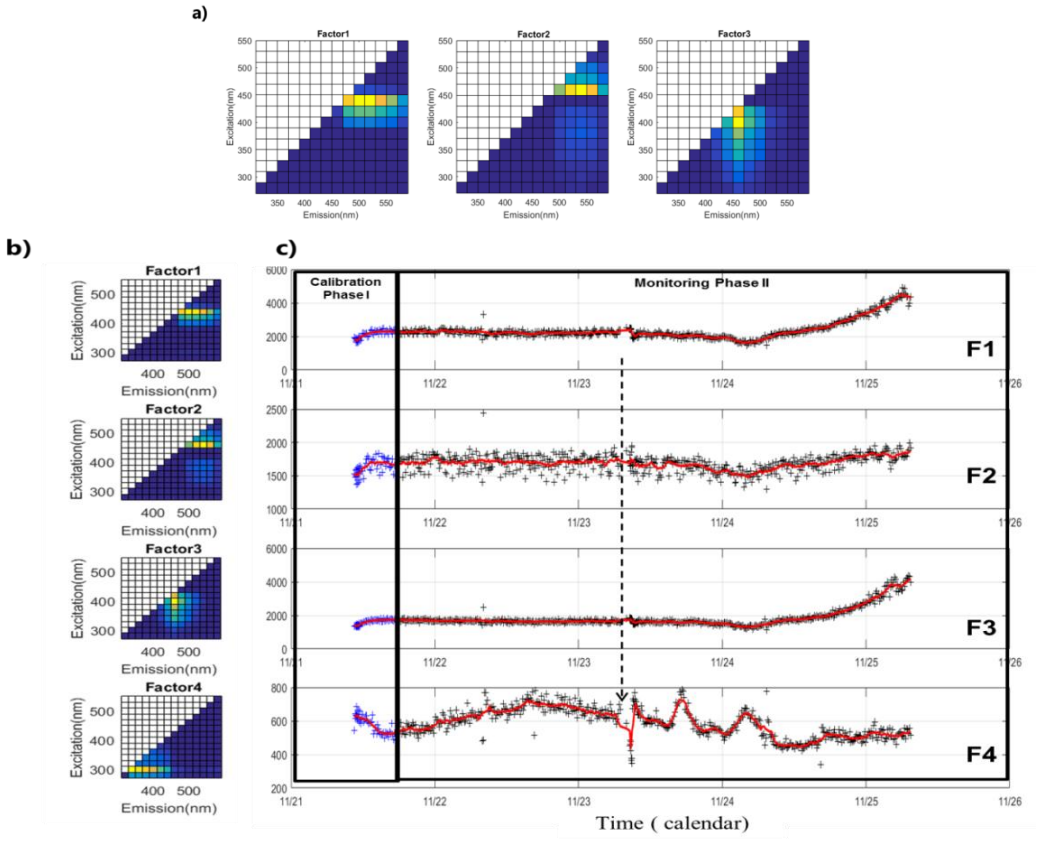

Figure 3.6. PARAFAC decomposition of EEMs recorded in Trial 3; a) PARAFAC components of clean conveyor belt measured in off-line mode, b) PARAFAC components based on calibration data in Trial3, c) concentration profile of PARAFAC scores for each component/factor.

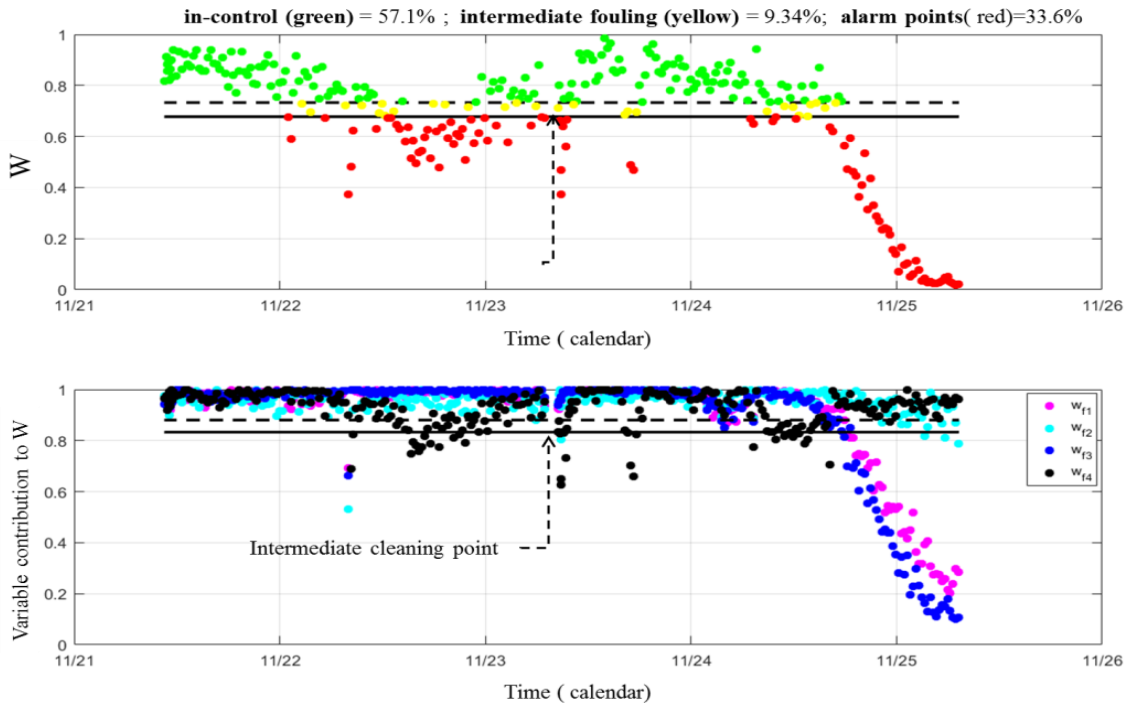

Figure 3.7. Wilks' ratio control chart for the monitoring Phase II under meat biofouling.

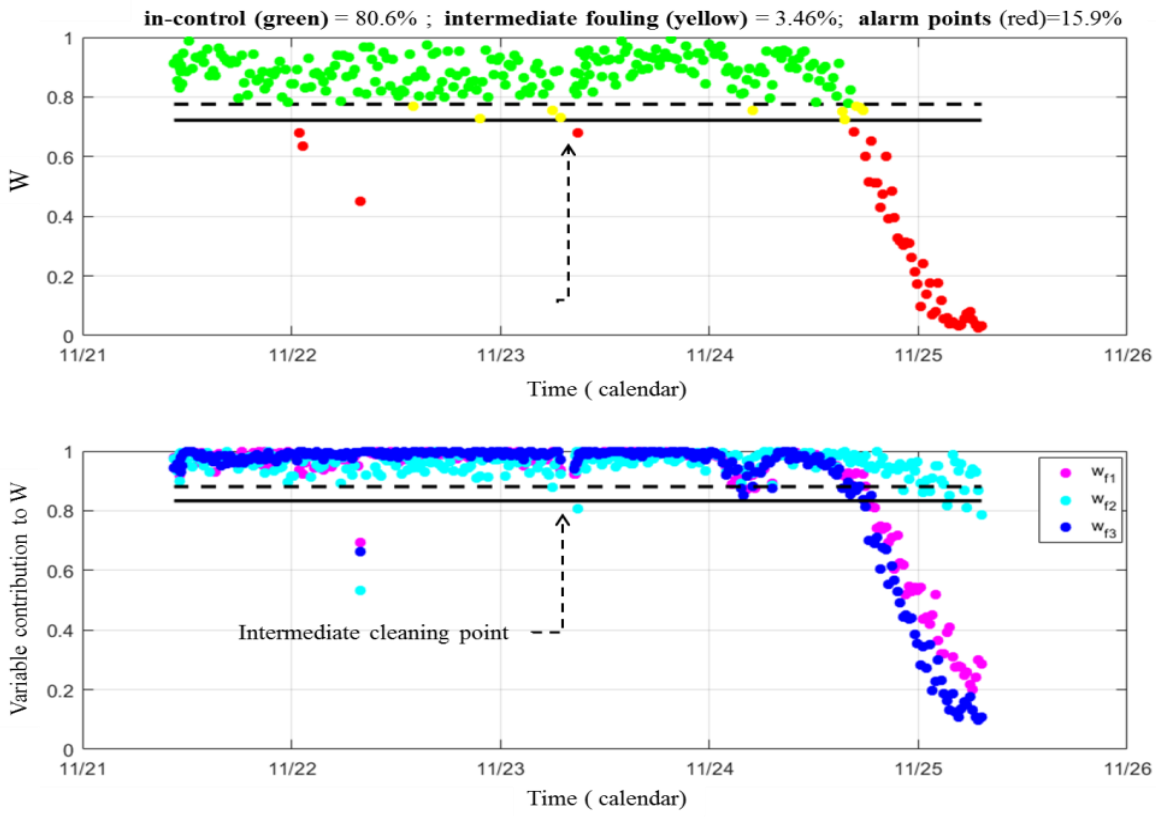

Figure 3.8 Wilks' ratio control chart calculated based on Factor 1, 2 and 3.

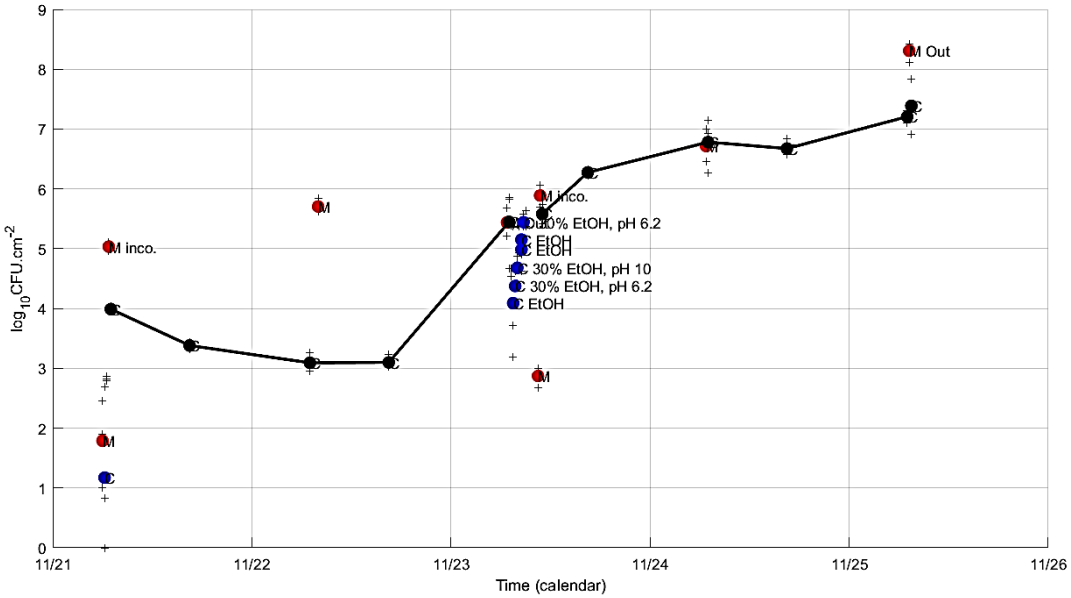

Figure 3.9 Total viable counts of Trial 3; (red)- microbial counts correspondent to meat product, (black)- microbial counts correspondent to conveyor surface, (blue)- microbial counts correspondent to conveyor surface after intermediate cleaning with ethanol wipes.

Even though at this stage the limit of detection appears to be around 6-7 $\log_{10}$ CFU·cm^{-2}**,** the results presented here offer a first step in demonstrating the potential of fluorescence spectroscopy in combination with statistical control in detecting potential microbial growths on conveyor surfaces under slaughterhouses conditions, on-line. Considering the recording principle of the BioView instrument, the efficiency of the Wilks method relies at this stage on the efficiency of capturing a good average *picture* of the entire 4.2m of scanned conveyor. Therefore, the case of a heterogeneous layer/localized contamination would hardly be captured in a recorded EEM; it would require instead a longer recording time based on averaging of more than 10 scans for each excitation wavelength in order to ensure that the entire 4.2m of conveyor has been exposed to each of the excitation wavelengths. However, when a uniform contamination layer is present across the entire conveyor length, which is expected to have happened in this case at 6-7 $\log_{10}$ CFU·cm^{-2}, the likelihood of capturing a representative *picture* of the fluorescing species in an EEM increases even if based on relatively short recording times.

More advanced fluorescence spectrophotometers capable of recording faster (based on e.g. charge-coupled devices (CCD) cameras, hence scanning simultaneously for all excitation wavelengths), with a higher signal-to-noise ratio and resolution can only bring positive improvements and allow for more localized detection. Another crucial aspect is tuning or selecting excitation wavelengths that result in minimal background interference while matching the excitation wavelength of biomolecules of interest. One should also be aware that the results provided by the reference culture and plate based methods are strongly biased by the culturing media and the chosen plating procedure. Selection of a more compatible method for comparison is therefore advisable, especially in the development phase, to demonstrate the method's power of microbial detection.

3.6. Assessment of a hand-held fluoresce device in evaluating surface biofouling

Near the end of this thesis project there was an opportunity to test a hand-held fluorescence device (BFD 100) which is currently sold by FreshDetect, Germany, as a commercial solution to quantify the bioburden level of minced pork meat. The device estimates Aerobic Plate Count in relation to bacterial porphyrins fluorescence signals when excited at 405nm. The recording of porphyrins fluorescence between 550-700nm is expected to fall outside the region where e.g. conveyor materials may interfere, as noticed from the BioView instrument experiments. Therefore, the main aim of the investigation was to determine if it is possible to distinguish between different bacterial suspensions when present on a conveyor surface.

3.6.1. Methods and materials

Pseudomonas fragi (CC4669) served as the model microorganisms and it was propagated in brain heart infusion broth for 2-3 days. Bacterial pellets from 50ml of inoculated broth were collected by centrifugation at 300rpm for 5min. A washing step with resuspension of bacterial cells into 0.9% NaCl saline water followed by collection of bacterial pellets through centrifugation (300rpm for 5min) was applied three times in order to remove any traces of broth. The final resuspension of cells served as the initial inoculum (equivalent to 8 $\log_{10}$ CFU·ml^{-1} as determined by culturing on standard PCA agar at 25°C) and from it tenfold dilution series were prepared at four levels in 0.9% NaCl saline water. Fluorescence spectra were recorded by fixing the probe on the surface of a conveyor coupon with level A damage (Figure 3.5) while holding within the measurement area 1.5ml from one bacterial solution (using a ring glued on the surface as well; demi-water served as a blank).

3.6.2. Results and discussion

Recording the emission spectra at only one excitation wavelength ($\lambda_{ex.}$= 405nm) falls under the first order calibration principle, which carries a set of weakness as previously explained in section 3.4. Starting from the hypothesis that an increase in the exposure time would result in a linear increase in the fluorescence intensity, hence follow the Beer-Lambert Law, the first interest was to check if possible to achieve a second-order calibration scenario by modeling data when organized in a three-way (or 3D) array X (IxJxK; where I is the dimension for samples, J dimension for emission spectra and K dimension for exposure time). With this aim, each of the bacterial dilutions were measured in five replicates while switching between different exposure times with the probe fixed on the measuring spot for the entire duration of the measurement. At first, the recordings were done in relation to a surface that presented minimal background interference.

From the raw emission spectra of the 7 $\log_{10}$ CFU·ml^{-1} Pseudomonas fragi bacterial suspension measured at different exposure times (0.02s, 0.06s and 0.1s) on the surface with minor background signal, a pronounced porphyrin fluorescence is observed between 600-700nm in particular at 0.1s exposure time, see Figure 3.10a. Based on recordings from all other bacterial suspensions measured under similar conditions, a three component PARAFAC model could be fit, see Figure 3.11. Inspecting the emission loadings, Factor 2 may be assigned to the background information whereas

Factor 3 resembles to the expected porphyrin profile (Figure 3.11b). Therefore, a distinction between the different bacterial dilutions is expected to be possible based on PARAFAC scores of Factor 3, which appears to function only until 5-6 $\log_{10}$ CFU·ml^{-1} level. Measuring the same bacterial dilutions but at increased exposure times (1.5s, 1.8s, 2s and 2.5s) did not bring much improvement in the model.

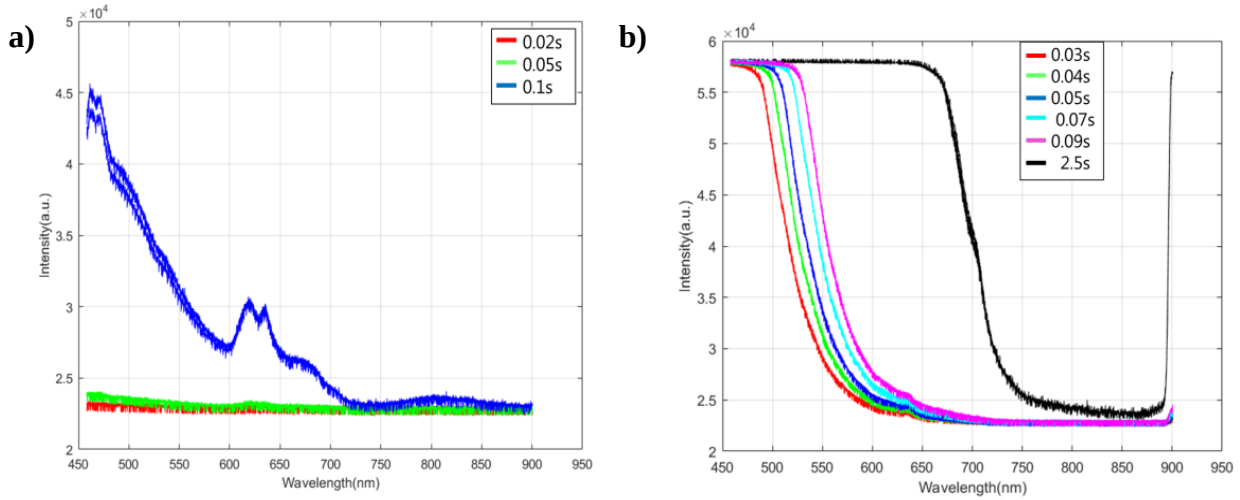

Figure 3.10 a) Emission spectra of 7 $\log_{10}$ CFU·ml^{-1} of Pseudomonas fragi bacterial suspension measured on surface with minimum background interference at different exposure times, b) Emission spectra of 8 $\log_{10}$ CFU·ml^{-1} of Pseudomonas fragi bacterial suspension measured on a conveyor surface with level A of damage at different exposure times.

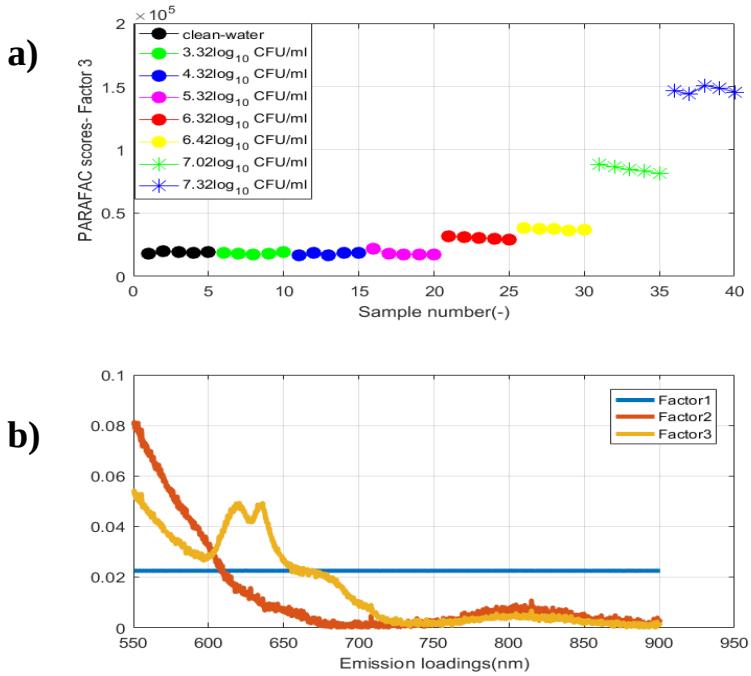

Figure 3.11 PARAFAC model of Pseudomonas fragi bacterial suspensions measured on surface with minimal background interference at 0.005s, 0.007s, 0.02s, 0.06s and 0.1s exposure time; a) pseudo-concentration profile of Factor 3, b) emission loadings of PARAFAC factors.

When recording a 8 $\log_{10}$ CFU·ml^{-1} of Pseudomonas fragi bacterial suspension on conveyor surface at comparable exposure times (0.03s, 0.04s, 0.05s, 0.07s, 0.09s and 2.5s), the information of porphyrins appear to be *diluted* by the background information (conveyor intrinsic autofluorescence), see Figure3.10b. Upon PARAFAC decomposition of recordings from all samples, again a three component PARAFAC model is found, with Factor 3 describing the porphyrins information. However, when looking at the concentration profile of the PARAFAC scores for Factor 3 (pseudo-concentrations), it shows that the model cannot distinguish between the different bacterial dilutions except the two level in the high range that correspondent to 7 and 8 $\log_{10}$ CFU·ml^{-1} respectively, see Figure 3.12a.

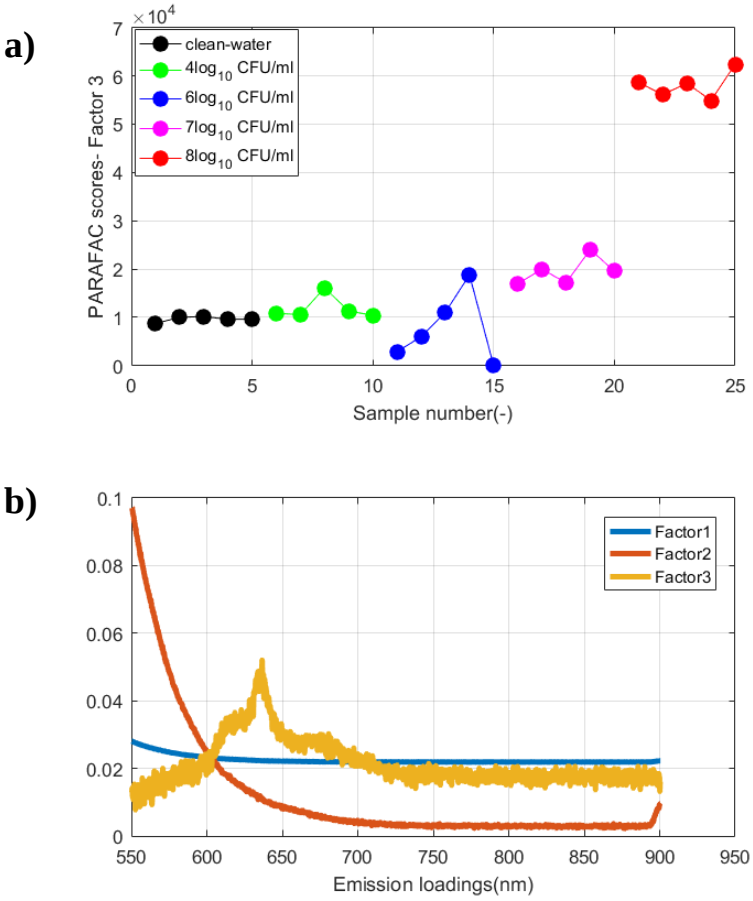

Figure 3.12 PARAFAC model of Pseudomonas fragi bacterial suspensions measured on a conveyor surface at 0.03s, 0.04s, 0.07s, and 0.09s exposure time; a) pseudo-concentration profile of Factor 3, b) emission loadings of PARAFAC factors.

Chapter 4

Characterization of reverse osmosis membrane fouling

4.1. Membrane fouling

The reverse osmosis membranes, most commonly available in the spiral wound configuration, are the active element in the water purification process[145]. A description of spiral wound configuration may be found in Paper II (page 4).

The most common cause of failure and decreased performance of RO membranes are due to accumulation of minerals, organic/ inorganic particles and microorganisms that deposit and interact with the membrane surface, in some cases becoming irreversible attached. This phenomenon is commonly known as membrane fouling. Overall, three (overlapping and interacting) types of fouling may be distinguished depending on the nature of deposits, see Box 3. Regardless of their nature, a fouling layer acts as a barrier with direct effect on flux reduction which requires an increased feed pressure in order to maintain in-spec permeate fluxes. It may also negatively affect product quality and ultimately it can shorten the membrane lifetime[146]. From an operation point of view, membrane fouling translates into increasing costs due to more energy consumption, system down time, inefficient use of membrane area and large amounts of water and chemicals needed for cleaning processes.
The mechanisms of fouling are complex and influenced by various factors, with probably the dominant ones being the feed composition (high organic matter will cause primarily organic fouling and high salt content will result in inorganic scaling), operational conditions (pH, temperature, fluxes, cleaning regimes, etc.) and membrane surface properties (smoothness, surface charge and hydrophilicity)[147]. Therefore, different circumstances will induce different fouling patterns, which stress the fact that knowledge attained from one production unit may not be entirely valid for a similar unit run under different conditions.

The limited number of available studies conducted on industrial scale RO membranes from the dairy industry report that accumulation of proteins and development of microorganisms are the main causes of fouling [148–151]. However, all these RO membranes were used in processing milk, whey or whey permeate for up-concentration purposes while water in the permeate stream was discharged. There is no available literature or data about the fouling trends of RO membranes that work in a process water recovery mode from whey UF permeate at industrial scale. The chemical composition of whey UF permeate, prevalent in minerals and lactose, is expected to change the fouling patters compared with what observed when feeding cheese whey to the RO system.
It is thus important to evaluate if implemented clean-in-place (CIP) regimes cope efficiently (or sufficiently) with removal of any biological, organic or inorganic deposits, and most important to

assess the impact on final quality of recovered water in the presence of any encountered fouling threats. Due to the closed nature and high pressure operations, the best way to obtain an accurate characterization of membrane fouling is through membrane autopsy.

Distinction between the different types of fouling and their prevalence on the membrane surface was evaluated by means of various analytical technologies in this thesis. Several industrial RO elements originating from a dairy plant that recover water from whey UF permeate were investigated with the aim to evaluate their main cause of fouling and provide insights for potential corrective actions if necessary. Paper II describes the main findings of membrane autopsy performed on the mentioned dairy RO membranes involved in recovery of process water. The paper is centered on the extensive biofouling trend that surprisingly appears to dominate the permeate surface of such membranes. The chapter is supplemented with results and discussion over the other types of membrane fouling, inorganic scaling and protein fouling respectively.

Box 3. Types of fouling

Organic fouling refers to the accumulation of organic matter. In food systems it consists mainly of proteins, lipids, polysaccharides, nucleic acids and organic acids. When processing cheese whey the organic fouling is caused primarily by the protein fraction which consists largely of β-lactoglobulin (55-65%). Fat may also be found in the organic layer; however its contribution is expected to be minimal in this work due to its removal in previous operations.

Biological fouling is caused by microorganism adhesion and proliferation on the membrane surface, hence formation of biofilms. Microorganisms have a remarkable capacity to adapt and attach to membrane surfaces under most operational conditions. Their encapsulation into a self-produce matrix renders their resistance to the operational conditions (high shear forces, pressures, etc.) and cleaning chemicals. Development of microorganisms into biofilms not only that has negative impact on overall membrane performance but may become also a hot-spot for cross-contamination of the product concentrated at the retentate side[148].

Inorganic scaling is the accumulation of inorganic salts and ions abundantly present in dairy systems such as Ca, Mg, K, etc. Supersaturation of soluble salts at the membrane surface causes salt precipitations and formation of scale. Surface crystallization takes place with production of crystal particles that may lead to perforation of the polyamide active layer of the membrane and allow passage of feed solutes and microorganisms into the permeate stream (recovered water). Such scale consists usually in calcium carbonate or calcium phosphate[147].

The very compact and nonporous nature of RO membranes determines that primarily surface fouling is encountered in such systems as opposed to low pressure membranes (MF and UF) where pore adsorption and clogging occurs aside from surface deposits (hence both internal and surface fouling)[147]. Ineffective cleaning or misuse of fundamental operational conditions may lead to the undesirable irreversible attachment of fouling compounds.

4.2. RO elements sampling overview

At Arla Foods Ingredients (AFI), Denmark, a two-stage RO unit is used to up-concentrate lactose from cheese whey UF permeate and recover process-water. The configuration of the RO unit is schematically shown in Figure 4.1. It consists of a first RO stage containing 5 loops followed by a reverse osmosis polisher (ROP) stage with 2 loops. In both cases, each of the loops contain several pressure vessels arranged in parallel, with each pressure vessel composed of 6 reverse osmosis elements connected in series. It is these RO-elements that were subjected to membrane autopsy and investigated for their fouling patterns. All sampled RO-elements were taken out from the described unit (except RO-E), with their details summarized in Table 4.1.

Table 4.1. Characteristics of sampled RO elements.

	RO-A	RO-B	RO-BB	RO-C	RO-D	RO-E	RO-F RO-F1;RO-F2;RO-F3	RO-G RO-G1;RO-G2;RO-G3
Sampling phase	Phase I		Phase II				Phase III	
Routine cleaning protocol	alkaline & acid solutions; Formulation A		alkaline & acid solutions; Formulation B			alkaline, acid & enzymatic solutions and sanitation at 78°C for 20min	alkaline & acid solutions; Formulation B	
Additional cleaning step	no cleaning; water flush	-	-	sanitation step at 78°C for 20min in pilot plant	-	-		
Manufacturer	Dow/Filmtec Hypershell RO-8038-30					Alfa Laval HSRO-8038-30	Dow/Filmtec Hypershell RO-8038-30	
Membrane material	Thin-film composite polyamide Polyethersulfone (PES)					Thin-film composite polyamide Polyester (PE)	Thin-film composite polyamide Polyethersulfone (PES)	
Operating time	3-4 years	3-4 years	3-4 years	3-4 years	6 months	3-4 years	3-4 years	
Loop/ location within pressure vessel	Loop 2 lead element	Loop 4 lead element	Loop 4 2nd element	Loop 4 3rd element	Loop 4 lead element	Different unit lead element	Loop 4 RO-F1: lead element RO-F2: 3rd element RO-F3: 6th element	Loop 5 RO-F1: lead element RO-F2: 3rd element RO-F3: 6th element

* Operating temperature: 15-18°C; Production cycle: >24h h; CIP cycle: 6h
** all RO elements are common spiral wound membrane that have a recommended max.CIP temperature of 55°C,exception RO-E that is specifically designed to withstand sanitization with hot water, max. sanitation temperature of 85°C

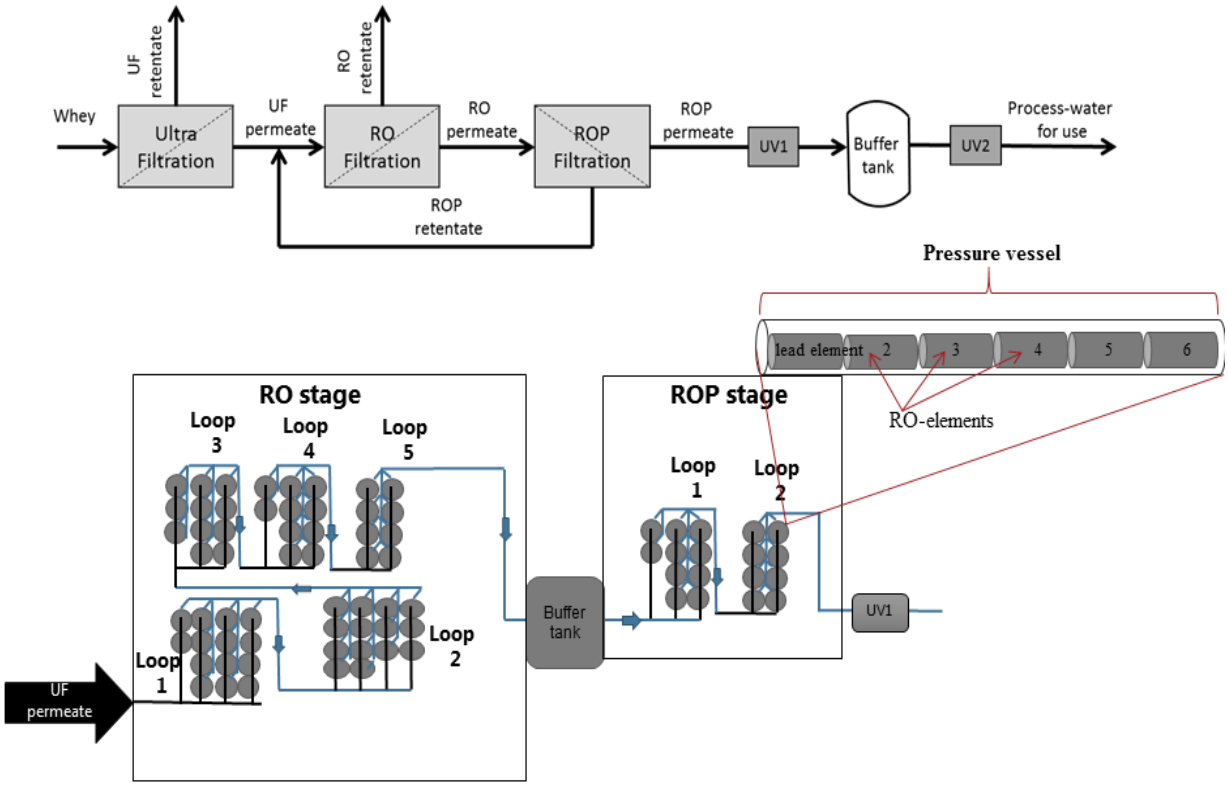

Figure 4.1 Configuration of RO/ROP unit.

Box 4. Cleaning-in-place (CIP)

Cleaning-in-place is the succession of operations conducted at the end of every production cycle with the aim of restoring the performance properties of membranes. In other words, the CIP operations are targeted to remove any (or most) of the fouling types. Due to the closed type of system, cleaning of membranes is a recipe based program that consists in recirculation of various cleaning chemicals which run in a specific sequence at particular temperature values, velocities, concentrations and time periods, without dismantling of equipment. Validation of membrane cleaning is routinely done by monitoring and comparing water fluxes before and after CIP operations. The sequence of cleaning solutions is not standard, but must be adapted and designed in relation to the type of fouling and equipment.

Box 4. Cleaning-in-place (CIP)

One should notice that inappropriate use and selection of cleaning agents may lead to irreversible attachment of fouling compounds. Therefore, the proper design of a cleaning program is crucial. In practice, decisions are best made in relation to observations and results of the membrane autopsy method that allows studying the nature and extent of fouling. The method provides useful information about distribution patterns and fouling composition, but due to its invasive and destructive way it can only be done occasionally.

Typically, a cleaning program would begin with water flushing of the entire system in order to displace (collected fraction) and remove (disposed fraction) any loose deposits and thus allow proper use of chemicals in the following treatments. Water flushing is conducted also in between each of the following treatment steps in order to wash away the cleaning agent and also the released foulants. An alkaline step (high pH cleaning at ~11-12) usually comes first to remove proteins, fats and biological matter. This alkaline treatment is based on formulations that contain NaOH or KOH as the main active ingredient, often combined with detergents or comparable alternatives to boost their cleaning power. In some applications, where heavy protein fouling is present as seen for example on membranes that process feed with high organic load such as cheese whey, an enzymatic cleaning step may be implemented. The enzymatic solutions contain in particular proteases, if necessary combined with lipases, to achieve an optimal cleaning level. Next, an acid step follows (low pH cleaning at ~2) with nitric acid or citric acid as main active ingredient, aimed to dissolve the mineral scale or metal oxides fouling. The dramatic changes in pH also ensure that any enzymes from a previous step are deactivated. It is worth noticing here that many of the cleaning formulations contain extra chemistry (e.g. surface active agents) and this is proprietary knowledge of the suppliers[152].

A disinfection step, not necessarily considered part of the CIP program but more like a stand-alone sanitation-in-place (SIP) step, can be added in applications where prevention of microbial growth is sought. One can distinguish two methods: chemical or heat sanitation. Evidently, proper cleaning is a prerequisite for effective membrane sanitation since the chemical sanitizers may react with the residues of organic matter. The chemical sanitation is more common due to its lower costs and involves the application of solutions based on a hydrogen peroxide / peroxyacetic acid blend. These compounds are efficient disinfectants, but their use may compromise membrane integrity. Heat sanitation is another possible way to prevent microbial growth in RO membranes, however most commercial membranes do not tolerate temperatures higher that 55°C, unless specially designed to withstand temperatures in the high range[153].

4.3. Confocal laser scanning microscopy (CLSM)

Confocal microscopy is a particular type of fluorescence microscopy, which uses fluorescence light from focal points to record magnified images of fluorescing specimens. Given that not all organic matter can undergo fluorescence (auto-fluorescence), a sample needs to be stained with fluorescent dyes (fluorochromes) prior imaging. Such fluorochromes are designed to bind to target molecules and upon excitation, particular parts of the specimen can be highlighted and subsequently imaged by means of a fluorescence microscope.

The greatest achievement that confocal microscopy brings is the three dimensional visualization of samples without performing a physical sectioning (so-called z-series with 3D imaging). CLSM is an important tool in biofilm research, useful to obtain information about spatial distribution of different constituents and understand more the interrelations within the biofilm matrix. When calibration and constant microscope settings are in place, quantification of the matrix building components based on measuring distances and determining their area/volume may also be possible[154]. In this thesis the quantification aspect was not explored, but CLSM was used instead as a qualitative tool in recording images on industrial RO membrane and evaluating the state of the microorganisms left on the membrane surface after CIP operations (microorganisms with or without biofilm matrix).

The aim of confocal microscopy is to only detect light from the focal point as this will be translated into sharper and better resolved images. Therefore, a confocal microscope is a modified conventional microscope, which instead of imaging simultaneously the entire specimen will direct light to only one single pin-point onto the sample and collect back only the emitted light from this focus point while rejecting anything else by means of a pinhole placed before the detector (in the conjugate plane), see Figure 4.2. The light source is typically a laser due to their powerful and coherent type of light compared to the traditional lamps, and a CLSM instrument will typically be equipped with several laser lines. A pinhole placed in front of the laser will create a point-wise illumination source as well. Afterwards, the beam is reflected by the dichroic mirror and focused onto the sample by the objective lenses just as in a conventional microscope. However, the sample will be illuminated, this time, in one single point instead of a wide area, due to the pinhole which restricts the amount of light to pass[155].

Fluorescence occurs in the illuminated area and light from the entire volume of confocal cone is collected by the objective lenses and transmitted towards the detector, most often a photomultiplier tube (PMT). If the entire collected light was to be sent directly to the detector, the image formed would still fall under the principle of conventional fluorescence microscopy since light out of focus would still be detected. Thus, a second pinhole, placed in the conjugated focus plane, allows passing light primarily from the focus point while rejecting to a high degree the out-of-focus light. The image formed in this way depicts just the image of the spot which was illuminated. It must be noted that it is the second pinhole that makes the set-up become confocal. The extent of light cut away is dictated by the pinhole size[156]. In order to visualize the entire picture, the point illumination

procedure has to be repeated across the entire specimen either by moving the sample or more often by scanning the laser beam across the sample, hence the confocal laser scanning moniker. In terms of laser beam scanning mode, different techniques are commercially available, each of them addressing improvements to overall image quality or speed:

- Systems which perform a single beam scanning, embedded in most confocal laser scanning microscope set-ups.
- Multiple beam scanning, found in the spinning disk (Nipkow disk) confocal microscope, characterized by high speed imaging.

A computer coupled to the detector is needed in order to store the incoming information and build-up the image one pixel at a time. In this case the images are digital and are not readily available to be seen at the viewing site as is the case in the conventional microscope. In the z-series, a set of optical sections are recorded sequentially for each focus plane while the stage moves along the z-axis at pre-defined depths. Furthermore, the z-stack of images collected can be assembled together in a 3D view by means of image processing software. The 3D-piezoelectric scanner in the stage ensures a precise movement and therefore an increased 3D confocal resolution. When recording the z-stacks the main inputs for the software are the number of x-y optical sections to be taken and the stage step as a measure of depth scanned[156].

A biofilm is expected to consist predominantly of proteins, nucleic acids, lipids and microorganisms largely dispersed within a sticky and dense matrix of polysaccharides [157]. Its complexity makes it challenging to capture all biofilm features with one single fluorescence label. In lack of such label, several fluorescent dyes are commonly used in combination to target individually the different components and record a qualitative confocal image of the overall biofilm structure. When selecting the types of fluorochromes to use one should first make sure that their absorption maximum is close to one of the laser lines available in the instrument as their emission signal will get weaker the further away the laser line is. Second, when more than one fluorochromes is used, it is important that the fluorescence dyes are chosen in such way that their emission signal have as minimal a spectral overlap as possible so that imaging and distinguishing between the several types of information is possible[154].

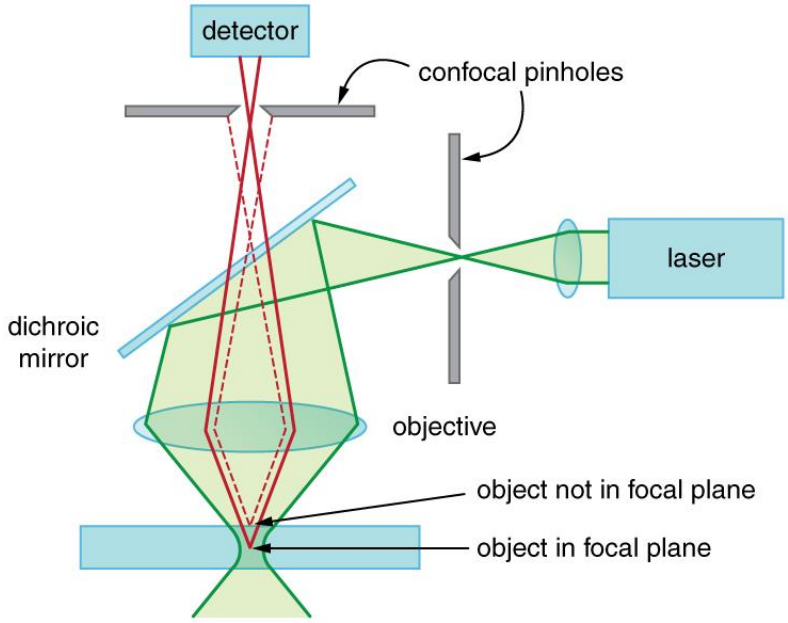

Figure 4.2 Illustration of a confocal microscope measurement interface.
Source: https://i.stack.imgur.com/jWIbC.jpg

Paper II

Biofouling on RO-membranes used for water recovery in the dairy industry

Iuliana Madalina Stoica, Eirini Vitzilaiou, Henriette Lyng Røder, Mette Burmølle, Dorrit Thaysen, Susanne Knøchel, Frans van den Berg

Journal of Water Process Engineering 24(2018)1-10

Journal of Water Process Engineering 24 (2018) 1–10

Contents lists available at ScienceDirect

Journal of Water Process Engineering

journal homepage: www.elsevier.com/locate/jwpe

Biofouling on RO-membranes used for water recovery in the dairy industry

Iuliana Madalina Stoica[a,*], Eirini Vitzilaiou[a], Henriette Lyng Røder[b], Mette Burmølle[b], Dorrit Thaysen[c], Susanne Knøchel[a], Frans van den Berg[a]

[a] Department of Food Science, Faculty of Science, University of Copenhagen, Rolighedsvej 26, DK-1958 Frederiksberg C, Denmark
[b] Department of Biology, Faculty of Science, University of Copenhagen, Universitetsparken 15, 2100, Copenhagen Ø, Denmark
[c] Arla Foods Ingredients, Sønderupvej 26, DK-6920 Videbæk, Denmark

ARTICLE INFO

Keywords:
Reverse osmosis (RO) membranes
Water recovery
Biofouling
CIP
Confocal laser scanning microscopy (CLSM)

ABSTRACT

Recovery followed by re-use of process-water obtained from dairy effluents by means of reverse osmosis technology is one route that can provide the dairy industry with the possibility to reach sustainable water regimes. However, membrane fouling is a phenomenon that limits both the efficiency and increases the running costs of such reverse osmosis units and can potentially alter the quality characteristics of permeate water. In this paper, several industrial-scale RO membranes used for recovery of process-water from whey UF permeate have been examined for their fouling tendency. At the end of a complete clean-in-place (CIP) protocol based on alkaline-acid formulations, biofouling appears to be the main issue in the investigated RO-elements. Between 4.19 and 5.69 $\log_{10}$ (CFU cm^{-2}) of viable microorganisms still remained on the membrane retentate surface and, more surprisingly, evidence of significant contamination was found on permeate side of these particular membranes. Microbiological analysis indicate that minor loads of microorganisms do pass into the permeate streams but final UV treatments ensured final process-water with non-detectable levels. There is a need for optimization of cleaning procedures and finding the best compromise for achieving surface disinfection while still preserving membrane integrity and not compromising the water quality.

1. Introduction

Climate change responsibilities, fresh water shortage, strict discharge regulations and financial gains are all factors that drive industries to seek out more sustainable practices and possibilities of water recovery in order to lower their effluents and water intake. Over the years, reverse osmosis (RO) membrane technology has demonstrated to be an excellent platform for recovery of water with high quality characteristics. Acting as a barrier to nearly all pollutants, the RO membranes produce water which can fulfill the strict quality regulations for public health and environment protection [1].

The food industries depend upon clean fresh water for a wide range of processes and cleaning operations and the implementation of safe and efficient water recovery strategies has become a major priority for many stakeholders [2]. Several examples of water recycling or reuse within the food sector have been reviewed by Vourch et al. [3] and Casani et al. [4]. Emerging originally as the biggest consumer and wastewater producer within the food area, the dairy industry is becoming one of the leaders in water reuse practices [5]. This is enabled primarily by their vast experience in applying membrane technology for concentrating or fractionating different liquid streams, but also due to the great potential of recovering water from different process streams such as milk or cheese whey [6,7]. This trend is also stimulated by the large volumes of water required for cleaning [8]. Raw whey was traditionally considered a big biological pollutant. However, using various membrane technologies in series, such as ultrafiltration (UF) followed by RO and possibly a RO-polisher, it can now be valorized by harvesting high nutritional products − whey and lactose powder − and ultimately the liquid can be recovered as water which can qualify for reuse in production steps such as heat exchangers and clean-in-place (CIP) operations [9].

RO units primarily use reverse osmosis membrane elements with a spiral wound configuration. The main reason for this is their compact format, advantageous price, high membrane surface area in relation to their volume, and fitness for multiple applications [10]. Unfortunately, when processing a product with increased organic loads, such as permeates from whey separation, organic fouling and more notable biofouling are major risks that need to be minimized. Next to the potential safety risks, the biofilm formation can have a serious negative impact on the performance of the filtration system by lowering the trans-membrane flux [11] and cause decreased salt rejection [12]. Most published works conclude that biofouling appears to be an inevitable

* Corresponding author.
E-mail address: iuliana.stoica@food.ku.dk (I.M. Stoica).

https://doi.org/10.1016/j.jwpe.2018.05.004
Received 30 January 2018; Received in revised form 1 May 2018; Accepted 3 May 2018

phenomenon, which dictates the need to develop strategies to keep it under control. These may include development of novel, more easily cleanable membrane configurations and materials or control of fouling of existing technologies by optimizing the cleaning formulation and operational conditions in relation to the characteristics of the feed product. However, the operation and maintenance costs combined with the risk of destroying the membranes structural integrity will increase if too frequent or too *harsh* cleaning is applied. An additional sanitation-in-place (SIP) step, right after CIP using e.g. peroxides or chlorine containing formulations, could shorten the lifetime of membrane elements considerably and is thus limited to special occasions. Like any technological solution in the food industry, a positive cost-benefit assessment will make the difference, and running costs of the equipment is an important aspect in this.

In spite of cleaning and technological improvements of membrane properties aimed to mitigate the issue, biofouling is still reported on whey concentration RO membranes by e.g. Hassan et al. (2009) [13], Adnan et al. [14] and Tang et al. [15]. Their findings showed that CIP was not entirely efficient in removing the resident microflora and could in the worst case result in cross-contaminating of the concentrated product. Similarly, when a new water recovery mode is added to the functionality of existing RO systems processing whey UF permeate, it becomes important to understand the biofouling trends, and even more, the impact on the RO permeates quality. The published work of Meneses and Flores [16] supports the feasibility and safety aspects of using the recovered process-water for cleaning purposes. Depending on the specific industry and application, the process water treatment operations may have multiple RO units in series and this is generally followed by UV treatment to further safeguard the microbiological quality.

Here we focus on the extent of biofouling on industrial-scale RO membrane elements used in recovering process-water from whey UF permeate. Operational conditions in industrial set-ups are in general complex due to factors which may be hard to be controlled, such as variable quality of whey UF permeate (batch-to-batch and dairy-to-dairy variations), unforeseen break-downs, leakages, or simply due to parameters that are occasionally tuned based on production demands. And even on a short term (i.e. weeks) the semi-continuous production chain in RO (-production-CIP-production-CIP-) has many unpredictable dynamic patterns where the previous run(s) can leave an imprint on the elements, influencing the present performance [17]. All these render any industrial RO-membrane to be exposed to a large set of varying conditions during their life-time, which are impossible to simulate realistically in laboratory studies. It is therefore important to derive operational practices based on observations attained from industrial-scale RO-membranes and evaluate the efficiency of industrial cleaning in removing any type of fouling. To do so, membrane autopsy is the best tool to gain accurate insights concerning fouling composition, patterns and their residing communities. In this study the condition of used industrial scale reverse osmosis membranes on both retentate and permeate surfaces will be characterized from a biofouling perspective in order to provide new knowledge which may help to improve practices for reusing process-water.

2. Methods and materials

2.1. Collection of RO membrane

A total of six RO-elements have been subjected to membrane autopsy and examined for their fouling tendencies. Elements are denoted alphabetically in Table 1 where their membrane specific characteristics can be found as well. With one exception, namely RO-E, all elements originate from the same processing plant, which uses cheese whey UF permeate trucked in from different dairies as a feed product for a two stage reverse osmosis system (RO plus RO-polisher) operated in a recovery mode for process-water, see Fig. 1a. The elements investigated were collected in particular from the first stage − RO − of the reverse osmosis process. The collection has been conducted in two steps, namely Phase I (RO-A and RO-B) and six months later Phase II (RO-BB, RO-C, RO-D and RO-E). Phase I was initiated as an exploratory stage, meant to assess the extent of fouling at this particular RO unit. In this phase the first interest was to determine the level of actual surface fouling at the end of a production cycle that a CIP protocol would have to remove or reduce. For that purpose, element RO-A was collected prior to cleaning, after flushing with water. Also in Phase I, element RO-B was collected (at a different location/loop), after subjecting the entire unit to the current CIP protocol, which at that time used an alkaline-acid cleaning formulation. This formulation had been in place for more than one year. In Phase II all elements have been collected after having completed their CIP cycle. It should be noted that due to a management decision, shortly after Phase I the routine CIP protocol for the RO units has been changed to a new alkaline-acid cleaning formulation. In Phase II it was also possible to inspect the surface of element RO-E from a different production plant. It was in particular interesting to examine RO-E due to the heat sanitation step included in the routine CIP-SIP regime. Such a SIP step, in particular via hydrogen peroxide or by short heat treatments is a known efficient way to counteract biofouling trends. To further explore this option, element RO-C was taken from production and moved to a pilot unit to undergo a heat sanitation step. Given their industrial history of use, distinct locations within the unit and the before-mentioned complex process dynamics of membrane operations, each inspected RO-element should be considered as a snapshot of its independent scenario. Direct, quantitative comparisons can thus not be made; this is only possible to a minor extent for RO-B, RO-BB, RO-C and RO-D due to their origin being the same pressure vessel. All RO-elements were transported in polyethylene bags from the production site to the university on the day of their removal, and stored at 5 °C for up to 5 days until autopsy and analysis.

2.2. Membrane configuration and autopsy procedure

The RO membrane itself is structured in a three layer configuration, namely a thin polyamide layer (< 200 nm), deposited on top of a polyethersulfone porous layer (about 50 μm), placed on top of a non-woven fabric support sheet, see Fig. 2b. The polyamide top layer is responsible for the permeability of water and rejection of dissolved impurities, whereas the other layers give the membrane mechanical strength. Therefore, the concentration of the feed product takes place at the side of the polyamide layer which will be further named as retentate surface side, while the bottom support layer represents the permeate surface side.

When constructing them in the spiral wound elements (Fig. 2a), several membrane sheets are laid out alternating their display, namely one facing inward while the next membrane faces outward. Following this arrangement in the whole stack, the retentate sides of consecutive membranes end up facing each other, and similar sorting happens for the permeate sides. The edges of consecutive membranes are glued by sealing their permeate sides together, with a fine permeate spacer in between, leaving only one side to serve as an exit for the permeate stream. The outer sides of the glued membrane envelopes (the retentate sides) are also separated, this time by coarser feed spacers in order to ensure flow of the feed product. Finally a central tube is attached to the exit side of each of the resulting envelopes and rolled around the tube creating the spiral shape, see Fig. 2a, which is further enclosed in a polypropylene hard outer shell for the elements investigated.

The autopsy was initiated by cutting the polypropylene hard outer shell and exposing the membranes by unrolling all leaves from their connection to the central permeate tube. For each RO-element, two non-consecutive envelopes with sufficient distance between each other were investigated. Next, a series of large coupons of 10 × 10 cm size were cut aseptically along each leaf surface, as illustrated in Fig. 1b, and inspected for biofilm presence by means of confocal laser scanning microscopy (CLSM). All coupons were stored at 5 °C until the following

Table 1
Characteristics of the sampled RO-elements.

	RO-A	RO-B	RO-BB	RO-C	RO-D	RO-E
Sampling phase	Phase I		Phase II			
Routine cleaning protocol	alkaline & acid solutions; Formulation A		alkaline & acid solutions; Formulation B			Alkaline, acid & enzymatic solutions and sanitation at 78 °C for 20 min
Additional cleaning step	no cleaning; water flush	–	–	sanitation step at 78 °C for 20 min in pilot plant	–	–
Manufacturer	Dow/Filmtec Hypershell RO-8038-30					Alfa Laval HSRO-8038-30
Membrane material	Thin-film composite polyamide Polyethersulfone (PES)					Thin-film composite polyamide Polyester (PE)
Operating time	3–4 years	3–4 years	3–4 years	3–4 years	6 months	3–4 years
Location within the unit	Loop 2	Loop 4, 1st	Loop 4, 2nd	Loop 4, 3rd	Loop 4, 1st	Different unit

Operating temperature: 15–18 °C; Production cycle: > 24 h; CIP cycle: ≈6 h.
All RO-elements are common spiral wound membrane that have a recommended maximum CIP temperature of 50 °C, exception RO-E which is specifically designed to withstand sanitization with hot water for prolonged times, up to 85 °C.

day when visualized with CLSM. Note that Phase I was conducted as an exploratory phase to capture any potential biofilm structure present across the RO-membranes. Thus, an extensive sampling pattern was employed in order to capture enough biofilm structure variation, and identifying a potential location-effect over one membrane surfaces due to different flow profiles [18]. Phase II was used as a verification experiment to collect more *snap-shots* (as described before) of normal production, and as demonstration for a relatively fast collection of information on CIP (and/or SIP) efficiency and residual surface fouling.

2.3. Isolation

Sample collection for isolation purposes was done via a scrapping or swabbing procedure. A 10 µL plastic sterile loop (SigmaAldrich) was used to scrape and collect samples from both the retentate and permeate side whenever thicker deposits could be seen on the membrane surface. These samples were streaked onto both standard MYPG selective agar prepared with 0.01% chloramphenicol and 0.005% chlortetracycline antibiotics for yeast isolation and plate-count-agar (PCA) plates for heterotrophic bacteria isolation. Whenever scrapping was not possible due to a lack of a visible residual fouling, samples were collected instead via the swab procedure using sterile 10 × 10 cm compress tissues. The swab samples were placed on agar plates at room temperature and then removed after one day. All plates (scraping and swabbing) followed incubation at 25 °C until growth and dominant colonies correspondent for both sides – retentate and permeate – were isolated and sequenced in a separate investigation (data not shown).

2.4. Microbiological analysis on membrane surface

Standard aerobic plate counting was performed on standard PCA substrate by the drop plating technique as described by Herigstad et al. [19]. The microbial population levels were estimated based on

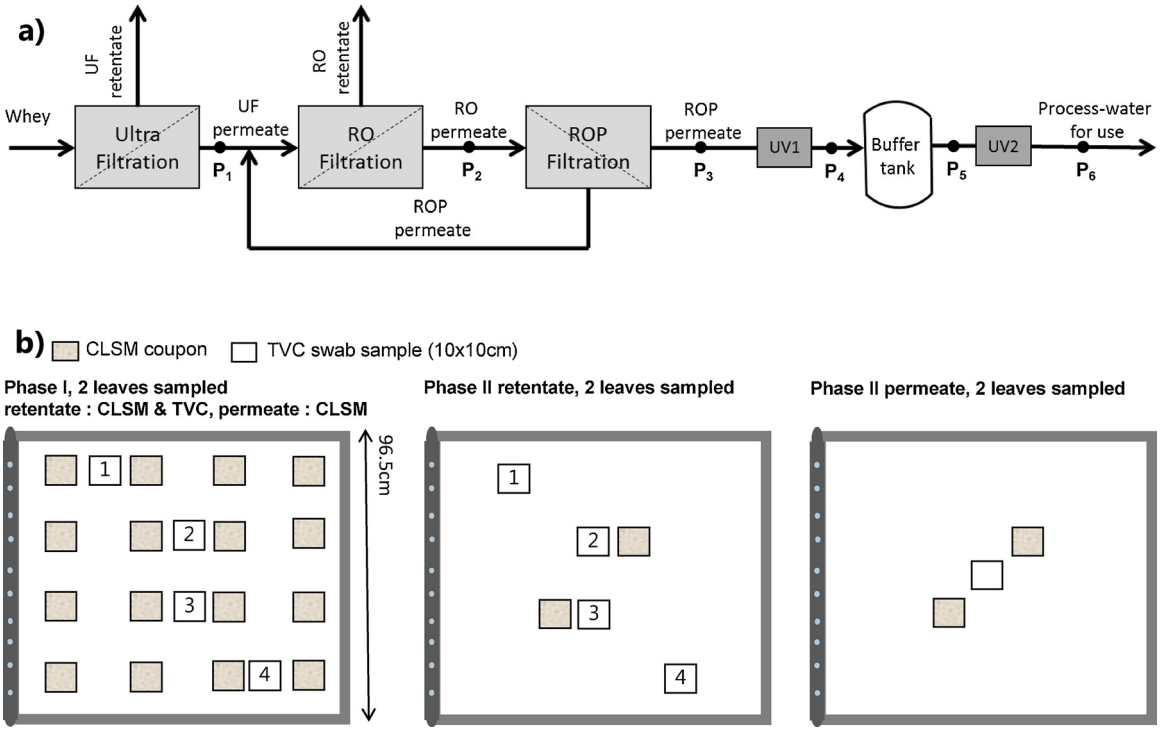

Fig. 1. (a) Overview of the Reverse Osmosis (RO)/RO polisher (ROP) water recovery system; (b) Membrane surface sampling design for Phases I (retentate side) and II (retentate and permeate) for Total Viable Counts (TVC) and Confocal Laser Scanning Microscopy (CLSM) analysis.

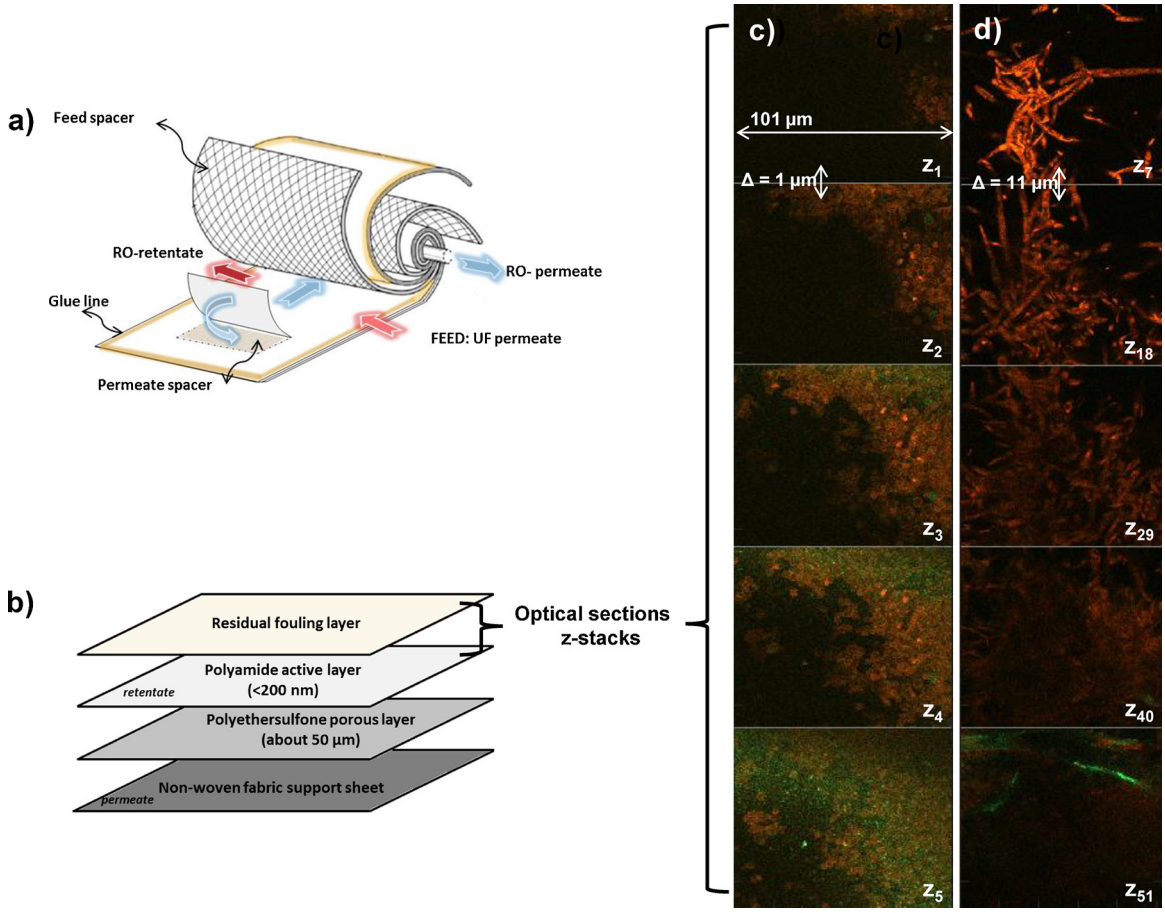

Fig. 2. (a) Overview of a spirally wound membrane element, design and functionality; (b) Schematic overview of a membrane leaf layer structure; (c) Representative CLSM depth profile (RO-B, retentate side) with 1 µm step distance; (d) Representative CLSM depth profile (RO-B, retentate side) with 11 µm distances.

10 × 10 cm areas, using four sampling spots on the retentate side (Fig. 1b). Note that microbial levels were determined also on the permeate side, however using one single spot per inspected leaf and conducted only for membrane samples originating from Phase II (Fig. 1b). Sample collection was done via a swabbing procedure. Briefly, sterile 10 × 10 cm compress tissues were first pre-hydrated in autoclaved 0.9% saline peptone water (SPO) in a sterile closed container. The moisturized tissues were used to swab the assigned area and placed in sterile stomacher bags. 50 mL of autoclaved 0.9% SPO was added to each bag under sterile conditions, followed by homogenization in a Stomacher® 400 Circulator (Seward Limited, UK) for 1 min. The homogenized solution from each bag served as zero-dilution for their corresponding sampling. Next, series of tenfold dilution were performed at four levels in 9 mL of 0.9% SPO for each sample and plated onto PCA agar plates by dispersing five evenly spaced 5 µL drops. After the drops on the agar dried (10–20 min) the PCA plates were inverted and incubated at 25 °C for 17–20 h. The total colony-forming-units (CFU) over all drops at the countable dilution level (30–300 colonies) were determined, scaled back and expressed as $\log_{10}(\text{CFU cm}^{-2})$.

2.5. Microbiological analysis on RO permeate streams

RO permeate samples were collected after 10 h of production(hence, following the last CIP cycle), from positions P_1- P_6 as indicated in Fig. 1 and transported in the same day to the University's lab. During transportation the temperature in containers fluctuated between 7 and 10 °C. At arrival, all samples were stored overnight at 4 °C, followed by microbial analysis next morning. Standard aerobic plate counting was conducted in PCA agar via the spread-plating technique. In addition, aerobic plate counting was conducted in parallel also on MYPG prepared with antibiotics, as described before, in order to support growth for only yeast species and thus estimate yeast population levels. Tenfold serial dilutions, done in duplicate at three levels, were performed for each of the initial samples (zero-dilutions) and spread further onto PCA and MYPG-antibiotics plates. During spread-plating a volume of 100 µL was taken from each dilution, and spread individually over one agar plate. Following this method, a limit of detection (LOD) of 10 CFU mL^{-1} could be achieved. Since low cell counts were expected in samples taken from P_3, P_4, P_5 and P_6, the spread plating technique has been supplemented with the triple plate method for only the initial sample (zero-dilution), in order to achieve an LOD of 1 CFU mL^{-1}. Triple plating here means that 1 mL was taken directly from the intended sample and equally distributed in three agar plates (approx. 0.33 mL per plate). At the end of plate incubation, the colonies grown on all the three plates were added. Incubation was done at 25 °C for all plates, followed for 10 days to ensure that slow growing or injured species (e.g. after UV treatment) will get sufficient time to develop. Due to low cell counts, results are shown as CFU mL^{-1} as opposed to microbiological analysis on membrane surface where counts are expressed in $\log_{10}(\text{CFU cm}^{-2})$.

2.6. Confocal laser scanning microscopy

Coupons dedicated for confocal laser scanning microscopy (CLSM) were analyzed within two days of their removal from membrane elements using a CLSM instrument (Zeiss LSM 800, Carl Zeiss Inc.) equipped with an inverted microscope and multiple laser lines. Note

that in the exploratory Phase I, a total number of 16 coupons for each sampled leaf were inspected, whereas in Phase II – given the aim of a quick spot check – only 2 coupons per leaf were visualized (Fig. 1b). Each coupon was divided into two sub-samples and dedicated to visualize their surface − one for the retentate side and the other for the permeate side. Observations of spatial distribution of microorganisms and extracellular polymeric substances (EPS) potentially present on the membrane samples were achieved by combining three fluorescent dyes selected based on literature [20,21]. All fluorochromes were purchased from Invitrogen/Molecular Probes (Eugene, OR, USA). Briefly, nucleic acids were stained with SYTO 9 (LIVE/DEAD® Biofilm Viability Kit, L10316), the entire biofilm matrix was stained with SYPRO Ruby (SYPRO® Ruby Biofilm Matrix Stain, F10318), labeling all types of proteins, whereas Concanavalin A (ConA, C860) was chosen to target specifically the glycoproteins within the entire biofilm matrix, thus the bacterial EPS glycoconjugates. The three stains (SYTO 9, SYPRO Ruby and ConA) were excited at 483 nm, 283 nm and 558 nm, respectively. Their detection wavelengths were optimized for minimum cross-talk based on pre-experiments and from there on applied to all samples. This resulted in emission from SYTO 9 (nucleic acids, bacterial cells) being recorded in the range of 480–520 nm, emission from SYPRO Ruby (biofilm matrix) acquired between 599 and 700 nm and emission from ConA (EPS glycoconjugates) was detected at 535–592 nm. During one recording an image for each channel was generated with a frame size of 512 × 512 pixels and a field of view of 101.41 × 101.41 µm, acquired via an oil objective 63 x (N.A. 1.2). A representative example is shown in Fig. 3; in all other figures in this paper the channel-merged image is used.

The staining procedure involved the preparation of a working solution which contained equal volumes of each stain prepared according to the supplier's instructions. A similar method of staining simultaneously with three fluorochromes has been employed by Bar-Zeev et al. (2014) [20]. A 200 µL volume of the final mixture was added on top of the coupon piece, on the surface side intended to be imaged. The prepared sample was incubated in darkness at room temperature for 30 min, followed by rinsing with 15 mL of sterile water in order to remove unbound stain and all loosely adherent cells or thicker deposits of organic matter. Generally, a gentle rinse with a few mL of water is recommended. In our study a more intensive washing was chosen to ensure that any remaining microorganisms were attached to the sample surface. Coupons were then fixed onto a glass slide using a cover glass and transparent nail polish. An example of a z-stack of the coupons can be seen in Fig. 2c for a layer of budding yeast cells of approximately 5 µm thickness, deposited on the RO-B retentate surface. In this case, z_1 represents the top image, while z_5 captures the bottom layer when reaching the membrane surface. Similarly, Fig. 2d shows a z-stack for a filamentous yeast layer deposited on the RO-B permeate surface. Due to its thickness, a fairly larger number of optical sections were needed here in order to capture the entire bulk structure where z_7 is the top/first image inside the layer and z_{51} is the optical section in the overall z-stack where the membrane surface is reached. We can assume that the corresponding yeast layer here reaches about a 47 µm thickness. For simplicity, all CLSM images presented in this paper are the most representative optical section within a particular z-stack, which could e.g. be z_2 and z_{18} for measurement series displayed in Figs. 2c and d, respectively.

3. Results and discussions

Several RO-elements utilized for processing whey UF permeate were screened for their fouling status and the microbial community characterized from a quantitative and morphological perspective based on total viable counts of aerobic microbial cells and microscopic analysis.

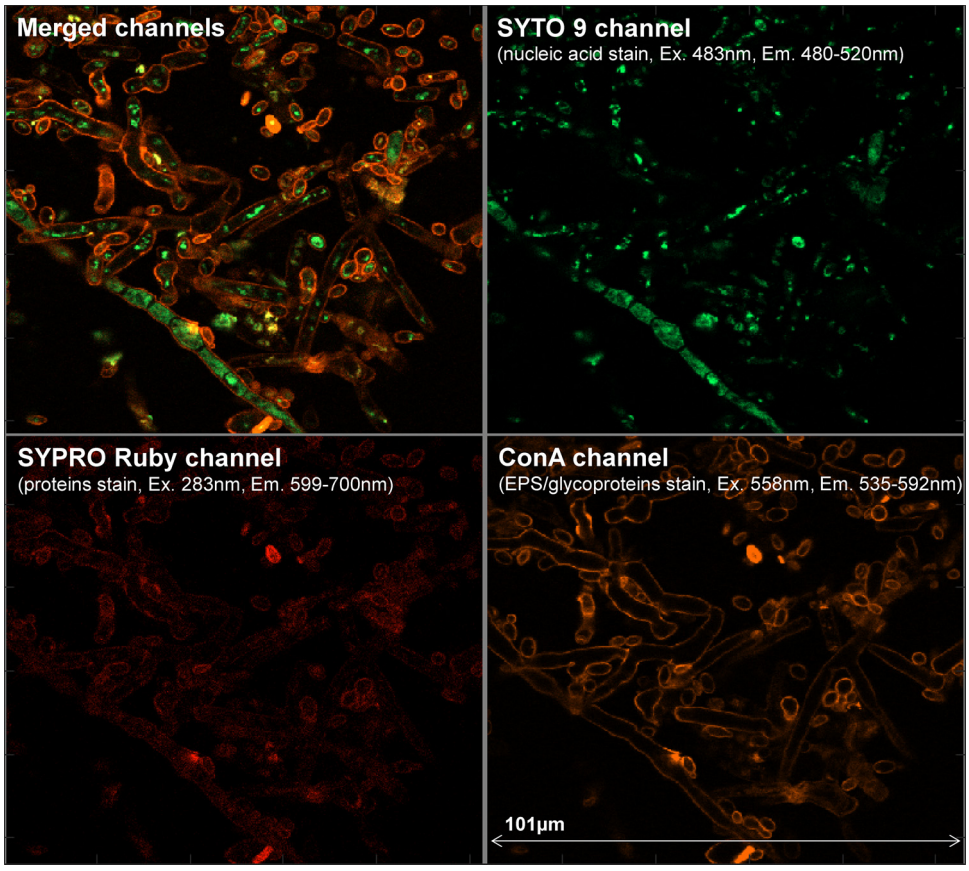

Fig. 3. Representative CLSM recording for merged channels and the three distinct staining agents.

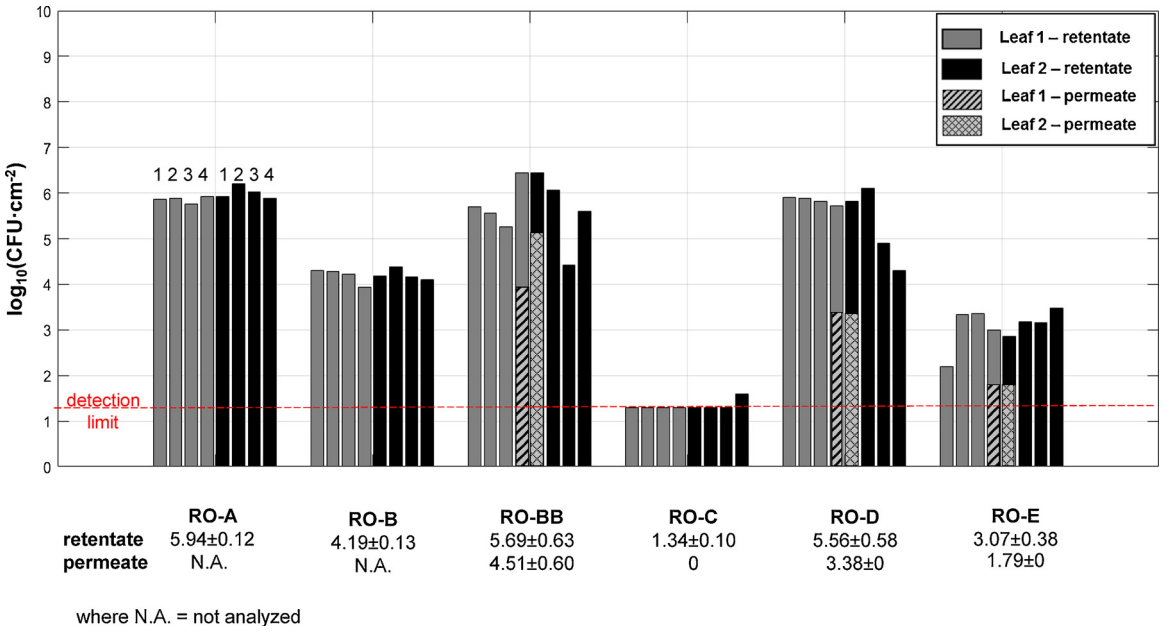

Fig. 4. Total Viable Counts (TVC, 25 °C) on the retentate side of membrane elements sampled in both Phase I and Phase II; TVC found on permeate side of elements sampled only in Phase II (see Table 1 and Fig. 1b for details; LOD 1.3 $\log_{10}$(CFU cm^{-2}).

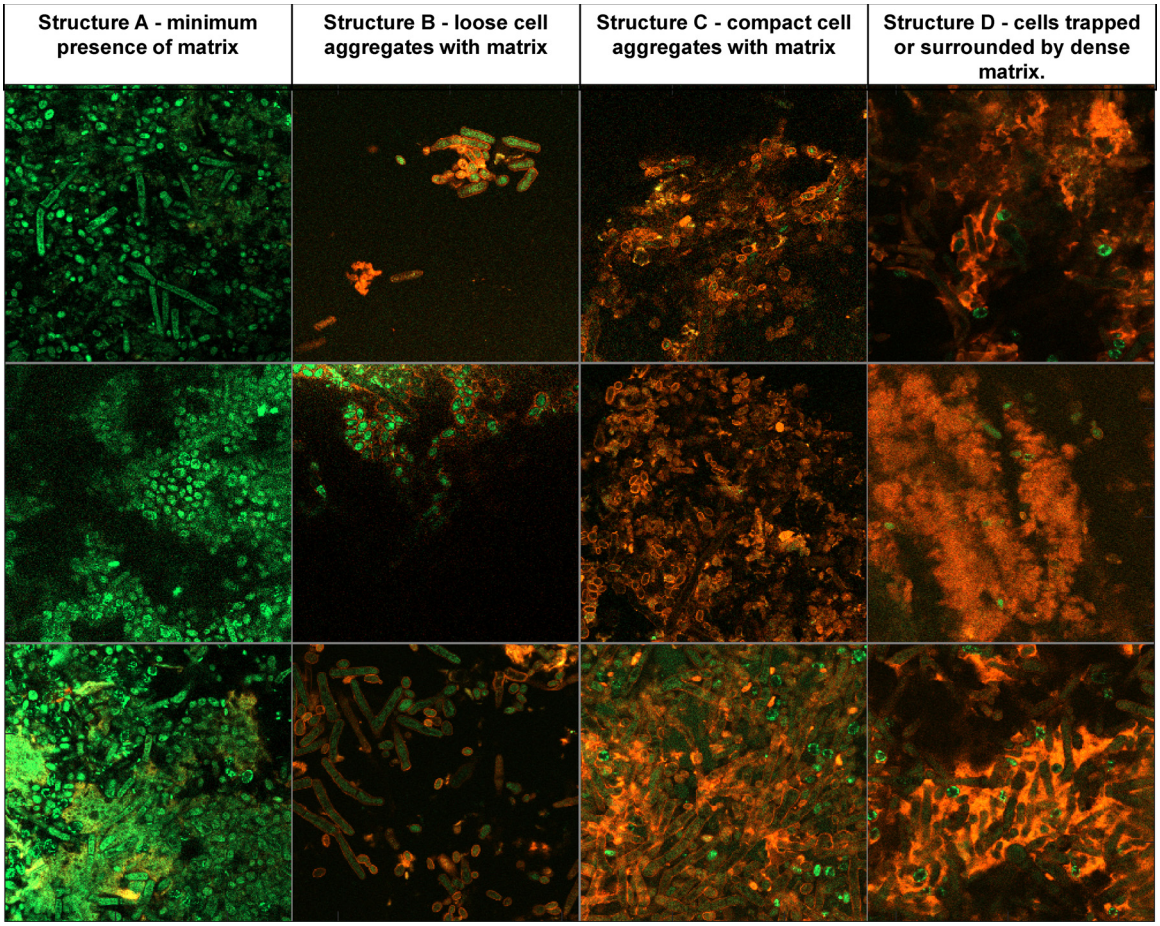

Fig. 5. Type of observed biofilm structures, visualized by three representative recordings, on the retentate side of industrial RO membranes used for water reclamation.

3.1. Visual characteristics of RO-elements

Collected prior to cleaning, after flushing, element RO-A displayed (as expected) wet yellow-colored deposits covering the entire retentate side of each membrane leaf. Both yeast and bacteria could be observed by microscopy in the correspondent foulant. Nothing could be seen on the permeate side of RO-A. The retentate side of all other elements appeared cleaned upon visual inspection. The overall appearance of a clean surface suggests the efficiency of the different CIP protocols in removing most organic fouling from the retentate side of the membranes. On inspection of the permeate surfaces of membranes from RO-B, RO-BB, RO−C and RO-D, all showed isolated white-colored deposits which contained mainly filamentous yeast. This foulant was in-homogeneously distributed across membrane's surface.

3.2. Microbiological analysis on membrane surface

Fig. 4 summarizes the counts on the retentate surface of each inspected membrane. Microbial levels did not vary significantly between the two leaves from the same element. As stated before, all cleaned RO-elements showed evidence of having undergone the CIP protocol, regardless of their cleaning formulation, as most of the organic matter was removed. However, certain levels of a microbial population still remained on the membrane retentate surface. An average microbial count of 4.19 $\log_{10}$(CFU cm^{-2}) was found on RO-B (CIPed), retentate side, whereas both RO-D and RO-BB (both CIPed) had a higher microflora level (between 5.56 and 5.69 $\log_{10}$(CFU cm^{-2})), which was unexpectedly comparable with an average of 5.94 $\log_{10}$(CFU cm^{-2}) detected on RO-A that had only a water flush (Fig. 4). Similar levels have been reported before by other researchers on industrial RO membranes where the feed product consisted of whey [22]. Considering that the inspected RO-elements all had been processing whey UF permeate, a general lower count would have been expected since the upstream ultrafiltration unit should retain most of the microbial load.

3.3. Confocal laser scanning microscopy

Next to the total counts, visualizing the status of residual microflora can assist in understanding the extent of surface attachment. Given the large number of recordings obtained in Phase I, it was observed that most images display structures that can be classified in four general categories; representative examples of these four biofilm structures are presented in Fig. 5. Applying this visual classification it can be determined that most structures identified on RO-B show loose bacterial cells surrounded or trapped in a biofilm matrix (Structures B and D), with significantly less recordings that display free cells (Structure A).

The microbial community of non-CIPed element RO-A, retentate side, consisted mainly of streptococci and rod shaped bacteria, plus budding and filamentous yeast, as isolated from PCA and MYPG-antibiotics selective plates. Upon inspection of the retentate side of RO-A coupons under the confocal microscope, it was found that the different isolates were in most cases present as free cells (Structure A) or packed in a dense protein-like matrix (Structure D; see Fig. 6 for a quantitative evaluation based on visual scoring of the CLSM recordings). It should be noted here that the areas involved (approximately 1m^2 per leaf, see Fig. 1b) in combination with microscopy make quantification challenging. Moreover, in the CLSM we actively searched for a contamination spot in each measurement sample coupon. Hence, the results presented should be interpreted as semi-quantitative. Several permeate side RO-A coupons, selected randomly, were investigated by confocal microscopy. None of them had evidence of contamination on the permeate surface. As a result, CLSM analysis continued by only evaluating the retentate surface of RO-A coupons.

The structures on RO-B (CIPed) retentate consisted mostly of loose yeast cell aggregates (Structure B), see Fig. 6. Mainly budding and filamentous yeast with the same morphology as found on RO-A could be isolated from RO-B retentate. Some evidence of remaining bacterial rods was found in the CLSM images captured, albeit only on one coupon. A common characteristic for RO-B and all other cleaned RO-elements is that the residual microflora present on the retentate surface exhibits cellular membranes stained primarily by ConA. It is known that microorganisms tend to encapsulating themselves in a self-produced extracellular polymeric matrix (EPS) in order to survive stressful conditions, such as shear stress, competition, low nutrients availability, etc. [23]. Such structures were not identified in most of the images recorded on the retentate RO-A coupons, which could suggest that the production of extracellular polysaccharides (EPS) may have been stimulated by the hostile conditions induced by cleaning, see Figs. 7 and 8. An alternative interpretation is that the applied cleaning treatments, specifically the alkaline step in the CIP recipe, may expose the deeper, attached layers that contain more EPS. To fully elucidate the biofouling status of these yeasts is not possible in a closed industrial system.

The permeate surface of all RO-B coupons was found widely covered by multiple layers of exclusively filamentous yeast that displayed the same type of structures (Fig. 7). The individual yeast cells were extremely long with branching hyphae that spread and covered a large area. Their structures were primarily stained by SYPRO Ruby and ConA. It was observed in the MYPG-antibiotics selective agar that the filamentous isolates grew slowly, taking between three and four days. The combination of slow growth and the relative low number of cells compared with bacterial cells in many cases may have prevented the detection of these yeast previously. The present direct microscopically approach indicates that they may have an important role in the biofouling due to the large coverage by each cell.

When RO-BB, RO-C and RO-D (originating from same pressure vessel as RO-B) were sampled several months later during Phase II, the same type of previously isolated budding and filamentous yeast were colonizing. This time they were seen on both retentate and permeate

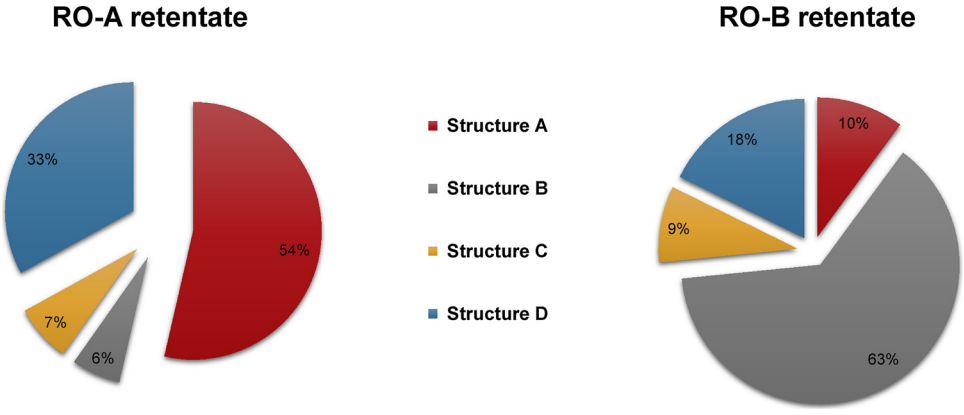

Fig. 6. Distribution of different biofilm structures(see Fig. 5) found on the surface of membrane elements in Phase I, RO-A (only water flush) retentate (n = 97 observations) and RO-B (CIPed) retentate (n = 79). No biofilm structures have been observed on the permeate side of RO-A, whereas all images recorded on the permeate surface of RO-B display the same type of filamentous yeast aggregates surrounded by a matrix (Structures C and D).

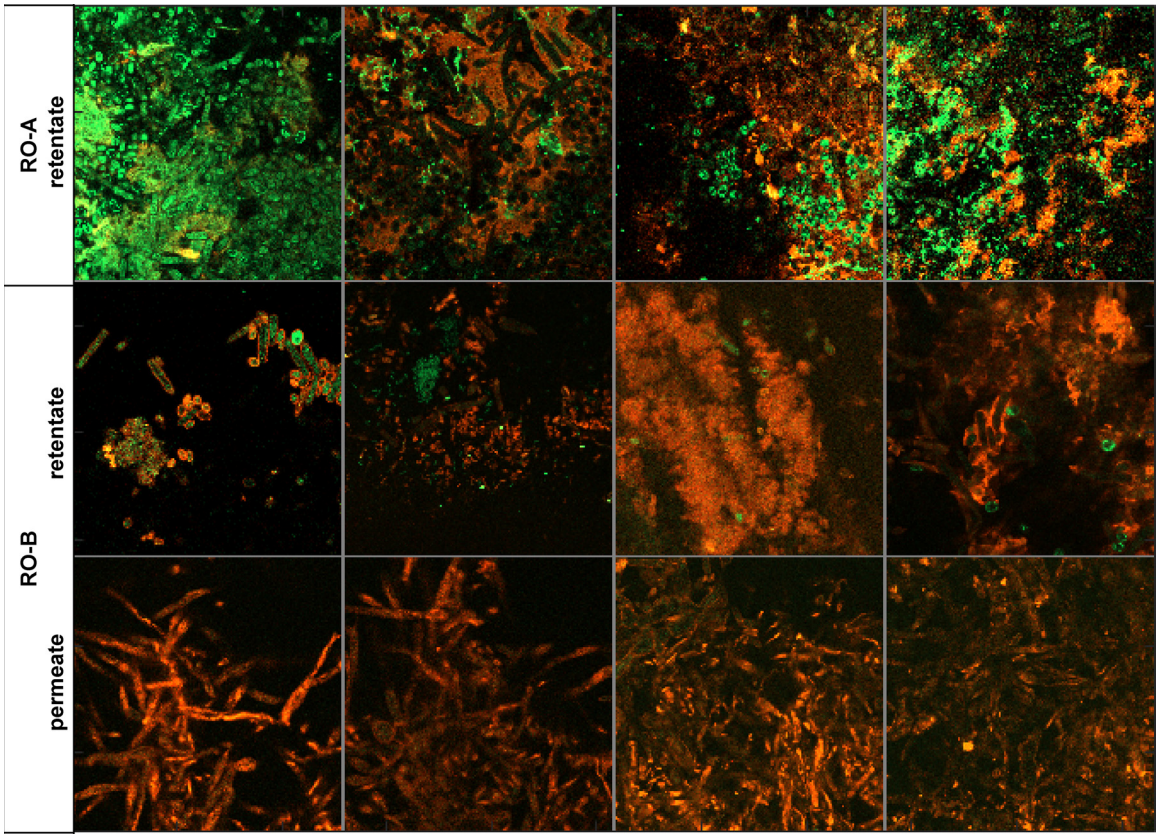

Fig. 7. Representative CLSM recordings; see Table 1 and text for details.

side of all three elements and rod shaped bacteria could be more easily spotted on each element's retentate surface, see Fig. 8. An additional experimental sanitation step at 78 °C for 20 min was applied on RO-C in a pilot facility. The low viable counts on the RO-C retentate side indicated the efficiency of this sanitation step.

Based on n = 8 observations for each surface side (retentate and permeate) for each RO-element sampled in Phase II, the CLSM images suggest that the microbial levels in RO-C were comparable with levels found in RO-BB and RO-D. Considering that RO-D and RO-BB had a distinct operating time, namely 6 months and 3–4 years respectively, one could expect to see differences in their biofouling structure. Overall, similar types of aggregates could however be observed across the retentate surface (Fig. 8). Compared to RO-B, the EPS surrounded cells were arranged in more dense clusters. Also, on the permeate surface of all Phase II RO-elements, filamentous cells were intertwined with budding yeast cells and in some cases without full coverage in an EPS matrix, as compared to RO-B (Figs. 7 and 8). This could indicate the presence of a younger microflora. The effective age of use did not seem to have an influence on present microbiota when judging solely on the results from the retentate side and the two operation times investigated. On the other hand, the CLSM images and the total counts detected on the permeate membrane surface suggest that RO-D had less microbial contamination here than the older RO-BB element although the character of the observations (one swab sample and two membrane coupons for each leaf visualized by confocal microscopy) makes the comparisons semi-quantitative.

CLSM images of the permeate side of the heat-sanitized RO-C show a fairly contaminated surface, but with no viable counts detected upon plating. This confirms the efficiency of the extreme heating step in inactivating any residual microorganisms on this membrane. On the other hand, viable counts were still detected – though at considerable lower level – on both the retentate and permeate side of RO-E element, which came from another process function but also had a 78 °C sanitation step included in its cleaning protocol. Little was observed upon confocal microscopy inspection of the sampled membrane coupons, but rods, cocci, pink budding yeast as well as filamentous yeast could be isolated in agar plates with samples from the RO-E retentate side while rod shaped bacteria were isolated from the RO-E permeate side samples (results not shown).

The hyphal cells may be responsible for an increased strength of the biofilm and show resistance to the shearing effect of the permeate streams. A dense filamentous yeast structure as found on RO-B (Fig. 7) might cause decreased permeate flux necessitating more pressure. This corrective measure is common in an industrial set-up and translates directly into increased costs for the production plant. Our findings indicate that yeast may play an important role in the biofouling process and that biofouling on the RO membranes' permeate side should not be overlooked.

3.4. Microbiological analysis on RO permeate streams

In the spiral wound configuration the permeate side is considered a closed space where only clean water is allowed to circulate. A CIP protocol can only restore the properties of retentate surface efficiently, while cleaning agents are not meant to reach the permeate side. Consequently, any opportunity for microorganisms to access the permeate space is undesirable. If microorganisms arrive on the permeate side, the non-woven fabric could act as an excellent type of surface for attachment and it has been observed that the very low nutrient levels are able to create suitable conditions for specific cells to proliferate [24]. Consequently, the development of microorganisms on membrane surface may lead to a permanent source of cross-contamination for permeate streams.

Our findings show that the feed product (whey UF permeate) contained viable microorganisms in the order of 100 CFU mL^{-1} while the RO permeate streams had levels below or at the detection limit. In the

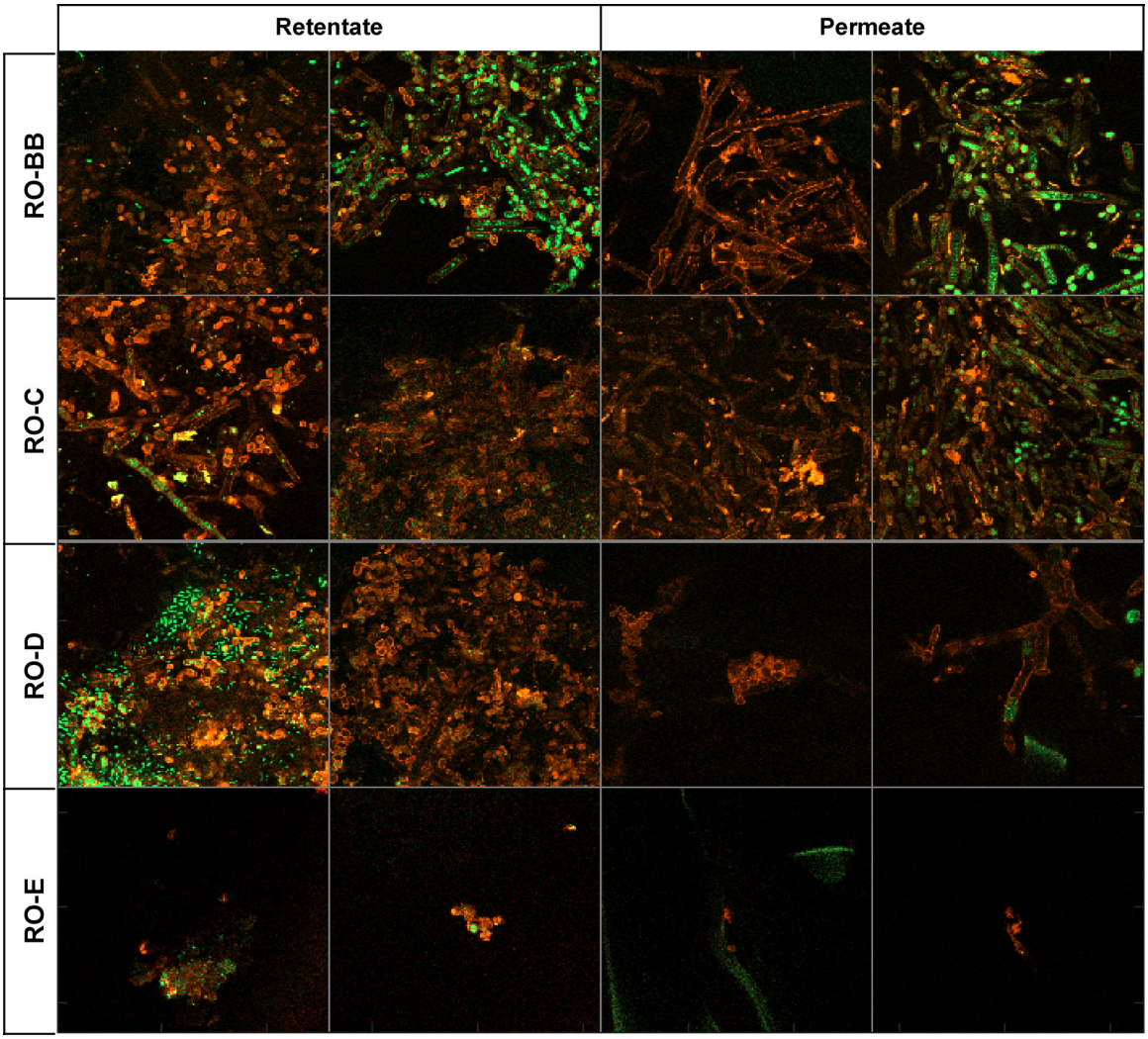

Fig. 8. Representative CLSM recordings taken on retentate and permeate surface of different CIPed RO-elements from Phase II; see Table 1 and text for more details.

Table 2
Total viable colonies found in permeate streams at different sampling points, see Fig. 1a. The exact number of colonies is presented for each of the two replicate determinations.

(CFU mL^{-1})	P_1 (UF perm.)	P_2 (RO perm.)	P_3 (ROP perm.)	P_4 (ROP + UV)	P_5 (buffer tank)	P_6 (process-water)
LOD	**10**	**10**	**1**	**1**	**1**	**1**
PCA aerobic 25 °C	65/144	0	1/2	1/2	0	0
MYPG-antibiotics aerobic 25 °C	66/65	2/0	0	0	0	0

final water, which in this case had been exposed to two RO treatments as well as UV before and after the buffer tank, no microorganisms were detected (Table 2). This suggests that in spite of evidence of high microbial contamination on membrane permeate surfaces, the microbial safety parameters of permeate streams do not necessarily reflect any risks. However, worse-case scenarios can potentially happen in industrial set-ups, which from a long-term perspective requires a strategy and monitoring procedure for reclaimed water suitable to prevent failures in operating such units.

The foremost issue seems to be the technological implications related to biofouling and flux decline. Routine checks conducted over time, with a strategic sampling for membrane autopsy, may be an example of a small compromise that can help industries to adapt and optimize their practices, especially when accurate real-time monitoring techniques are difficult to implement for such closed, high-pressure and compact systems. Even better, these types of checks could start with the membrane autopsy of elements that show low performance and are intended for replacement anyway. Valuable insights can be gained from understanding their particular cause of failure. Such data bases may help on the one hand to identify if any trends occur within the production plant, but also to formulate new specifications for developing membranes with improved properties or configurations based on full-scale practice rather than small-scale experiments. Different feed, spacers, materials or flow regimes may dictate biofilm morphology and potentially influence the type of microbial community. Thus, optimization, e.g. by periodical/low frequency heat sanitation, should be seen as a continuous process since one adjustment will lead to new issues. Consequently, tuning the process conditions based on results of the autopsy procedure can be a better approach compared to sticking to fixed recipes until significantly low performance arises.

Sampling and achieving true quantitative comparisons for large surface areas is difficult to conduct in an industrial set-up. A production

plant is a system far from the ideal scenario since its operational conditions, feed product characteristics, and cleaning efficiency are variables that change continuously, thereby influencing the overall unit performance and *state* of the system. In spite of this, process-water recovery is a rapidly growing area and more investigations as hereby presented – in full-scale production – are needed to get a better understanding and a route to further optimization.

4. Conclusions

Autopsy was performed on industrial scale reverse osmosis membrane elements that have been used for water recovery from whey separation permeate and their different biofouling structures were characterized via CLSM. Extensive biofouling was seen on membranes after simple flushing but biofouling was also present on membranes after routine CIP treatment on the retentate side and, more surprisingly, on the permeate side. A mixed microbial community was generally found on the retentate surface of all inspected membranes, visually primarily composed of yeast. Filamentous yeast with numerous, long hyphae were observed on the permeate surfaces and the layer stained primarily by ConA, labeling glycoconjugates. Microbiological analysis of the reclaimed, double UV treated process-water streams showed no detectable microbial activity.

Acknowledgements

This work was supported by the REuse of WAteR in the food and bioprocessing inDustries (REWARD) consortium funded by the Danish Council for Strategic Research, Programme Commission on Health Food and Welfare (Copenhagen).

References

[1] I.G. Wenten, Khoiruddin, Reverse osmosis applications: prospect and challenges, Desalination 391 (2016) 112–125, http://dx.doi.org/10.1016/j.desal.2015.12.011.
[2] H. Ölmez, Water consumption, reuse and reduction strategies in food processing, Sustain. Food Process, (2013), pp. 401–434, http://dx.doi.org/10.1002/9781118634301.ch17.
[3] M. Vourch, B. Balannec, B. Chaufer, G. Dorange, Nanofiltration and reverse osmosis of model process waters from the dairy industry to produce water for reuse, Desalination 172 (2005) 245–256, http://dx.doi.org/10.1016/j.desal.2004.07.038.
[4] S. Casani, M. Rouhany, S. Knøchel, A discussion paper on challenges and limitations to water reuse and hygiene in the food industry, Water Res. 39 (2005) 1134–1146, http://dx.doi.org/10.1016/j.watres.2004.12.015.
[5] L. Levidow, P. Lindgaard-Jørgensen, Å. Nilsson, S.A. Skenhall, D. Assimacopoulos, Process eco-innovation: assessing meso-level eco-efficiency in industrial water-service systems, J. Clean. Prod. 110 (2016) 54–65, http://dx.doi.org/10.1016/j.jclepro.2014.12.086.
[6] P. Kumar, N. Sharma, R. Ranjan, S. Kumar, Z.F. Bhat, D.K. Jeong, Perspective of membrane technology in dairy industry: a review, Asian-Aust. J. Anim. Sci. 26 (2013) 1347–1358, http://dx.doi.org/10.5713/ajas.2013.13082.
[7] A. Suárez, F.A. Riera, Production of high-quality water by reverse osmosis of milk dairy condensates, J. Ind. Eng. Chem. 21 (2015) 1340–1349, http://dx.doi.org/10.1016/j.jiec.2014.06.004.
[8] S.J. Rad, M.J. Lewis, Water utilisation, energy utilisation and waste water management in the dairy industry: a review, Int. J. Dairy Technol. 67 (2014) 1–20, http://dx.doi.org/10.1111/1471-0307.12096.
[9] C. Aydiner, U. Sen, S. Topcu, D. Ekinci, A.D. Altinay, D.Y. Koseoglu-Imer, B. Keskinler, Techno-economic viability of innovative membrane systems in water and mass recovery from dairy wastewater, J. Memb. Sci. 458 (2014) 66–75, http://dx.doi.org/10.1016/j.memsci.2014.01.058.
[10] J. Johnson, M. Busch, Engineering aspects of reverse osmosis module design, Desalin. Water Treat. 15 (2010) 236–248, http://dx.doi.org/10.5004/dwt.2010.1756.
[11] C. Li, Y. Yang, S. Ding, L.A. Hou, Dynamics of biofouling development on the conditioned membrane and its relationship with membrane performance, J. Memb. Sci. 514 (2016) 264–273, http://dx.doi.org/10.1016/j.memsci.2016.04.066.
[12] M. Herzberg, M. Elimelech, Biofouling of reverse osmosis membranes: role of biofilm-enhanced osmotic pressure, J. Memb. Sci. 295 (2007) 11–20, http://dx.doi.org/10.1016/j.memsci.2007.02.024.
[13] A.N. Hassan, S. Anand, M. Avadhanula, Microscopic observation of multispecies biofilm of various structures on whey concentration membranes1, J. Dairy Sci. 93 (2010) 2321–2329, http://dx.doi.org/10.3168/jds.2009-2800.
[14] S. Anand, D. Singh, Resistance of the constitutive microflora of biofilms formed on whey reverse-osmosis membranes to individual cleaning steps of a typical clean-in-place protocol, J. Dairy Sci. 96 (2013) 6213–6322, http://dx.doi.org/10.3168/jds.2013-7012.
[15] X. Tang, S.H. Flint, J.D. Brooks, R.J. Bennett, Factors affecting the attachment of micro-organisms isolated from ultrafiltration and reverse osmosis membranes in dairy processing plants, J. Appl. Microbiol. 107 (2009) 443–451, http://dx.doi.org/10.1111/j.1365-2672.2009.04214.x.
[16] Y.E. Meneses, R.A. Flores, Feasibility, safety, and economic implications of whey-recovered water in cleaning-in-place systems: a case study on water conservation for the dairy industry, J. Dairy Sci. 99 (2016) 3396–3407, http://dx.doi.org/10.3168/jds.2015-10306.
[17] A. Klimkiewicz, A.E. Cervera-Padrell, F. Van Den Berg, Modeling of the flux decline in a continuous ultrafiltration system with multiblock partial least squares, Ind. Eng. Chem. Res. 55 (2016) 10690–10698, http://dx.doi.org/10.1021/acs.iecr.6b01241.
[18] J.K. Jensen, N. Ottosen, S.B. Engelsen, F. Van Den Berg, Investigation of UF and MF membrane residual fouling in full-scale dairy production using FT-IR to quantify protein and fat, Int. J. Food Eng. 11 (2015) 1–15, http://dx.doi.org/10.1515/ijfe-2014-0254.
[19] B. Herigstad, M. Hamilton, J. Heersink, How to optimize the drop plate method for enumerating bacteria, J. Microbiol. Methods. 44 (2001) 121–129, http://dx.doi.org/10.1016/S0167-7012(00)00241-4.
[20] E. Bar-Zeev, K.R. Zodrow, S.E. Kwan, M. Elimelech, The importance of microscopic characterization of membrane biofilms in an unconfined environment, Desalination 348 (2014) 8–15, http://dx.doi.org/10.1016/j.desal.2014.06.003.
[21] C. Sun, L. Fiksdal, A. Hanssen-Bauer, M.B. Rye, T. Leiknes, Characterization of membrane biofouling at different operating conditions (flux) in drinking water treatment using confocal laser scanning microscopy (CLSM) and image analysis, J. Memb. Sci. 382 (2011) 194–201, http://dx.doi.org/10.1016/j.memsci.2011.08.010.
[22] S. Anand, A. Hassan, M. Avadhanula, The effects of biofilms formed on whey reverse osmosis membranes on the microbial quality of the concentrated product, Int. J. Dairy Technol. 65 (2012) 451–455, http://dx.doi.org/10.1111/j.1471-0307.2012.00848.x.
[23] H.-C. Flemming, EPS—Then and now, Microorganisms 4 (2016) 41, http://dx.doi.org/10.3390/microorganisms4040041.
[24] P.B. Skou, B. Khakimov, S.D. Aunsbjerg, S. Knøchel, F. van den Berg, T.H. Hansen, D. Thaysen, Chemical characterization by gas chromatography-mass spectrometry and inductively coupled plasma-optical emission spectroscopy of membrane permeates from an industrial dairy ingredient production used as process water, J. Dairy Sci. (2018).

4.4. Protein fouling

Fourier Transformed Infrared in Attenuated Total Reflectance (FTIR-ATR) mode, see Box 5, was used as a rapid method to evaluate the extent of organic residual-fouling present on RO membranes after their industrial CIP. The technique emerges as a fast method to characterize the type of fouling[84,158,159] and cleaning status of membranes since any attached layer of organic compounds may be identified in relation to their functional groups (with primary interest in this case being the amide absorption bands originating from the whey protein fractions). FTIR-ATR helps also in establishing the spatial distribution of organic foulants, which is probably the method's most attractive feature. In order to obtain also a quantitative figure over the residual protein level, the same membrane coupons were subjected to the BCA (bicinchoninic acid) protein assay test. The BCA test is referred herein as the quantitative method of total protein level, determined on extraction from membrane coupons of fouling into a solution. It uses as a principle the reduction of the cupric ion (Cu^{2+}) to the cuprous ion (Cu^{+}) in the presence of proteins when in an alkaline medium. Upon interaction of BCA with the cuprous ion, a BCA/copper complex with purple color is formed. The resulting complex is stable, water-soluble and with a strong absorbance at 562 nm that is nearly linear with protein concentration. Therefore, the estimation of protein levels in unknown samples can be done in relation to a standard curve achieved from a known protein sample, in this case Albumin Standard (BSA), that was treated in a similar way as the unknown samples.

4.4.1. Methods and materials

Coupons of 4x4 cm were sampled across two distinct leaves from RO-A, RO-B, RO-BB and RO-D elements in a 3 by 3 pattern as indicated in Figure 4.3a. Each coupon was first scanned with the FTIR-ATR instrument (ABB Bomen model 100, detector DTGS Model SMH307AT) in two distinct locations per coupon side (retentate and permeate). The ATR sampling technique was used with the accessory that uses a triple bounce small diamond probe of about 2 mm in diameter and with a metal pin that allows pressing the membrane material against diamond as shown in Figure 4.3b. Spectra were collected in the spectral range 4,000-500 cm^{-1} with 4 cm^{-1} resolution, averaged over 64 scans. Samples were pressed against the diamond at a pressure level 3 (arbitrary units) and a background that was measured under similar conditions based on empty interface was in computing absorbance spectra. IR spectra were recorded also on a new RO membrane surface (virgin membrane) and on a (assumed mainly) biofilm sample scrapped from the permeate side of an entire separate leaf, air dried and then measured with the FTIR-ATR technique under similar conditions.

The non-destructive way of IR measurements made it possible that same coupons could be further subjected to the BCA protein assay, only performed on coupons from RO-BB and RO-D. Briefly, the method consisted in an extraction step where the 4x4 cm coupons were cut in small fragments, immersed in 20ml of 0.1M NaOH solution and left for extraction overnight at room temperature

while continuous mixing on a roller table. Before analysis each sample was vortexed for approx. 1 min and the resulting suspension was used in the BSA assay following the microplate procedure (25µL of each standard and unknown sample in 3 replicates were mixed with 200µL of the working reagent, incubated at 37°C for 30 minutes and absorbance measured at 562nm on a plate reader after approx. 10 min. when sampled reached room temperature)[160].

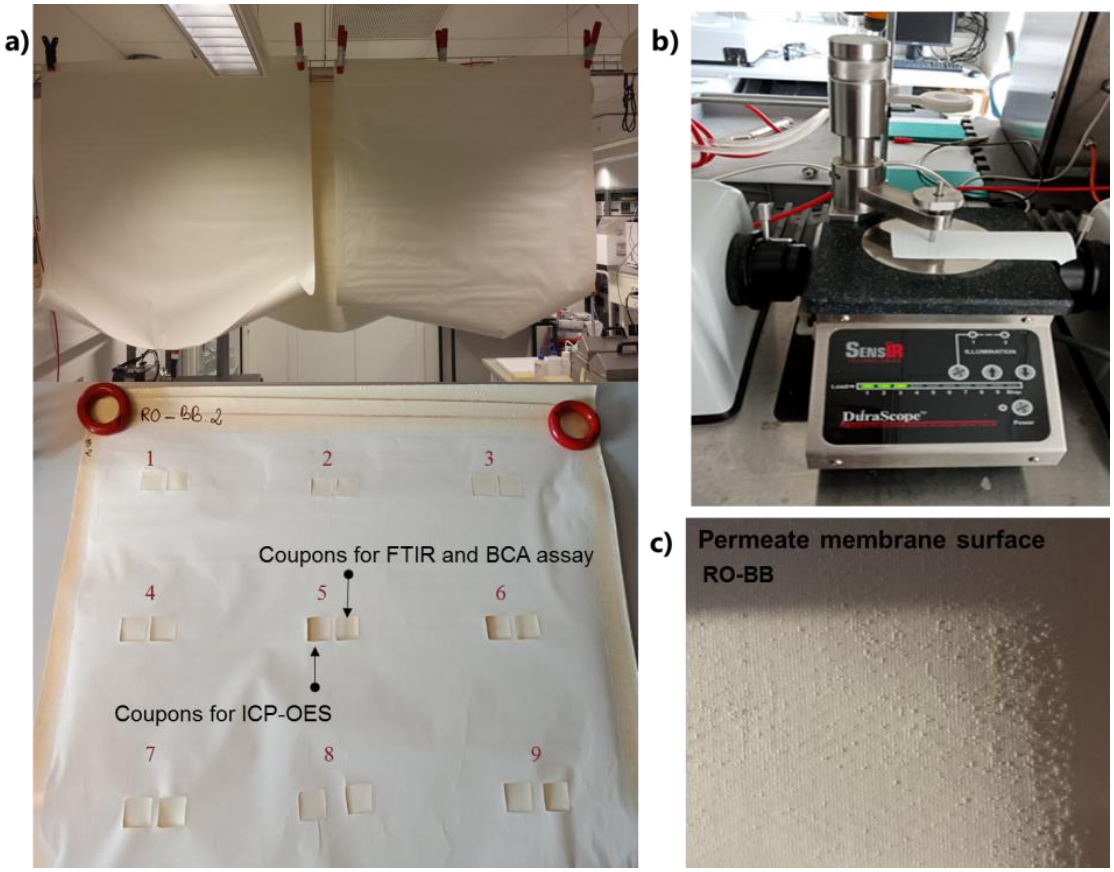

Figure 4.3 a) Coupon sampling pattern across RO membrane leaves, b)ATR accessory with triple bounce showing a membrane material pressed against the diamond at pressure level 3, c) example of physical appearance of biofilm as found on RO membrane permeate surface (visualizing fouling - accumulated due to drying - and imprint of the membrane spacer)

Box 5. Principle of Fourier Transformed Attenuated Total Reflectance (FTIR-ATR) spectroscopy

Infrared spectroscopy is one of the vibrational spectroscopy techniques that can be used to resolve the chemical nature of a sample based on the absorbance patterns that occur under interaction with radiation from infrared region. All molecules exhibit molecular vibrations that are characteristic to their structure and molecular bonds. Light, in particular from mid-infrared region (MIR, 14000-4000 cm^{-1}), has the property to resonate with most of these fundamental vibrational or vibrational-rotational transitions, at the requirement that a change in the dipole moment occurs. Such dipole moments happen to exist in most molecules (i.e. water, carbohydrates, proteins and fats) with importance for food industry which makes infrared spectroscopy an attractive analytical tool[161].

The traditional way of measuring IR would require transmission of a beam through a sample, which due to the high absorption levels in most cases would be limited to very small path lengths and extensive sample preparation for solid samples. The Attenuated Total Reflectance (ATR) sampling idea overcomes these issues and opens the possibility to measure solid samples *as is*, hence with no extra preparation steps involved. The same principle can be used with liquid samples that have extremely high absorbance. The principle of ATR is based on measuring changes in the total internal reflected infrared beam at contact with a sample. It involves the use of a material that has a higher refractive index than the sample to be analyzed. Most often a diamond crystal is used due to its high refractive index (n=2.4) but also due to the fact that is extremely hard (and high pressure may be applied to get good contact with the measurement object) and chemically inert. When the infrared beam is directed onto the diamond, its internal reflectance creates an evanescent wave that propagates beyond the crystal surface and penetrates into the sample. Upon contact with the sample, the energy of the evanescent wave is attenuated at the infrared frequencies where the sample absorbs and then passed back to the infrared beam, which exits the crystal and reaches a detector, see Figure 4.4. The evanescent wave has an exponential intensity-decay from the boundary of crystal surface and thus can only protrude the sample a few microns (0.5- 5µm; dependent on the material measured). This implies that the sample must be in close contact with the crystal and sample homogeneity is highly important to achieve reproducible spectra[162]. Consequently, the information contained in recorded spectra is strictly restricted to the information contained at the immediate sample surface. The penetration depth is less than 200 nm over 4,000–2,600 cm^{-1} wave numbers, and is greater than 300 nm at wave numbers lower than 2000 cm^{-1} [163].

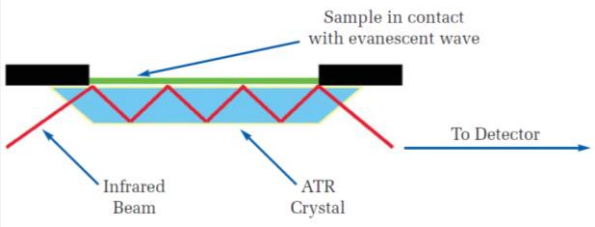

Figure 4.4 Principle of Attenuated Total Reflectance. Source: PerkinElmer(2005)[162]

4.4.2. Results and discussion

Figure 4.5 present examples of the raw FTIR spectra collected for both retentate and permeate membrane sides of RO elements before and after CIP, complimented with the spectra of new membrane and a biofilm sample. A possible assignment of the identified vibrational bands was done based on literature[164,165] and summarized in Table 4.2.

Table 4.2. Possible assignment of vibrational bands identified in the FTIR spectra recorded fouled RO membranes.

Wavenumber (cm^{-1})	Possible assignment
3283	N-H streching of amide A in proteins
2926	C-H asymmetric stretching of $-CH_3$ in fatty acids
2851	C-H symmetric stretching of $>CH_2$ in fatty acids
1745	>C=O stretching of lipid esters
1664	C=O stretching and/ or bending C-N streching and C-C-N deformation vibration in secondary amide group for amide I and in aromatic polyamide
1637	Amide I streching of β- sheet structures of proteins
1624	Amide I streching of β- sheet structures of proteins
1585	C-C streching vibration of aromatic in -plane ring for polysulfone
1541	Amide II band of proteins- coupled C-N stretch, N-H bend
1489	C-C stretching vibration of aromatic in-plane ring for polysulfone.
1294	Symmetric SO_2 stretching vibration for polysulfone.
1242	Asymmetric C-O-C stretching vibration of the aryl-O-aryl group for polysulfone and/or Amide III vibration.
1105	Asymmetric SO_2 stretching vibration for polysulfone.
1085	P=O symmetric stretching in DNA, RNA and phospholipids
833	In-phase out-of-plane hydrogen deformation vibration of para-substituted phenyl groups for polysulfone.

Comparing the FTIR spectra of coupons from RO-A with the new membrane it is observed that at the end of a production cycle (>24h) the retentate membrane surface is coated with a layer that contains primarily carbohydrates (mostly lactose which is concentrated at this side of the membrane) noticed from the strong absorption band near 1031 cm^{-1} of the C-O stretching vibration, and proteins which are evident from the strong signals in the amide bands at 1634 cm^{-1} (amide I of C=O stretch), 1541 cm^{-1} (amide II of N-H bend and C-N stretch) and 3279 cm^{-1} (amide A of N-H stretch). Additionally, indication of fat accumulation is evident from the peak observed at 1745 cm^{-1} that originates from the C=O stretching of lipid esters, but also the absorption bands at 2924 cm-1 from C-H asymmetric stretching of -CH3 in fatty acids and at 2851 cm^{-1} from the C-H symmetric stretching of >CH2 in fatty acids (Figure 4.5a).

One can note the effect of CIP operations when comparing the FTIR spectra of RO-A with those from elements that followed their standard industrial CIP cleaning protocol. To a great extent the fouling layer is removed, but some fat, proteins and carbohydrates is still observed at their correspondent absorption bands, see Figure 4.5a.

a)

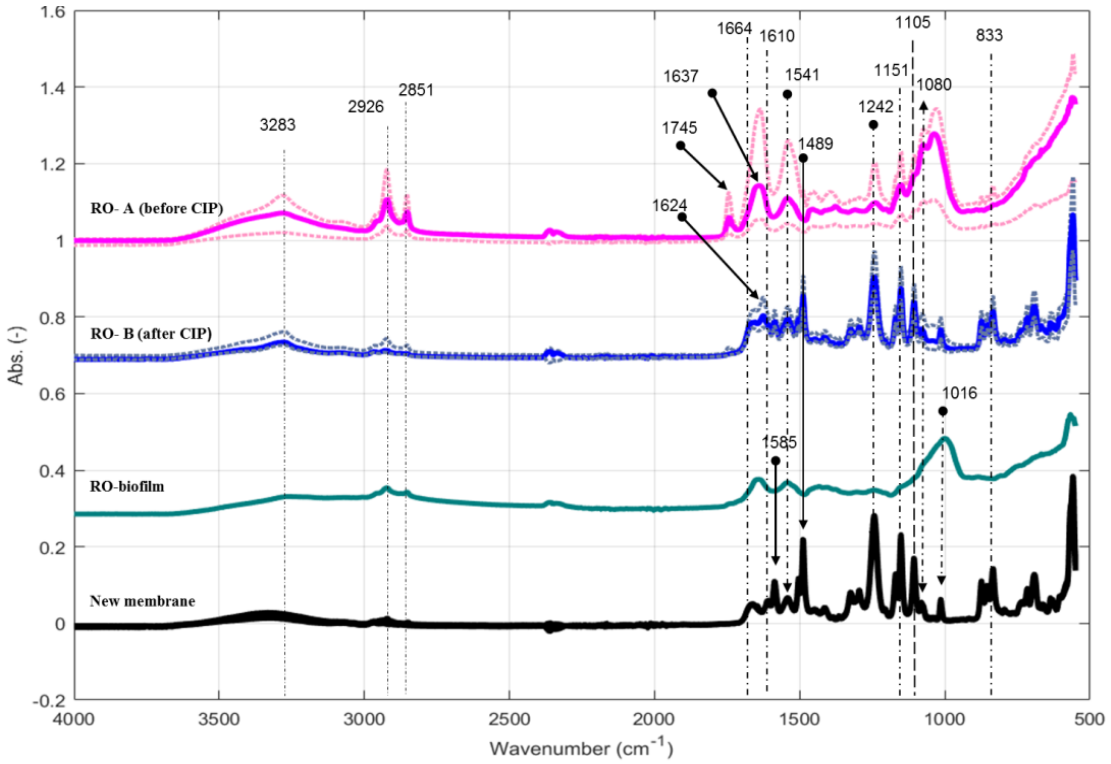

b)

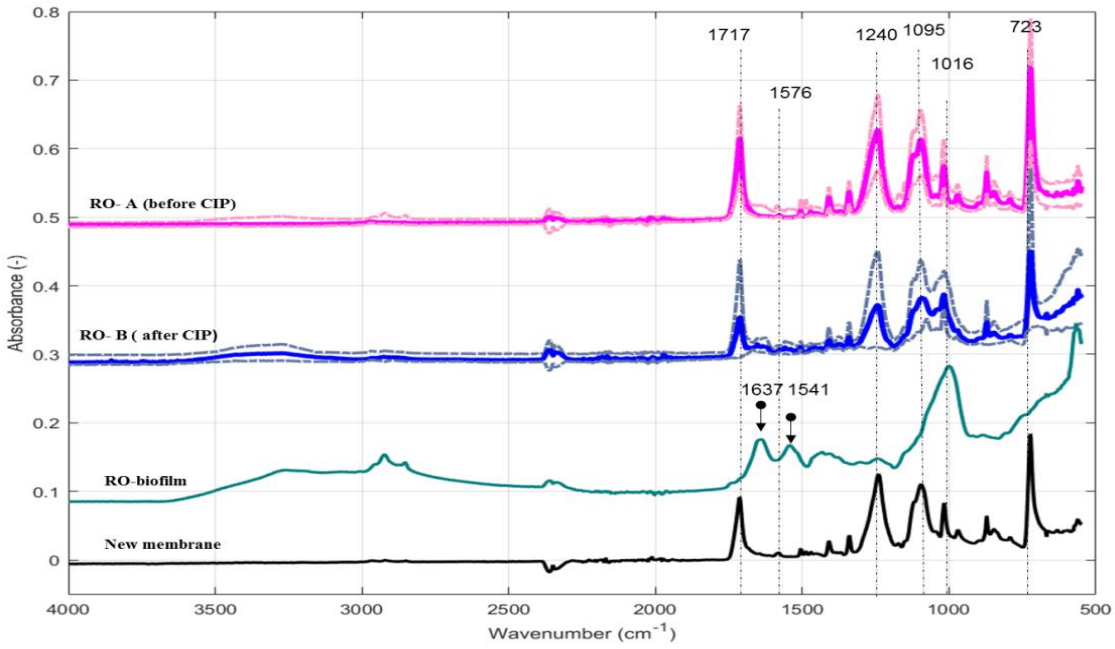

Figure 4.5 a) FTIR spectra of RO membrane retentate; b) FTIR spectra of RO membrane permeate; (offsets introduced for visual clarity, example of a recorded FTIR spectra and envelope over all measurements are plotted).

Typically, the permeate side of the spiral wound RO membranes is not tested for fouling, neither when looking at literature discussing RO membranes used exclusively in dairy applications, nor in other investigations where membrane autopsy was done on RO membranes used in wastewater reclamation[166] or desalination purposes[167]. This may be attributed to the fact that the membrane permeate side is generally not an *interesting* surface to characterize considering that the nonporous structure of the active polyamide layer and its working mechanism based on molecule-diffusion is expected to let primarily water molecules pass through. Therefore, the permeate side is considered generally a clean *support-side/layer* due to its exposure to only water molecules that are recovered from the processed feed solution. However, when cutting open the permeate side of the sampled RO elements, visible deposits were found, see Figure 4.3c. As described in Paper II, such deposits were found to be of a microbiological nature caused by extensive growth of a yeast strain with filamentous morphology.

From the FTIR spectra collected on the permeate side of the sampled coupons (Figure 4.5b), it is safe to assume that the information contained in the amide bands corresponds to the functional groups of proteins found in the biofilm layer. Since on the permeate side the membrane material does not overlap with the amide I and amide II bands, a concentration profile of the biofouling layer can be determined by simply calculating the height of relative absorbance at one of these amide peaks. To do so all spectra were baseline corrected in relation to the spectral area 2000-1800 cm^{-1} (no information detected in this region) and the height of the amide I band at 1645 cm^{-1} was determined based on the formula according to Bégoin et al. (2006)[159], that takes into account the variable penetration depth of the IR beam in the membrane material:

$$\text{Height ratio} = \frac{H^{amide\ I}}{H^{membrane\ pure\ band}} \qquad \text{Eq. (4.1)}$$

where membrane pure band is relative absorption at 1240 cm^{-1}.

Similarly, on the retentate side, the protein concentration was calculated in relation to the amide I band at 1624 cm^{-1} due to its little interference with the membrane peaks.

Both the BCA protein assay and the FTIR based protein concentration profiles indicated that overall RO-BB was more contaminated than the RO-D element. From the FTIR spectra it could be determined that the retentate surface of RO-BB membrane (4 years old) had comparable levels with its younger homologue RO-D (6 months) - average of amide height peak across all leaves was 0.44±0.05 and 0.40±0.03 respectively. A difference could be seen instead in relation to their permeate side where the older RO-BB membrane was found more fouled than its younger version RO-D) - average of amide height peak across of 0.64±0.35 and 0.077±0.10 respectively.

This is in good agreement with the total viable count values of 4.51 $\log_{10}$ CFU·cm^{-2} on permeate side of RO-BB compared to 3.38 $\log_{10}$ CFU·cm^{-2} of permeate RO-D, see Paper II. From Figure 4.6 it is noticed that the BCA assay values correlate to some extent (r^2= 0.76) with the amide I height ratio calculated on the membranes permeate side. This suggests that the bulk part of the protein extracted into solution originates primarily from the permeate side. In an attempt to evaluate the

efficiency of the extraction step, five coupons taken from the RO-BB element were measured for their protein content via the BCA assay at different extraction points. From Figure 4.7, it appears that the extraction step is not absolute and first after approx. 32 hours the level of protein in solution does not show a notable increase.

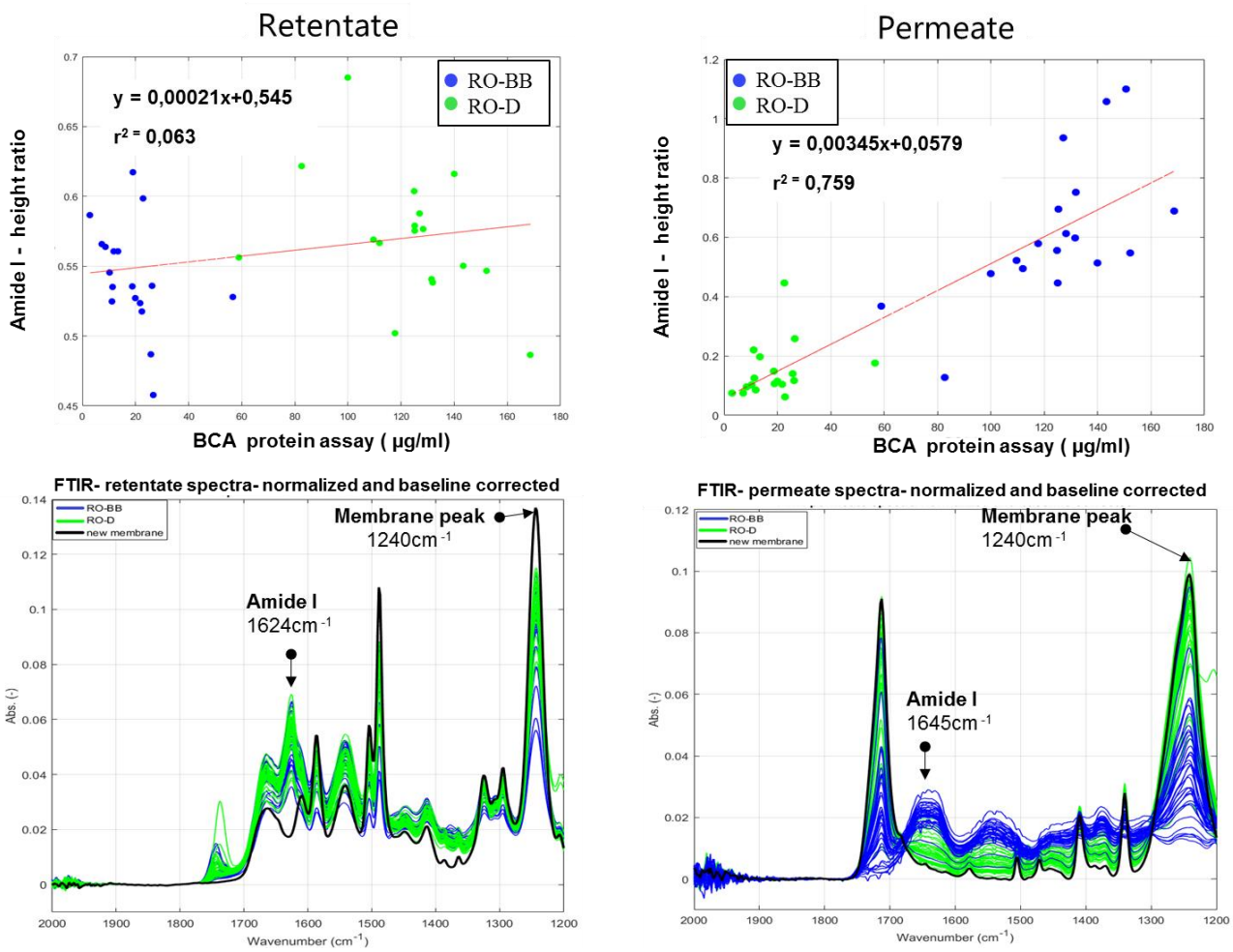

Figure 4.6 BCA assay values vs. amide I height ratio on RO-BB and RO-D

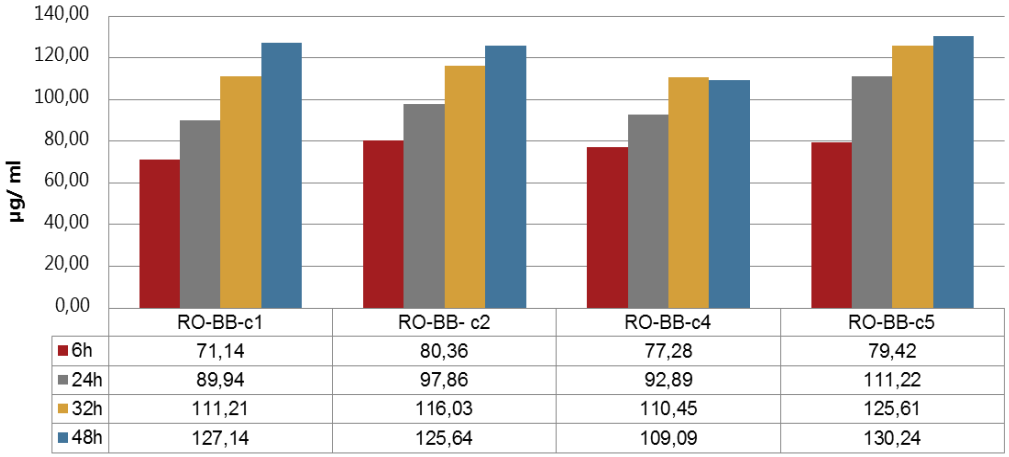

	RO-BB-c1	RO-BB- c2	RO-BB-c4	RO-BB-c5
6h	71,14	80,36	77,28	79,42
24h	89,94	97,86	92,89	111,22
32h	111,21	116,03	110,45	125,61
48h	127,14	125,64	109,09	130,24

Figure 4.7 Time effect on protein extraction from five distinct membrane coupons (4x4 cm) into alkaline solution

4.5. Inorganic scaling

A limited number of coupons from RO-BB and RO-D (three from each sampled leaf) were assessed for their inorganic elements fouling via inductively coupled plasma-optical emission spectroscopy (ICP-OES)[168].

4.5.1. Methods and materials

Sample preparation followed first an extraction step where room temperature dried coupons were immersed in an acid mixture composed of 12 ml HCl: 4 ml HNO_3 and left to rest overnight. Membrane material was then removed and 500µl H_2O_2 was added into the solution, which was further microwave digested (ramp/temp/hold step1:10min/100°C/10min and step2: 10min/180°C/10min) in order to reduce any matrix interference (in this case organic fouling and the biofilm matrix). After digestion, the resulting solution was diluted 1:1 in MiliQ water and measured on a 5100 ICP-OES (Agilent Technologies) equipped with a Meinhard nebulizer and a cyclonic spray chamber. A 5-point external calibration standard was prepared from a Multielement standard solution 5 for ICP(54704, Sigma-Aldrich) diluted 1:1 dilutions in MiliQ water and measured in sequence with all samples.

4.5.2. Results

The inorganic fraction as extracted from the sampled coupons is presented in Table 4.2

Table 4.2. Concentration of inorganic elements extracted in 16ml of acid solution from 4x4cm coupons sampled across membrane leaves of RO-BB and RO-D; where (n.d.) refers to element found below limit of detection in relation to the calibration standard.

	RO-D						RO-BB					
Element (µg)	Leaf 1			Leaf2			Leaf 1			Leaf2		
Al	n.d.	n.d	n.d	n.d	n.d	n.d	n.d	0.87	0.93	0.84	0.31	0.63
Ca	n.d.	n.d	n.d	n.d	n.d	n.d	n.d	34.99	61.27	27.70	14.58	35.70
Fe	n.d.	n.d	n.d	n.d	n.d	n.d	n.d	0	0	0	0	0
K	n.d.	n.d	n.d	n.d	n.d	4.08	36.19	14.72	16,59	7.39	2.05	21.99
Mg	n.d.	n.d	n.d	n.d	n.d	5.08	23.40	19.41	11.95	8.23	10.32	11.74
Na	60.55	62.90	62.66	60.97	62.39	69.02	74.89	77.67	80.40	74.65	72.77	77.11
Zn	n.d.	n.d	n.d	n.d	n.d	n.d.	n.d	n.d.	n.d	n.d	n.d	n.d

4.6. Biofouling

When addressing the biofouling aspect, quantification was the main focus whereas identification and characterization of the RO-membrane microflora was out of scope of this thesis work. The aerobic plate count (APC) was determined by the reference culture and plating method and additionally by MicroSnap™ Total. The MicroSnap™ Total served in this case as a rapid test that allowed more extensive sampling.

4.6.1. Reference culture and plating method

Aerobic plate count determination took place by culturing the collected surface samples onto standard plate-count-agar (PCA) substrate with aerobic incubation at 25°C. Several steps were necessary before the estimation of the APC levels.

Step1. Surface sampling and ten-fold dilution series

Surface sample collection took place via a swabbing procedure from membrane surface areas of 10x10 cm using compress tissues that were moisturized prior to their use with 0.9% saline peptone water (SPO). Sampling was done under sterile conditions using gloves sanitized with 70% ethanol. Once a sample was collected it was placed into a sterile stomacher bag with 50mL of autoclaved 0.9% SPO. The extraction of microbial cells into the solution happened by homogenization in a Stomacher® 400 Circulator (Seward Limited, UK) for 1 minute. The homogenized solution from each bag served as zero-dilution and next, series of ten-fold dilutions were performed at four levels in 9mL of 0.9% SPO for each sample. Each ten-fold dilution in the series was inoculated on a PCA agar plate (and on MYPG agar if applicable). Depending on the investigation and workload, two different plating methods have been applied for the different investigations. An illustration of the drop plate and spread plate method may be seen in Figure 4.8.

Step2.1 - Drop plate method

The agar plate is divided into two parts, with each side of the agar being assigned for one dilution level of a sample. The inoculation of any of the ten-fold dilutions series took place by dispersing five evenly spaced 5µl drops onto their dedicated plate space. The drops were allowed to dry on the agar (10-20 minutes), the plates inverted and incubated at 25°C for 17-20 hours.

Advantage: requires less time and smaller number of agar plates.

Disadvantage: slow growing microorganisms may be overgrown by faster ones; requires precise electronic pipettes; not suitable for microorganisms that have a swarming type of motility[169].

Step 2.2 - Spread plate method

Under aseptic conditions a volume of 0.1ml from the dilution sample is transferred onto the center of agar plate and spread evenly over the entire plate surface with an L-shaped spreader. The inoculated plates were allowed to dry (10-20 minutes), plates inverted and incubated afterwards at 25°C for up to 4-5 days.

Advantage: useful for isolating aerobic microorganisms.

Disadvantages: strict aerobes are favored while microaerophilic tend to grow slower.

Step3.Colony counting and estimation of log_{10} CFU·cm^{-2} in the initial sample

At the end of the incubation period the number of colonies was determined in relation to the dilution sample that resulted in visible and distinguishable colonies observed on the agar plate. In the case of the drop plate method (Step 2.1), the number of colonies for a sample is the sum of colonies visible within all five drops, whereas for the spread plate method (Step 2.2) the total number of colonies visible in the whole plate is used. In both cases estimations of the total number of CFU in the initial sample was done according to the formula:

$$\log_{10} \text{CFU}\cdot\text{cm}^{-2} = \log_{10} \frac{(nr.of\ colonies \cdot plated\ volume \cdot 10^{dilution\ level}) \cdot 50ml}{sampled\ area\ (cm^2)} \qquad \text{Eq.(4.2)}$$

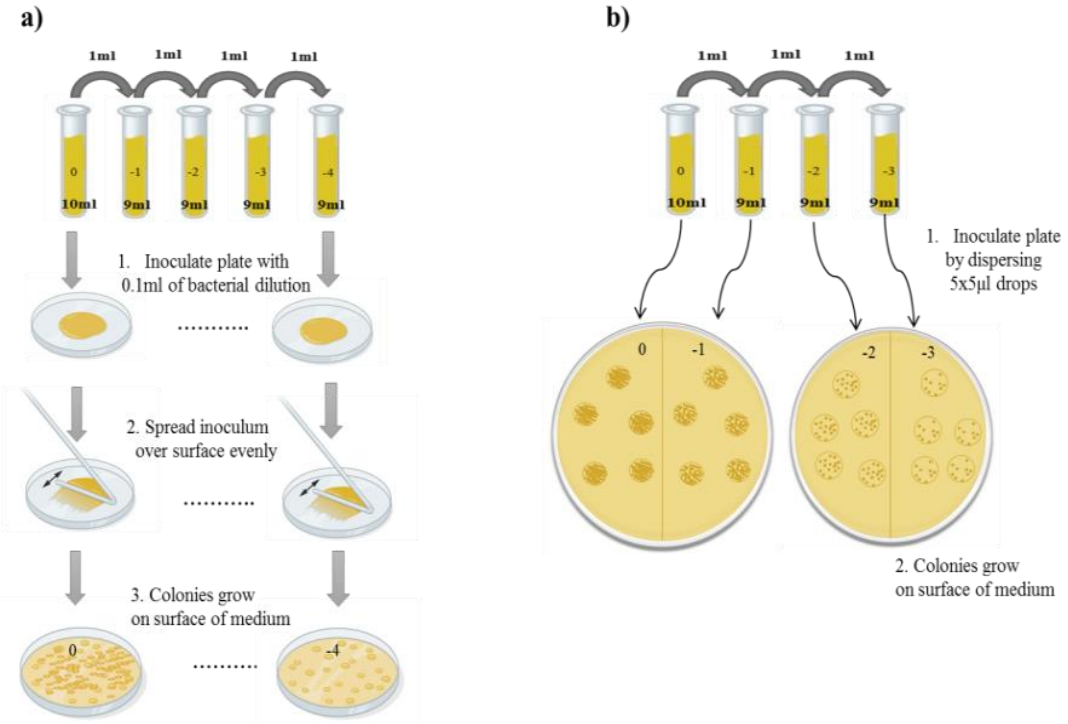

Figure 4.8 Illustration of the plating methods a) spread plate method, b) drop plate method. adapted from https://microbeonline.com/spread-plate-technique-principle-procedure-results

4.6.2. MicroSnap™ Total

The MicroSnap™ Total from Hygiena was used in parallel with the reference culture and counting methods as a rapid alternative to enumerate the total viable aerobic bacteria present on the surface of autopsied RO-membranes. The test is designed to use ATP as a biomarker for estimating the bacterial concentrations in a sample, either solid, liquid or surface. Considering the need to distinguish between bacterial ATP and extracellular ATP originating from the food matrix, the assay follows two-step procedure.

In the initial phase - *the enrichment step* - the sample is added to a growth media (broth) that supports the growth of most foodborne bacterial cells and additionally contains ATPase enzymes capable to reduce the extracellular ATP level. This phase takes place with incubation of the Enrichment pens at 30°C and takes 7 hours, when the background ATP is considered to reach minimal interference. In the second phase - *the detection phase* - an aliquot is transferred into a Detection pen containing a bioluminescence reagent that inactivates the ATPase enzyme, and via a lysis agent the bacterial ATP is extracted into solution. Upon reaction with the firefly enzyme the amount of light produced is measured with a luminometer. The light signal detected with the luminometer is assumed proportional with the concentration of present cells and can be converted into colony-forming-units (CFU).

One should note that the estimation of CFU is approximate since different microorganisms contain different amounts of ATP. Stressed cells also may contain lower amount of ATP, hence their detection and quantification may be inaccurate. Presence of fungi renders higher errors since the extraction buffer of the method is not designed for the extraction of ATP from the fungi cell, and also the ATP level of a fungi cell is typically several orders higher than of a bacterial cell. Therefore, the MicroSnap™ Total detection system is primarily designed for quantification of aerobic heterotrophic bacteria. The detection range for MicroSnap is <100 to 100,000 CFU· ml^{-1} (corresponding to <10 to 50,000 Relative Light Units – RLU – in the vendors *parlance*)[105].

Sample collection was done from a 5x5 cm area directly from the membrane via the stick swab of the MicroSnap™ Total enrichment device. The swab pen was brought back into the device placed for incubation at 30°C for 7 hours followed by detection of RLU units according to supplier's indications. Conversion of RLU units into $\log_{10}$ CFU·cm^{-2} was done via Eq.4.3.
Advantage: fast; dilutions are not required; minimal equipment / materials necessary.
Disadvantage: limited to a fixed range of detection level; human error introduced by swab pen procedure / application / handling; limited to small area as a compromise for falling within detection limits.

$$\log_{10} \text{CFU}\cdot\text{cm}^{-2} = \log_{10}\left(\frac{RLU\ value\cdot 10}{sampled\ area}\right) \qquad \text{Eq.(4.3)}$$

4.6.3. Results and discussion

Because of a management decision to exchange all RO elements in the entire RO/ROP unit, it was possible to collect and evaluate the extent of permeate biofouling on six more RO elements. Element details may be found in Table 4.1. Aerobic plate count was determined exclusively on the permeate surface of all RO elements by the plating method (via the spread plate technique) with sample collection from two distinct areas (10x10 cm) only one leaf (Figure 4.8c). Additional aerobic plate count values were obtained with MicroSnap™ Total from five sampling areas (5 x5 cm) across the same leaf. Given the fast result nature of the MicroSnap™ Total test, two additional leaves per RO element were sampled via MicroSnap™ Total, without performing any other reference plating.
Results obtained via MicroSnap™ Total correlate to some extent with the aerobic plate count values determined via reference plating (Figure 4.9d). Overall, both methods showed lower counts on RO-F1, RO-F2 and RO-F3 originating from the same pressure vessel in loop 4 when compared to RO-G1, RO-G2 and RO-G3 from loop 5, see Figure 4.9a. Across the surface of a sampled leaf, no significant differences were found between the five distinct measurements done via MicroSnap™ Total. Thus, results are presented in Figure 4.9b as average of the five measurements across a sampled leaf together with their standard deviations. Differences could be made instead between leaves within same RO elements. However, these observations are made based on the MicroSnap™ Total test and results should be viewed as semi-quantitative considering the inherited errors of the method when performed on yeast containing samples.

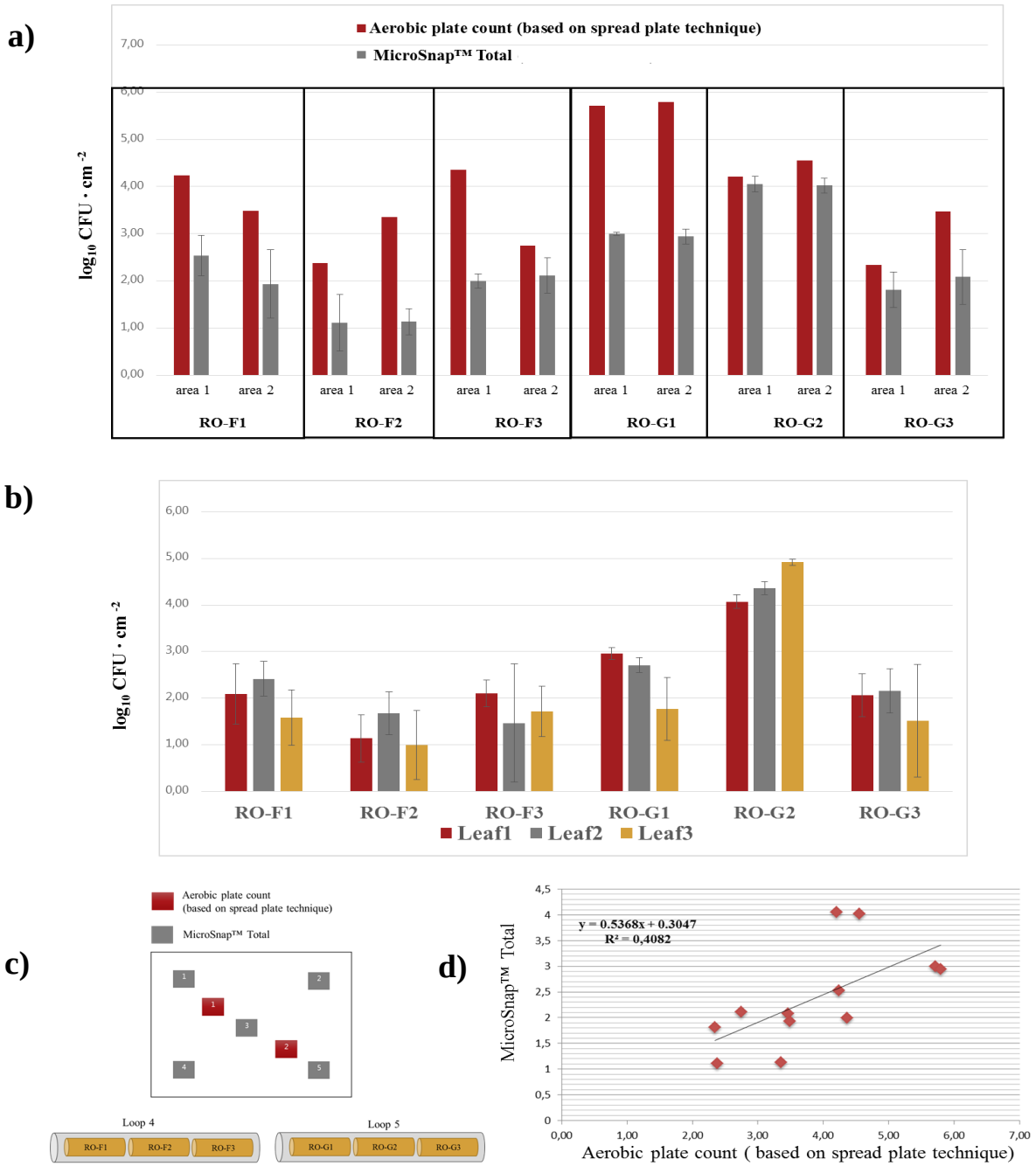

Figure 4.9 a) Aerobic plate count values across RO elements from sampling Phase 3; (red) counts determined via reference plating in area 1 and 2 while (grey) average of MicroSnap™ Total results from area 1,2 and 3 plotted against reference counts from area 1 and average of MicroSnap™ Total results in area 3,4 and 5plotted against reference counts from area 2 b) results of the MicroSnap™ Total test across three distinct leaves per element and presented as average of the whole five sampling spots within each leaf c) sampling pattern for reference plating and MicroSnap™ Total, d) reference plating vs. average MicroSnap™ Total results.

Chapter 5

Conclusions and perspectives

5.1. Conclusions

This PhD project has dealt both with exploring the possibility to develop a rapid method to signal critical microbial levels on conveyor belts under slaughterhouses conditions and with characterization of membrane surface fouling when processing UF whey permeate with recovery of process water.

The interest in the two scenarios comes from industry's aim to seek alternative ways to minimize their effluents and reduce their dependence on potable water e.g. by reducing the number of cleaning cycles. Evidently, this triggers the need for more active monitoring and control of key quality process attributes. Equipment surface hygiene is a crucial step in ensuring cost efficient operational practices and safe products. However, monitoring their hygiene status comes with a set of challenges. On open surfaces such as conveyor belts, evaluation of surface hygiene requires strategic and manual sample collection followed by labor intensive conventional plating. Results are typically biased by the efficiency of sample collection and chosen plating conditions (growth media, incubation temperature, plating method). In closed systems such as RO membrane, surfaces are inaccessible and evaluation of their hygiene status must be inferred from other monitored parameters (such as permeate fluxes and feed pressure). Cleaning of such closed systems takes place based on fixed recipes, which should be optimized in order to avoid insufficient or over cleaning. Decisions based on statistical control have probably the highest power to account for the considerable variability and unpredictable factors of (food) industrial practices. The investigations presented in this thesis were therefore targeted to improve the settings for an appropriate process quality control strategy when applied to the two scenarios.

In *Chapter 3*, devices based on front-face fluorescence spectroscopy were used to capture in a non-destructive way the autofluorescence characteristics of the measured conveyor belt (fouled/not fouled). Molecules such as NADH, FAD, tryptophan and porphyrins are expected to exhibit contributions in the EEMs as a function of microbial metabolic activity, as widely described in literature (Table3.1). However, the food matrix (in this case meat product) will contribute as well, with a similar type of information. The structural information recorded in EEMs was therefore extracted through PARAFAC decomposition in order to benefit of the power of second-order calibration methods to isolate unique information when new interferences are encountered. As extra challenge, the type of conveyor belt used for this investigation presented a strong intrinsic fluorescence overlapping with most signals of interest. Upon PARAFAC decomposition of data recorded on clean conveyor, three fluorescing species were identified and it was established that

their ratio varied across the conveyor length as a function of surface damage. Based on a Wilks' ratio statistic applied on PARAFAC scores, contaminates (emerging contributions in the EEMs) are identified in relation to shifts in the variance and covariance structure of the three conveyor fluorophores as determined in the calibration phase (calibration based on surface characteristics at to beginning of production). In this way the variable background interference is neutralized during decision making and the model is adaptable to the changes in surface topology as induced by process operations (wear-and-tear). The working principle of the statistical control chart based on Wilk's ratio was demonstrated both under artificial contamination (i.e. riboflavin) and also – conceptually - under meat biofouling in pilot-scale.

At this stage only high microbial loads can be detected and if distributed uniformly across the measuring surface. Detection in the interested range of 3-6 $\log_{10}$ CFU·cm^{-2} would require more advanced instruments capable of recording faster a complete EEM. An important factor in reaching a solution is fine tuning the selection of excitation wavelengths. The optimal choice should be made in such way that excitation of conveyor fluorophores is kept at a minimum. In this regard, the FreshDetect hand-held device was tested for its property to measure information that falls at the edge of what is considered conveyor background. However, the instrument relies on only one single excitation wavelength and its power to distinguish between bacterial growth is minimal for the conveyer surface task.

In *Chapter 4* several RO elements were sampled at various time points, originating from an RO/ROP unit which is used to recover process water from whey UF permeate. All elements were subjected to membrane autopsy with as main purpose evaluating the efficiency of CIP operations and determining the nature of their fouling. With respect to the findings on retenate membrane surfaces the microbial levels were comparable with what it has been reported in literature. The information contained in the amide bands as shown in the FTIR spectra indicate that after CIP operations, the retentate surface is coated with a layer consisting primarily of a protein like material. From the FTIR spectra it is also evident that most of the fouling layer is removed after cleaning. The overall levels of inorganic elements extracted from membrane coupons were minor, suggesting that scaling has only a limited contribution to the fouling layer for the membrane unit investigated. The membrane microflora was characterized strictly from a morphological point of view. In literature the membrane microflora of RO membranes processing cheese whey is strictly found as a diverse bacterial community. However, on all inspected RO membranes yeasts with a budding and filamentous morphology were found in combination with bacterial strains. In particular on the membrane permeate sides, extensive coverage with filamentous yeast was found.

The filamentous yeast had slow growth rates with colonies detectable in plating usually first after four or five days. Their presence in permeate streams could therefore potentially pass undetected by the routinely microbial analysis at the production plant which stresses the importance of UV treatment in ensuring the microbial safety quality of permeate streams. Targeted microbial analysis on

samples from water permeates streams throughout the entire RO/ROP unit showed only few yeast colonies and none after the UV disinfection points. However, it must be noted that at the sample collection stage all RO elements across the entire unit, with the exception of those in loop 4 and 5, were recently replaced with new membrane elements (based on a management decision).

The contamination source with yeast and their ultimate passage through the RO membrane is unknown and remains an open question. In literature, filamentous yeast is reported to be commonly isolated in tap water and water distribution systems[170]. Preliminary rRNA sequencing results[171] show that the yeast isolates found on the sampled RO membranes may be identified as Geotrichum clavatum or Magnusiomyces spicifer (filamneotus yeast) and Sporopachydermia lactativora (the budding yeast). In the report by Defra (2011)[172], Geotrichum clavatum is one of the fungal species commonly isolated from treated drinking water. This suggests that the intake of potable water in itself may represent a potential entrance route for yeast in the production plant.

5.2. Perspectives

Considering their important role in cross-contamination of food product, open food contact surfaces require great attention and a (typically) very labor intensive monitoring procedure. Switching to an on-line or at-line evaluation of surface hygiene would have obvious advantages over the time consuming plating methods. Although in an early development stage, the fluorescence based monitoring procedure described in this thesis is one option that may lead to a valid solution for on-line or at-line surface monitoring. Only one type of conveyor material was investigated, but the presented strategy may in practice turn to be easier to implement on conveyor surfaces subjected to less physical changes or with a minor spectral influence. Important to consider is the bias and limitations characteristic to conventional plating techniques which may add an extra challenge in method validation. Perhaps, in the development phase, compatible methods that account in their result for the presence of both cultivable and non-cultivable microorganisms (for example flow cytometry) should be considered for comparison besides the aerobic plate count values.

Spiral wound membranes are closed systems with no possibility to inspect their surface unless causing permanent damage. The findings described in this thesis are a proof that their behavior under industrial conditions cannot be predicted since the membrane permeate surface should – at least in theory - be a contaminant free area. With the identified biofouling trend, heat sanitation would be the preferred alternative to reduce and avoid the further growth of surface attached microorganisms. However, present membranes are characterized by a upper-temperature limit of 55°C and switching to heat sanitizable RO membrane is not always a financial viable option. Therefore, on a short term, a production plant would have to live with the technical implications of the biofouling layer and actively check that the final safety quality of permeate streams is routinely reached. In this regard, the efficiency of current UV treatment in inactivating any yeast or bacterial strains should be investigated.

Microorganisms are known to be capable to restore their metabolic functions[173] after UV treatment through either photo-reactivation or dark repair mechanisms. Although, reactivation is much slower under dark conditions, temperature, pH and ionic strength could have an effect on dark repair of microorganisms after UV treatment[174]. It should thus be evaluated if the processing operations offer conditions for such restore mechanisms. Even if not detected in the permeate streams, the proof of extensive biofouling on permeate surfaces indicate that cross-contamination is a constant danger and stresses the dependence on UV treatment.

On a long perspective, a sampling program (e.g. every six months) of some membranes, including autopsy and analysis, may offer a periodical window into the actual hygiene and physical status of RO elements. It may serve as a platform to identify occurrence of potential microbial threats that could pass undetected in the permeate water streams (e.g. due to a dilution effect in the overall processing volumes) and this way optimize future microbial analysis accordingly. Therefore, results from such strategic membrane sampling could serve as an internal reference and comparison points. Large amounts of data are collected everyday through classical process monitoring techniques (e.g. conductivity, pH, temperature, turbidity, permeate fluxes, etc.). Their dynamics should be linked through a multiway approach with observations attained from membrane autopsy and based on this, one could establish what constitutes a normal cleaning profile. Optimization of membrane cleaning should thus be seen as a continuous process. This way, over-cleaning or ineffective cleaning, as it is most likely to occur with the current recipe based cleaning method, could be minimized.

References

1. Ölmez H. Water Consumption, Reuse and Reduction Strategies in Food Processing. In: *Sustainable Food Processing*. ; 2013:401-434. doi:10.1002/9781118634301.ch17.
2. Sethu V, Viramuthu VA. 23 – Water recycling in the food industry. In: *Handbook of Water and Energy Management in Food Processing*. ; 2008:647-662. doi:10.1533/9781845694678.5.647.
3. Water Framework Directive. Directive 2000/60/EC of the European Parliament and of the Council of 23 October 2000 establishing a framework for Community action in the field of water policy. *Off J Eur Parliam*. 2000;L327(October 2000):1-82. doi:10.1039/ap9842100196.
4. Directive 2006/11/EC of the European Parliament and of the Council on pollution caused by certain dangerous substances discharged into the aquatic environment of the Community. *Off J Eur Union*. 2006. https://eur-lex.europa.eu/LexUriServ/LexUriServ.do?uri=OJ:L:2006:064:0052:0059:EN:PDF.
5. *Directive 98/83/EC on the Quality of Water Intended for Human Consumption*. Vol L 269.; 2000. doi:2004R0726 - v.7 of 05.06.2013.
6. Food and Agriculture Organization of the United Nations. *The Future of Food and Agriculture: Trends and Challenges.*; 2017. doi:ISBN 978-92-5-109551-5.
7. Nagy E. Advances in membrane technology for the treatment and reuse of food processing wastewater. In: *Handbook of Water and Energy Management in Food Processing*. ; 2008:663-699. doi:10.1533/9781845694678.5.663.
8. Walstra P, Wouters JTM, Geurts TJ. *Dairy Science and Technology*. Vol 146.; 2006. doi:10.1007/s007690000247.
9. Baldasso C, Barros TC, Tessaro IC. Concentration and purification of whey proteins by ultrafiltration. *Desalination*. 2011;278(1-3):381-386. doi:10.1016/j.desal.2011.05.055.
10. Meneses YE, Flores RA. Feasibility, safety, and economic implications of whey-recovered water in cleaning-in-place systems: A case study on water conservation for the dairy industry. *J Dairy Sci*. 2016;99(5):3396-3407. doi:10.3168/jds.2015-10306.
11. Bustillo-Lecompte C, Mehrvar M, Quiñones-Bolaños E. Slaughterhouse Wastewater Characterization and Treatment: An Economic and Public Health Necessity of the Meat Processing Industry in Ontario, Canada. *J Geosci Environ Prot*. 2016;4(4):175-186. doi:10.4236/gep.2016.44021.
12. Soares VM, Pereira JG, Zanette CM, et al. Cleaning Conveyor Belts in the Chicken-Cutting Area of a Poultry Processing Plant with 45°C Water. *J Food Prot*. 2014;77(3):496-498. doi:10.4315/0362-028X.JFP-13-340.
13. Amorim AKB, de Nardi IR, Del Nery V. Water conservation and effluent minimization: Case study of a poultry slaughterhouse. *Resour Conserv Recycl*. 2007;51(1):93-100. doi:10.1016/j.resconrec.2006.08.005.
14. Matsumura EM, Mierzwa JC. Water conservation and reuse in poultry processing plant-A case study. *Resour Conserv Recycl*. 2008;52(6):835-842. doi:10.1016/j.resconrec.2007.10.002.

15. Mavrov V, Bélières E. Reduction of water consumption and wastewater quantities in the food industry by water recycling using membrane processes. *Desalination*. 2000;131(1-3):75-86. doi:10.1016/S0011-9164(00)90008-0.

16. Suárez A, Riera FA. Production of high-quality water by reverse osmosis of milk dairy condensates. *J Ind Eng Chem*. 2015;21:1340-1349. doi:10.1016/j.jiec.2014.06.004.

17. Suárez L, Diez MA, Riera FA. Recovery of detergents in food industry: an industrial approach. *Desalin Water Treat*. 2015;56(4):967-976. doi:10.1080/19443994.2014.942384.

18. Vourch M, Balannec B, Chaufer B, Dorange G. Nanofiltration and reverse osmosis of model process waters from the dairy industry to produce water for reuse. *Desalination*. 2005;172(3):245-256. doi:10.1016/j.desal.2004.07.038.

19. Aydiner C, Sen U, Topcu S, et al. Techno-economic viability of innovative membrane systems in water and mass recovery from dairy wastewater. *J Memb Sci*. 2014;458:66-75. doi:10.1016/j.memsci.2014.01.058.

20. Casani S, Hansen TB, Christensen J, Knochel S. Comparison of methods for assessing reverse osmosis membrane treatment of shrimp process water. *J Food Prot*. 2005;68(4):801-807.

21. Blöcher C, Noronha M, Fünfrocken L, et al. Recycling of spent process water in the food industry by an integrated process of biological treatment and membrane separation. *Desalination*. 2002;144(1-3):143-150. doi:10.1016/S0011-9164(02)00303-X.

22. Selma M V., Allende A, López-Gálvez F, Conesa MA, Gil MI. Disinfection potential of ozone, ultraviolet-C and their combination in wash water for the fresh-cut vegetable industry. *Food Microbiol*. 2008;25(6):809-814. doi:10.1016/j.fm.2008.04.005.

23. Lopez D, Vlamakis H, Kolter R. Biofilms. *Cold Spring Harb Perspect Biol*. 2010;2(7):a000398. doi:10.1101/cshperspect.a000398.

24. Holah JT. Cleaning and disinfection practices in food processing. In: *Hygiene in Food Processing*. ; 2014:259-261. doi:http://dx.doi.org/10.1533/9780857098634.3.259.

25. Janknecht P, Melo LF. Online biofilm monitoring. *Rev Environ Sci Biotechnol*. 2003;2(2-4):269-283. doi:10.1023/B:RESB.0000040461.69339.04.

26. WHO. The Top 10 causes of Death. World Health Organization. doi:/entity/mediacentre/factsheets/fs310/en/index.html.

27. WHO, FAO. CODEX ALIMENTARIUS. *Food Hyg Basic texts*. 2009. http://www.fao.org/docrep/012/a1552e/a1552e00.htm.

28. Jha SN, Jha SN. Chapter 1 – Food Safety and Quality. In: *Rapid Detection of Food Adulterants and Contaminants*. ; 2016:1-24. doi:10.1016/B978-0-12-420084-5.00001-9.

29. EC. White Paper on Food Safety. 2000. https://ec.europa.eu/food/sites/food/files/safety/docs/animal-feed-pub06_en.pdf.

30. EC. Regulation (EC) No 852/2004 of the European Parliament and of the Council on the hygiene of foodstuffs. *EC*. 2004. https://eur-lex.europa.eu/LexUriServ/LexUriServ.do?uri=OJ:L:2004:139:0001:0054:en:PDF.

31. EC. Regulation (EC) No 853/2004 of the European Parliament and of the Council laying laying down specific hygiene rules for food of animal origin. 2004. https://eur-

lex.europa.eu/legal-content/EN/TXT/PDF/?uri=CELEX:32004R0853&from=EN.

32. EC. Regulation (EC) No 183/2005 of the European Parliament and of the Council laying down requirements for feed hygiene. 2005. https://eur-lex.europa.eu/legal-content/EN/TXT/HTML/?uri=CELEX:32005R0183&from=EN.

33. EC. Regulation (EC) No 178/2002 of the European Parliament and of the Council laying down the general principles and requirements of food law, establishing the European Food Safety Authority and laying down procedures in matters of food safety. 2002. https://eur-lex.europa.eu/legal-content/EN/TXT/PDF/?uri=CELEX:32002R0178&from=EN.

34. Van der Meulen B, Van de Weerd H. 1 – Food hygiene regulation in the European Union (EU). In: *Hygiene in Food Processing*. ; 2014:3-20. doi:10.1533/9780857098634.1.3.

35. Adley CC, Ryan MP. The Nature and Extent of Foodborne Disease. In: *Antimicrobial Food Packaging*. ; 2016:1-10. doi:10.1016/B978-0-12-800723-5.00001-2.

36. Lelieveld HLM, Holah JT. Hazards, sources and vectors of contamination. In: *Hygiene in Food Processing: Principles and Practice: Second Edition*. ; 2013:21-50. doi:10.1533/9780857098634.1.21.

37. Smoot L, Cordier JL. Emerging foodborne pathogens and the food industry. In: *Foodborne Pathogens: Hazards, Risk Analysis and Control: Second Edition*. ; 2009:154-181. doi:10.1533/9781845696337.1.154.

38. Blackburn C. Managing microbial food spoilage: An overview. In: *Food Spoilage Microorganisms*. ; 2006:147-170. doi:10.1533/9781845691417.2.147.

39. Blanchfield JR. Good manufacturing practice (GMP) in the food industry. In: *Handbook of Hygiene Control in the Food Industry*. ; 2005:324-347. doi:10.1533/9781845690533.3.324.

40. Mortimore S, Wallace C. An introduction to HACCP. In: *HACCP*. ; 1998:1-11. doi:10.1007/978-1-4615-5781-4_1.

41. European Community. Directive (2000/60/EC) of the European Parliament and of the Council establishing a framework for Community action in the field of water policy. *Off J Eur Communities*. 2000;L 327:1-72. doi:https://eur-lex.europa.eu/legal-content/EN/TXT/HTML/?uri=CELEX:32000L0060&from=EN.

42. Moerman F, Kastelein J. Hygienic Design and Maintenance of Equipment. In: *Food Safety Management: A Practical Guide for the Food Industry*. ; 2014:673-739. doi:10.1016/B978-0-12-381504-0.00026-3.

43. EC. Regulation (EC) No 1935/2004 of the European Parliament and of the Council and articles intended to come into contact with food. 2004. https://eur-lex.europa.eu/legal-content/EN/TXT/HTML/?uri=CELEX:32004R1935&from=EN.

44. EHEDG M of CS of the. Materials of construction for equipment in contact with food. *Trends Food Sci Technol*. 2007;18, Supple:S40-S50. doi:http://dx.doi.org/10.1016/j.tifs.2006.11.025.

45. Schmidt RH, Erickson DJ, Sims S, Wolff P. Characteristics of food contact surface materials: Stainless steel. *Food Prot Trends*. 2012;32(10):574-584.

46. Lai JKL, Lo K., Shek CH. *Stainless Steel an Introduction and Their Recent Developments*.; 2012. doi:10.2174/97816080530561120101.

47. Lewan M, Partington E. Food processing equipment construction materials. In: *Hygiene in Food Processing*. ; 2014:142-154. doi:10.1533/9780857098634.2.142.

48. Moerman F, Partington E. Materials of Construction for Food Processing Equipment and Services: Requirements, Strengths and Weaknesses. *J Hyg Eng Des*. 2014:10-37. http://www.jhed.mk/filemanager/JHED Vol 6/01. HED/02. Frank Moerman.pdf.

49. Sidwell J. Global legislation for rubber materials in contact with food. In: *Global Legislation for Food Contact Materials*. ; 2015:141-160. doi:10.1016/B978-1-78242-014-9.00006-1.

50. Garrett TR, Bhakoo M, Zhang Z. Bacterial adhesion and biofilms on surfaces. *Prog Nat Sci*. 2008;18(9):1049-1056. doi:10.1016/j.pnsc.2008.04.001.

51. Monroe D. Looking for chinks in the armor of bacterial biofilms. *PLoS Biol*. 2007;5(11):2458-2461. doi:10.1371/journal.pbio.0050307.

52. Flemming HC, Wingender J. The biofilm matrix. *Nat Rev Microbiol*. 2010;8(9):623-633. doi:10.1038/nrmicro2415.

53. Limoli DH, Jones CJ, Wozniak DJ, Cruz S. Bacterial Extracellular Polysaccharides in Biofilm Formation and Function. *Microbiol Spectr*. 2015;3(3):1-30. doi:10.1128/microbiolspec.MB-0011-2014.Bacterial.

54. Vu B, Chen M, Crawford RJ, Ivanova EP. Bacterial extracellular polysaccharides involved in biofilm formation. *Molecules*. 2009;14(7):2535-2554. doi:10.3390/molecules14072535.

55. Sinde E, Carballo J. Attachment of *Salmonella spp*. and *Listeria monocytogenes* to stainless steel, rubber and polytetrafluorethylene: the influence of free energy and the effect of commercial sanitizers. *Food Microbiol*. 2000;17(4):439-447. doi:10.1006/fmic.2000.0339.

56. Celmer D, Oleszkiewicz JA, Cicek N. Impact of shear force on the biofilm structure and performance of a membrane biofilm reactor for tertiary hydrogen-driven denitrification of municipal wastewater. *Water Res*. 2008;42(12):3057-3065. doi:10.1016/j.watres.2008.02.031.

57. Whitehead KA, Verran J. Formation, architecture and functionality of microbial biofilms in the food industry. *Curr Opin Food Sci*. 2015;2:84-91. doi:10.1016/j.cofs.2015.02.003.

58. Giaouris EE, Simões M V. Chapter 11 - Pathogenic Biofilm Formation in the Food Industry and Alternative Control Strategies. In: *Handbook of Food Bioengineering*. ; 2018:309-377. doi:https://doi.org/10.1016/B978-0-12-811444-5.00011-7.

59. Pugh SJ, Hewitt GF, Müller-Steinhagen H. Fouling During the Use of Seawater as Coolant—the Development of a User Guide. *Heat Transf Eng*. 2005;26(1):35-43. doi:10.1080/01457630590890148.

60. Matsumura Y, Yamada K, Takahashi M, Kikuchi Y, Tsuchido T. Properties of bacterial corrosion of stainless steel and its inhibition by protamine coating. *Biocontrol Sci*. 2007;12(1):21-29. doi:10.4265/bio.12.21.

61. Herzberg M, Elimelech M. Biofouling of reverse osmosis membranes: Role of biofilm-enhanced osmotic pressure. *J Memb Sci*. 2007;295(1-2):11-20. doi:10.1016/j.memsci.2007.02.024.

62. Bridier A, Briandet R, Thomas V, Dubois-Brissonnet F. Resistance of bacterial biofilms to disinfectants: A review. *Biofouling*. 2011;27(9):1017-1032. doi:10.1080/08927014.2011.626899.

63. Milojević L, Velebit B, Baltić T, Nikolić A, Mitrović R, Dordević V. Characterization of biofilms produced by Escherichia coli O157 isolated from cattle hides. In: *IOP Conference Series: Earth and Environmental Science*. Vol 85. ; 2017. doi:10.1088/1755-1315/85/1/012076.

64. Liu NT, Nou X, Lefcourt AM, Shelton DR, Lo YM. Dual-species biofilm formation by Escherichia coli O157:H7 and environmental bacteria isolated from fresh-cut processing facilities. *Int J Food Microbiol*. 2014;171:15-20. doi:10.1016/j.ijfoodmicro.2013.11.007.

65. Gomes LC, Piard JC, Briandet R, Mergulhão FJ. Pseudomonas grimontii biofilm protects food contact surfaces from Escherichia coli colonization. *LWT - Food Sci Technol*. 2017;85:309-315. doi:10.1016/j.lwt.2017.03.005.

66. Lianou A, Koutsoumanis KP. Strain variability of the biofilm-forming ability of Salmonella enterica under various environmental conditions. *Int J Food Microbiol*. 2012;160(2):171-178. doi:10.1016/j.ijfoodmicro.2012.10.002.

67. Shaheen R, Svensson B, Andersson MA, Christiansson A, Salkinoja-Salonen M. Persistence strategies of Bacillus cereus spores isolated from dairy silo tanks. *Food Microbiol*. 2010;27(3):347-355. doi:10.1016/j.fm.2009.11.004.

68. de Souza EL, Meira QGS, Barbosa I de M, Athayde AJAA, da Conceição ML, de Siqueira JP. Biofilm formation by Staphylococcus aureus from food contact surfaces in a meat-based broth and sensitivity to sanitizers. *Brazilian J Microbiol*. 2014;45(1):67-75. doi:10.1590/S1517-83822014000100010.

69. EC. REGULATION (EC) No 2073/2005 on microbiological criteria for foodstuffs. 2005. https://eur-lex.europa.eu/LexUriServ/LexUriServ.do?uri=OJ:L:2005:338:0001:0026:EN:PDF.

70. Ismaïl R, Aviat F, Michel V, et al. Methods for recovering microorganisms from solid surfaces used in the food industry: A review of the literature. *Int J Environ Res Public Health*. 2013;10(11):6169-6183. doi:10.3390/ijerph10116169.

71. HONG C-H, TODD ECD, BAHK G-J. Aerobic Plate Counts as a Measure of Hazard Analysis Critical Control Point Effectiveness in a Pork Processing Plant. *J Food Prot*. 2008;71(6):1248-1252. doi:10.4315/0362-028X-71.6.1248.

72. Gracias KS, McKillip JL. A review of conventional detection and enumeration methods for pathogenic bacteria in food. *Can J Microbiol*. 2004;50(11):883-890. doi:10.1139/w04-080.

73. Nivens DE, Co BM, Franklin MJ. Sampling and quantification of biofilms in food processing and other environments. In: *Biofilms in the Food and Beverage Industries*. ; 2009:539-568. doi:10.1533/9781845697167.5.539.

74. ISO. ISO 4833-1:2013. 2013. https://www.iso.org/obp/ui/#iso:std:59509:en.

75. ISO. ISO 18593:2018. 2018. https://www.iso.org/obp/ui/#iso:std:iso:18593:ed-2:v1:en.

76. Griffith C. Surface Sampling and the Detection of Contamination. In: *Handbook of Hygiene Control in the Food Industry: Second Edition*. ; 2016:673-696. doi:10.1016/B978-0-08-100155-4.00044-3.

77. Orion Diagnostica. A Guide to Monitoring Surface Hygiene. http://www.lifesignmed.com/sites/default/files/Hygicult Guide To Monitoring Cleanliness.pdf.

78. FDA. Guidance for Industry PAT: A Framework for Innovative Pharmaceutical Development, Manufacuring, and Quality Assurance. *FDA Off Doc*. 2004;(September):16. doi:http://www.fda.gov/CDER/guidance/6419fnl.pdf.

79. van den Berg F, Lyndgaard CB, Sørensen KM, Engelsen SB. Process Analytical Technology in the food industry. *Trends Food Sci Technol*. 2013;31(1):27-35. doi:10.1016/j.tifs.2012.04.007.

80. Tajammal Munir M, Yu W, Young BR, Wilson DI. The current status of process analytical technologies in the dairy industry. *Trends Food Sci Technol*. 2015;43(2):205-218. doi:10.1016/j.tifs.2015.02.010.

81. Hitzmann B, Hauselmann R, Niemoeller A, Sangi D, Traenkle J, Glassey J. Process analytical technologies in food industry – challenges and benefits: A status report and recommendations. *Biotechnol J*. 2015;10(8):1095-1100. doi:10.1002/biot.201400773.

82. Roussel S, Preys S, Chauchard F, Lallemand J. Process Analytical Technology for the Food Industry. *Springer*. 2014;(VII):301. doi:10.1007/978-1-4939-0311-5.

83. Lyndgaard CB, Rasmussen MA, Engelsen SB, Thaysen D, Van Den Berg F. Moving from recipe-driven to measurement-based cleaning procedures: Monitoring the Cleaning-In-Place process of whey filtration units by ultraviolet spectroscopy and chemometrics. *J Food Eng*. 2014;126:82-88. doi:10.1016/j.jfoodeng.2013.10.037.

84. Jensen JK, Ottosen N, Engelsen SB, Van Den Berg F. Investigation of UF and MF membrane residual fouling in full-scale dairy production using FT-IR to quantify protein and fat. *Int J Food Eng*. 2015;11(1):1-15. doi:10.1515/ijfe-2014-0254.

85. Stoica IM, Vitzilaiou E, Lyng Røder H, et al. Biofouling on RO-membranes used for water recovery in the dairy industry. *J Water Process Eng*. 2018;24:1-10. doi:10.1016/j.jwpe.2018.05.004.

86. Joseph R. Lakowicz. Principles of Fluorescence Spectroscopy. Introduction to Fluorescence. In: *Introduction to Fluorescence Joseph R. Lakowicz Lakowicz,*. ; 1999:1-23. doi:10.1007/978-1-4757-3061-6_1.

87. M.H. P. Basic Principles of Spectroscopy. In: Editions 2nd, ed. *Food Analysis*. Srpinger, Boston,MA; 2010. doi:https://doi.org/10.1007/978-1-4419-1478-1_21.

88. Valeur B, Berberan-Santos MN. *Molecular Fluorescence: Principles and Applications, Second Edition*.; 2012. doi:10.1002/9783527650002.

89. Martynov VI, Pakhomov AA, Popova N V., Deyev IE, Petrenko AG. Synthetic Fluorophores for Visualizing Biomolecules in Living Systems. *Acta Naturae*. 2016;8(4):33-46.

90. Leblanc L, Dufour E. Monitoring the identity of bacteria using their intrinsic fluorescence. *FEMS Microbiol Lett*. 2002;211(2):147-153. doi:10.1111/j.1574-6968.2002.tb11217.x.

91. Sugiyama J, Fujita K, Yoshimura M, Tsuta M, Shibata M, Kokawa M. Detection of food hazards using fluorescence fingerprint. In: *IFAC Proceedings Volumes (IFAC-PapersOnline)*. Vol 4. ; 2013:70-74. doi:10.3182/20130828-2-SF-3019.00035.

92. B. Valeur MNB. Effects of Intermolecular Photophysical Processes on Fluorescence Emission. In: *Molecular Fluorescence: Principles and Applications*. 2nd editio. ; 2012:141-179. doi:10.1002/9783527650002.

93. Ogikubo S, Nakabayashi T, Adachi T, et al. Intracellular pH sensing using autofluorescence

lifetime microscopy. *J Phys Chem B*. 2011;115(34):10385-10390. doi:10.1021/jp2058904.

94. Valeur B, Berberan-Santos MN. Environmental Effects on Fluorescence Emission. In: *Molecular Fluorescence*. ; 2012:109-140. doi:10.1002/9783527650002.ch5.

95. Rinnan Å, Andersen CM. Handling of first-order Rayleigh scatter in PARAFAC modelling of fluorescence excitation-emission data. *Chemom Intell Lab Syst*. 2005;76(1):91-99. doi:10.1016/j.chemolab.2004.09.009.

96. Eilers PHC, Kroonenberg PM. Modeling and correction of Raman and Rayleigh scatter in fluorescence landscapes. *Chemom Intell Lab Syst*. 2014;130:1-5. doi:10.1016/j.chemolab.2013.09.002.

97. Clarke RJ, Oprysa A. Fluorescence and Light Scattering. *J Chem Educ*. 2004;81(5):705. doi:10.1021/ed081p705.

98. Lakowicz JR. Instrumentation for Fluorescence Spectroscopy 2.1. In: *Principles of Fluorescence Spectroscopy*. ; 2006:36. doi:10.1002/9783527633500.ch1.

99. Bro R. PARAFAC. Tutorial and applications. In: *Chemometrics and Intelligent Laboratory Systems*. Vol 38. ; 1997:149-171. doi:10.1016/S0169-7439(97)00032-4.

100. Stoica IM, Babamoradi H, van den Berg F. A statistical strategy to assess cleaning level of surfaces using fluorescence spectroscopy and Wilks' ratio. *Chemom Intell Lab Syst*. 2017;165. doi:10.1016/j.chemolab.2017.03.014.

101. Andersen CM, Bro R. Practical aspects of PARAFAC modeling of fluorescence excitation-emission data. *J Chemom*. 2003;17(4):200-215. doi:10.1002/cem.790.

102. Yang L, Bashir R. Electrical/electrochemical impedance for rapid detection of foodborne pathogenic bacteria. *Biotechnol Adv*. 2008;26(2):135-150. doi:10.1016/j.biotechadv.2007.10.003.

103. Jiang J, Wang X, Chao R, et al. Smartphone based portable bacteria pre-concentrating microfluidic sensor and impedance sensing system. *Sensors Actuators, B Chem*. 2014;193:653-659. doi:10.1016/j.snb.2013.11.103.

104. Kim H, Jung Y, Doh IJ, Lozano-Mahecha RA, Applegate B, Bae E. Smartphone-based low light detection for bioluminescence application. *Sci Rep*. 2017;7. doi:10.1038/srep40203.

105. Meighan P, Smith M, Datta S, Katz B, Nason F. The validation of the microsnap total for enumeration of total viable count in a variety of foods. *J AOAC Int*. 2016;99(3):686-694. doi:10.5740/jaoacint.16-0016.

106. Veal DA, Deere D, Ferrari B, Piper J, Attfield P V. Fluorescence staining and flow cytometry for monitoring microbial cells. *J Immunol Methods*. 2000;243(1-2):191-210. doi:10.1016/S0022-1759(00)00234-9.

107. Casalinuovo IA, Di Pierro D, Coletta M, Di Francesco P. Application of electronic noses for disease diagnosis and food spoilage detection. *Sensors*. 2006;6(11):1428-1439. doi:10.3390/s6111428.

108. Nadkarni MA, Martin FE, Jacques NA, Hunter N. Determination of bacterial load by real-time PCR using a broad-range (universal) probe and primers set. *Microbiology*. 2002;148(1):257-266. doi:10.1099/00221287-148-1-257.

109. Castillo M, Martín-Orúe SM, Manzanilla EG, Badiola I, Martín M, Gasa J. Quantification of

total bacteria, enterobacteria and lactobacilli populations in pig digesta by real-time PCR. *Vet Microbiol*. 2006;114(1-2):165-170. doi:10.1016/j.vetmic.2005.11.055.

110. Davis R, Mauer L. Fourier transform infrared (FT-IR) spectroscopy: a rapid tool for detection and analysis of foodborne pathogenic bacteria. *Curr Res Technol Educ Top Appl Microbiol Microb Biotechnol A Méndez-Vilas*. 2010;(1):1582-1594. http://www.formatex.info/microbiology2/1582-1594.pdf.

111. Wang P, Pang S, Chen J, et al. Label-free mapping of single bacterial cells using surface-enhanced Raman spectroscopy. *Analyst*. 2016;141(4):1356-1362. doi:10.1039/C5AN02175H.

112. Nicolaou N, Xu Y, Goodacre R. Fourier transform infrared and raman spectroscopies for the rapid detection, enumeration, and growth interaction of the Bacteria Staphylococcus aureus and Lactococcus lactis ssp. cremoris in Milk. *Anal Chem*. 2011;83(14):5681-5687. doi:10.1021/ac2008256.

113. Cheng JH, Sun DW. Recent Applications of Spectroscopic and Hyperspectral Imaging Techniques with Chemometric Analysis for Rapid Inspection of Microbial Spoilage in Muscle Foods. *Compr Rev Food Sci Food Saf*. 2015;14(4):478-490. doi:10.1111/1541-4337.12141.

114. Zheng XC, Peng YK, Wang WX. A Nondestructive Real-Time Detection Method of Total Viable Count in Pork by Hyperspectral Imaging Technique. *Appl Sci*. 2017;7(3):213. doi:10.3390/app7030213.

115. Tito NB, Rodemann T, Powell SM. Use of near infrared spectroscopy to predict microbial numbers on Atlantic salmon. *Food Microbiol*. 2012;32(2):431-436. doi:10.1016/j.fm.2012.07.009.

116. Quintelas C, Mesquita DP, Lopes JA, Ferreira EC, Sousa C. Near-infrared spectroscopy for the detection and quantification of bacterial contaminations in pharmaceutical products. *Int J Pharm*. 2015;492(1-2):199-206. doi:10.1016/j.ijpharm.2015.07.005.

117. Oberreuter H, Mertens F, Seiler H, Scherer S. Quantification of micro-organisms in binary mixed populations by Fourier transform infrared (FT-IR) spectroscopy. *Lett Appl Microbiol*. 2000;30(1):85-89. doi:10.1046/j.1472-765x.2000.00694.x.

118. Ellis DI, Broadhurst D, Kell DB, Rowland JJ, Goodacre R. Rapid and quantitative detection of the microbial spoilage of meat by fourier transform infrared spectroscopy and machine learning. *Appl Environ Microbiol*. 2002;68(6). doi:10.1128/AEM.68.6.2822-2828.2002.

119. Ammor MS, Argyri A, Nychas GJE. Rapid monitoring of the spoilage of minced beef stored under conventionally and active packaging conditions using Fourier transform infrared spectroscopy in tandem with chemometrics. *Meat Sci*. 2009;81(3):507-514. doi:10.1016/j.meatsci.2008.10.015.

120. Hassan M, Gonzalez E, Hitchins V, Ilev I. Detecting bacteria contamination on medical device surfaces using an integrated fiber-optic mid-infrared spectroscopy sensing method. *Sensors Actuators, B Chem*. 2016;231:646-654. doi:10.1016/j.snb.2016.03.044.

121. Escoriza MF, VanBriesen JM, Stewart S, Maier J, Treado PJ. Raman spectroscopy and chemical imaging for quantification of filtered waterborne bacteria. *J Microbiol Methods*. 2006;66(1):63-72. doi:10.1016/j.mimet.2005.10.013.

122. Zhu Q, Quivey RG, Berger AJ. Raman spectroscopic measurement of relative concentrations

in mixtures of oral bacteria. *Appl Spectrosc*. 2007;61(11):1233-1237. doi:10.1366/000370207782597021.

123. Fischer M, Wahl M, Friedrichs G. Design and field application of a UV-LED based optical fiber biofilm sensor. *Biosens Bioelectron*. 2012;33(1):172-178. doi:10.1016/j.bios.2011.12.048.

124. Mita Mala D, Yoshimura M, Kawasaki S, et al. Fiber optics fluorescence fingerprint measurement for aerobic plate count prediction on sliced beef surface. *LWT - Food Sci Technol*. 2016;68:14-20. doi:10.1016/j.lwt.2015.11.065.

125. Fischer M, Triggs GJ, Krauss TF. Optical sensing of microbial life on surfaces. *Appl Environ Microbiol*. 2016;82(5):1362-1371. doi:10.1128/AEM.03001-15.

126. Beier BD, Quivey RG, Berger AJ. Raman microspectroscopy for species identification and mapping within bacterial biofilms. *AMB Express*. 2012;2(1):1-7. doi:10.1186/2191-0855-2-35.

127. Chisanga M, Muhamadali H, Ellis DI, Goodacre R. Surface-Enhanced Raman Scattering (SERS) in Microbiology: Illumination and Enhancement of the Microbial World. *Applied Spectroscopy*. 2018.

128. Schlücker S. Surface-enhanced raman spectroscopy: Concepts and chemical applications. *Angew Chemie - Int Ed*. 2014;53(19):4756-4795. doi:10.1002/anie.201205748.

129. Iulietto MF, Sechi P, Borgogni E, Cenci-Goga BT. Meat spoilage: A critical review of a neglected alteration due to ropy slime producing bacteria. *Ital J Anim Sci*. 2015;14(3):316-326. doi:10.4081/ijas.2015.4011.

130. Abdi H, Williams LJ. Principle component analysis. *Wiley Interdiscip Rev Comput Stat*. 2010;2(4):433-459.

131. Haaland DM, Thomas E V. Partial Least-Squares Methods for Spectral Analyses. 1. Relation to Other Quantitative Calibration Methods and the Extraction of Qualitative Information. *Anal Chem*. 1988;60(11):1193-1202. doi:10.1021/ac00162a020.

132. Aït-Kaddour A, Boubellouta T, Chevallier I. Development of a portable spectrofluorimeter for measuring the microbial spoilage of minced beef. *Meat Sci*. 2011;88(4):675-681. doi:10.1016/j.meatsci.2011.02.027.

133. Sahar A, Boubellouta T, Dufour É. Synchronous front-face fluorescence spectroscopy as a promising tool for the rapid determination of spoilage bacteria on chicken breast fillet. *Food Res Int*. 2011;44(1):471-480. doi:10.1016/j.foodres.2010.09.006.

134. Strathmann M, Mittenzwey KH, Sinn G, Papadakis W, Flemming HC. Simultaneous monitoring of biofilm growth, microbial activity, and inorganic deposits on surfaces with an in situ, online, real-time, non-destructive, optical sensor. *Biofouling*. 2013;29(5):573-583. doi:10.1080/08927014.2013.791287.

135. Kilungo AP, Carlton-Carew N, Powers LS. *Journal of Biosensors & Bioelectronics.*; 2013. https://www.omicsonline.org/continuous-real-time-detection-of-microbial-contamination-in-water-using-intrinsic-fluorescence-2155-6210.S12-002.php?aid=14627.

136. Lefcourt AM, Wiederoder MS, Liu N, Kim MS, Martin Lo Y. Development of a portable hyperspectral imaging system for monitoring the efficacy of sanitation procedures in food processing facilities. *J Food Eng*. 2013;117(1):59-66. doi:10.1016/j.jfoodeng.2013.01.043.

137. Hassoun A, Karoui R. Front-face fluorescence spectroscopy coupled with chemometric tools for monitoring fish freshness stored under different refrigerated conditions. *Food Control*. 2015;54:240-249. doi:10.1016/j.foodcont.2015.01.042.

138. Beck EA, Lefcourt AM, Lo YM, Kim MS. Use of a portable fluorescence imaging device to facilitate cleaning of deli slicers. *Food Control*. 2015;51:256-262. doi:10.1016/j.foodcont.2014.11.031.

139. Durek J, Fröhling A, Bolling J, Thomasius R, Durek P, Schlüter OK. Non-destructive mobile monitoring of microbial contaminations on meat surfaces using porphyrin fluorescence intensities. *Meat Sci*. 2016;115:1-8. doi:10.1016/j.meatsci.2015.12.022.

140. Oto N, Oshita S, Makino Y, Kawagoe Y, Sugiyama J, Yoshimura M. Non-destructive evaluation of ATP content and plate count on pork meat surface by fluorescence spectroscopy. *Meat Sci*. 2013;93(3):579-585. doi:10.1016/j.meatsci.2012.11.010.

141. Shirai H, Oshita S, Makino Y, Sugiyama J, Yoshimura M. Nondestructive Hygiene Monitoring on Pork Meat Surface Using Excitation–Emission Matrices with Two-Dimensional Savitzky–Golay Second-Order Differentiation. *Food Bioprocess Technol*. 2014;7(12):3455-3465. doi:10.1007/s11947-014-1353-3.

142. Shirai H, Oshita S, Makino Y. Detection of fluorescence signals from ATP in the second derivative excitation-emission matrix of a pork meat surface for cleanliness evaluation. *J Food Eng*. 2016;168:173-179. doi:10.1016/j.jfoodeng.2015.07.032.

143. Yoshimura M, Sugiyama J, Tsuta M, et al. Prediction of Aerobic Plate Count on Beef Surface Using Fluorescence Fingerprint. *Food Bioprocess Technol*. 2014;7(5):1496-1504. doi:10.1007/s11947-013-1167-8.

144. Everard CD, Kim MS, Lee H. Assessment of a handheld fluorescence imaging device as an aid for detection of food residues on processing surfaces. *Food Control*. 2015;59:243-249. doi:10.1016/j.foodcont.2015.05.030.

145. Bódalo-Santoyo A, Gómez-Carrasco JL, Gómez-Gómez E, Máximo-Martín MF, Hidalgo-Montesinos AM. Spiral-wound membrane reverse osmosis and the treatment of industrial effluents. *Desalination*. 2004;160(2):151-158. doi:10.1016/S0011-9164(04)90005-7.

146. Penña N, Gallego S, del Vigo F, Chesters SP. Evaluating impact of fouling on reverse osmosis membranes performance. *Desalin Water Treat*. 2013;51(4-6):958-968. doi:10.1080/19443994.2012.699509.

147. Jiang S, Li Y, Ladewig BP. A review of reverse osmosis membrane fouling and control strategies. *Sci Total Environ*. 2017;595:567-583. doi:10.1016/j.scitotenv.2017.03.235.

148. Anand S, Hassan A, Avadhanula M. The effects of biofilms formed on whey reverse osmosis membranes on the microbial quality of the concentrated product. *Int J Dairy Technol*. 2012;65(3):451-455. doi:10.1111/j.1471-0307.2012.00848.x.

149. Anand S, Singh D. Resistance of the constitutive microflora of biofilms formed on whey reverse-osmosis membranes to individual cleaning steps of a typical clean-in-place protocol. *J Dairy Sci*. 2013;96(10):6213-6222. doi:10.3168/jds.2013-7012.

150. Hassan AN, Anand S, Avadhanula M. Microscopic observation of multispecies biofilm of various structures on whey concentration membranes1. *J Dairy Sci*. 2010;93(6):2321-2329. doi:10.3168/jds.2009-2800.

151. Tang X, Flint SH, Brooks JD, Bennett RJ. Factors affecting the attachment of micro-organisms isolated from ultrafiltration and reverse osmosis membranes in dairy processing plants. *J Appl Microbiol*. 2009;107(2):443-451. doi:10.1111/j.1365-2672.2009.04214.x.

152. Moerman F, Rizoulières P, Majoor FA. Cleaning in place (CIP) in food processing. In: *Hygiene in Food Processing: Principles and Practice: Second Edition*. ; 2013:305-383. doi:10.1533/9780857098634.3.305.

153. DOW. Water & Process Solutions, FILMTEC ™ Reverse Osmosis Membranes: Technical Manual. *Dow Chem Co*. 2013:181. http://www.dow.com/en-us/water-and-process-solutions/products/reverse-osmosis#/accordion/F36C1D89-9385-480A-9242-575D600E6F81.

154. Schlafer S, Meyer RL. Confocal microscopy imaging of the biofilm matrix. *J Microbiol Methods*. 2017;138:50-59. doi:10.1016/j.mimet.2016.03.002.

155. Semwogerere D, Weeks ER. Confocal Microscopy. *Encycl Biomater Biomed Eng*. 2005:1–10. doi:10.1081/E-EBBE-120024153.

156. Diaspro A, Chirico G. Two-photon excitation microscopy. *Adv Imaging Electron Phys*. 2003;126. doi:10.1016/S1076-5670(03)80016-2.

157. Branda SS, Vik Å, Friedman L, Kolter R. Biofilms: The matrix revisited. *Trends Microbiol*. 2005;13(1):20-26. doi:10.1016/j.tim.2004.11.006.

158. Chan R, Chen V. Characterization of protein fouling on membranes: Opportunities and challenges. *J Memb Sci*. 2004;242(1-2):169-188. doi:10.1016/j.memsci.2004.01.029.

159. Bégoin L, Rabiller-Baudry M, Chaufer B, et al. Methodology of analysis of a spiral-wound module. Application to PES membrane for ultrafiltration of skimmed milk. *Desalination*. 2006;192(1-3):40-53. doi:10.1016/j.desal.2005.10.010.

160. Scientific T. BCA ™ Protein Assay Kit. *BCA Protein Assay Kit*. 2007;747(23225):6-7. doi:10.1016/j.ijproman.2010.02.012.

161. Pavia DL, Lampman GM, Kriz GS. *Introduction to Spectroscopy BT - Introduction to Spectroscopy*.; 2001. papers3://publication/uuid/DA5E8589-68A0-4D2F-BB5E-7C12F3FA0CC3.

162. PerkinElmer. FT-IR Spectroscopy Attenuated Total Reflectance (ATR). 2005. https://www.utsc.utoronto.ca/~traceslab/ATR_FTIR.pdf.

163. Tang CY, Kwon Y-N, Leckie JO. Effect of membrane chemistry and coating layer on physiochemical properties of thin film composite polyamide RO and NF membranes. *Desalination*. 2009;242(1-3):149-167. doi:10.1016/j.desal.2008.04.003.

164. Xuamei Tang. Controling biofilm development on ultrafiltration and reverse osmosis membranes used in dairy plants. *PhD thesis*. 2011. http://hdl.handle.net/10179/2302.

165. Davis R, Mauer LJ. Fourier tansform infrared (FT-IR) spectroscopy: A rapid tool for detection and analysis of foodborne pathogenic bacteria. In: *Current Research, Technology and Education Topics in Applied Microbiology and Microbial Biotechnology*. ; 2010:1582-1594. https://www.researchgate.net/profile/Reeta_Davis/publication/257781807_Fourier_Transform_Infrared_FT-IR_Spectroscopy_A_Rapid_Tool_for_Detection_and_Analysis_of_Foodborne_Pathogenic_

Bacteria/links/5614e8f108ae4ce3cc649412.pdf.

166. Yu T, Meng L, Zhao QB, Shi Y, Hu HY, Lu Y. Effects of chemical cleaning on RO membrane inorganic, organic and microbial foulant removal in a full-scale plant for municipal wastewater reclamation. *Water Res*. 2017;113:1-10. doi:10.1016/j.watres.2017.01.068.

167. Kim S-J, Oh BS, Yu H-W, et al. Foulant characterization and distribution in spiral wound reverse osmosis membranes from different pressure vessels. *Desalination*. 2015;370:44-52. doi:10.1016/j.desal.2015.05.013.

168. Boss CB, Fredeen KJ. *Concepts, Instrumentation and Techniques in Inductively Coupled Plasma Optical Emission Spectrometry*. Vol 1542.; 2015.

169. Herigstad B, Hamilton M, Heersink J. How to optimize the drop plate method for enumerating bacteria. *J Microbiol Methods*. 2001;44(2):121-129. doi:10.1016/S0167-7012(00)00241-4.

170. Novak Babič M, Zalar P, Ženko B, Džeroski S, Gunde-Cimerman N. Yeasts and yeast-like fungi in tap water and groundwater, and their transmission to household appliances. *Fungal Ecol*. 2016;20:30-39. doi:10.1016/j.funeco.2015.10.001.

171. Vitzilaiou E. Mater Thesis-Biofilm forming microorganisms from reverse osmosis membranes in dairy industry. 2017.

172. Defra. *A Review of Fungi in Drinking Water and the Implications for Human Health.* Paris; 2011. http://www.dwi.gov.uk/research/completed-research/reports/DWI70-2-255.pdf.

173. Quek PH, Hu J. Indicators for photoreactivation and dark repair studies following ultraviolet disinfection. *J Ind Microbiol Biotechnol*. 2008;35(6):533-541. doi:10.1007/s10295-008-0314-0.

174. Salcedo I, Andrade JA, Quiroga JM, Nebot E. Photoreactivation and dark repair in UV-treated microorganisms: Effect of temperature. *Appl Environ Microbiol*. 2007;73(5):1594-1600. doi:10.1128/AEM.02145-06.